MECHANISMS OF ATP RELEASE IN AIRWAY EPITHELIAL CELLS

Lucia Seminario Vidal

A dissertation submitted to the faculty of the University of North Carolina at Chapel Hill in partial fulfillment of the requirements for the degree of Doctor of Philosophy in the Department of Cell and Molecular Physiology

Chapel Hill
2010

Approved by:

Eduardo R. Lazarowski

James M. Anderson

Richard C. Boucher

Kay Lund

Scott Randell

ABSTRACT

LUCIA SEMINARIO VIDAL: Mechanisms of ATP release in airway epithelial cells
(Under the direction of Eduardo R. Lazarowski, Ph.D.)

The mucociliary clearance (MCC) process that removes foreign particles and pathogens is the primary innate defense mechanism in the airways. Major components of MCC, i.e., ion transport, mucin secretion, and ciliary beat frequency, are regulated by extracellular ATP and adenosine, acting on cell surface purinergic receptors. Given the physiological importance of purinergic regulation of MCC activities, the objective of this dissertation was to elucidate signaling elements and pathways relevant for ATP release from airway epithelial cells.

The protease-activated receptor (PAR) agonist thrombin elicited a rapid Ca^{2+}-dependent release of ATP. In contrast, the $P2Y_2$ receptor agonist UTP caused negligible ATP release, despite promoting a robust Ca^{2+} response. Thrombin-elicited ATP release was associated with Rho activation, was accompanied by enhanced cellular uptake of the hemichannel fluorescence probe propidium iodide in a Ca^{2+}- and Rho kinase-dependent manner, and was inhibited by connexin/pannexin hemichannel blockers. These studies suggested that thrombin promotes ATP release from airway epithelial cells via Rho- and Ca^{2+}-dependent activation of connexin/pannexin hemichannels.

Similarly to thrombin, hypotonic challenge triggered ATP release, which was accompanied by RhoA activation, MLC phosphorylation, and dye uptake. ATP release and dye uptake in hypotonic challenge-stimulated cells were inhibited by transfecting cells with a dominant negative mutant of RhoA, and by inhibiting or knocking-down pannexin 1.

Transient receptor potential-4 (TRPV4) inhibitors reduced RhoA activation, dye uptake, and ATP release. Thus, hypotonic stress-induced ATP release occurs via Rho-dependent pannexin 1 hemichannel opening, and TRPV4 likely transduces osmotic stress into Rho-mediated ATP release.

In goblet cells, PAR agonists stimulated the concomitant release of mucins and ATP, which was dependent on intracellular Ca^{2+} mobilization and cytoskeletal reorganization. Mucin granules contained ATP, but levels of ADP and AMP within granules exceeded those of ATP. Direct release of ADP/AMP from mucin granules likely represents an important source of ASL adenosine, promoting A_{2b} receptor-dependent ion/water secretion necessary for mucin hydration.

In sum, this dissertation suggests a major mechanism for ATP release from non-mucous cells, i.e., Rho-dependent pannexin 1 opening. These studies also reveal that PARs promote Ca^{2+}-regulated secretion of ATP/ADP/AMP-rich mucin granules from goblet cells.

To Prem, Liliana, and Mosso.

ACKNOWLEDGEMENTS

It was a challenge to embark in a basic science Ph.D. training after graduating from medical school. While my passion for the advancement of knowledge and my innate curiosity drove my decision to immerse myself into the Ph.D. studies and kept me motivated throughout these years, this dissertation would not have been possible without the support and guidance of several individuals. To them I would like to express my gratitude.

First and foremost, I would like to thank my advisor and mentor Dr. Eduardo Lazarowski for his contribution to my development as a scientist, supporting me with his patience and knowledge while allowing for my independent growth throughout the years. I appreciate all the time and effort that he invested into teaching me everything from signaling pathways on the white board to hands-on radioisotopic- and HPLC-based assays. It has been an honor to be his student.

I would like to express my gratitude to all of the Lazarowski lab members, who have provided a fun working environment for the past four years. I am most indebted to Dr. Silvia Kreda for her advice and crucial contributions to the studies of nucleotide release from goblet cells, which made her an essential part of this research. She also trained me in several techniques, including confocal microscopy and immunoprecipitation assays. I am grateful to Silvia in every possible way and hope to collaborate with her in the future. Many thanks go in particular to my friends Dr. Juliana Sesma and Catja van Heusden. I thank Juliana for discussing exciting ideas during "coffee break" some late afternoons. I am much indebted to

TABLE OF CONTENTS

LIST OF TABLES

LIST OF FIGURES

ABBREVIATIONS

5'-NT	5'-nucleotidase
B,γ-metATP	β,γ-methylene ATP
AC	adenylyl cyclase
ADA1	adenosine deaminase 1
ADO	adenosine
AK	adenylate kinase
ALU	arbitrary light units
ASL	airway surface liquid
BAPTA-AM	1,2-bis(o-aminophenoxy)ethane-N,N,N',N'-tetraacetic acid (acetoxymethyl ester)
$[Ca^{2+}]ex$	extracellular calcium concentration
cAMP	cyclic AMP
CaCC	Ca^{2+}-activated Cl^- channel
CBF	ciliary beat frequency
CF	cystic fibrosis
CFTR	cystic fibrosis transmembrane conductance regulator
DAG	diacylglycerol
DMEM	Dulbecco's modified eagle's medium
DMSO	dimethyl sulfoxide
Ebselen	2-phenyl-1,2-benzisoselenazol-3(2H)-one
EDTA	ethylenedinitrilotetraacetic acid
ENaC	epithelial sodium channel

E-NPPs	ecto-nucleotide pyrophosphatases/phosphodiesterase
ER	endoplasmic reticulum
GAPDH	glyceraldehyde 3-phosphate dehydrogenase
GlcNAc	N-Acetylglucosamine
GEF	guanine nucleotide exchange factor
GPCR	G protein-coupled receptor
HBSS	Hank's balanced salt solution
HEPES	4-(2-hydroxyethyl)-1-piperazine ethanesulfonic acid
HPLC	high performance liquid chromatography
INO	inosine
$InsP_3$	inositol 1,4,5-trisphosphate
MCC	mucociliary clearance
MLC	myosin light chain
MLCK	MLC kinase
NDPK	nucleoside diphosphokinase
NTPDase	nucleoside triphosphate diphosphohydrolase
PAR	protease-activated receptor
PAR-AP	PAR activating peptide
PBS	phosphate buffered saline
PCL	periciliary liquid layer
PI3K	phosphoinositide 3-kinase
PIP_2	phosphatidylinositol 4,5-bisphosphate
PLC	phospholipase C

PKA	protein kinase A
PKC	protein kinase C
ROCK	rho-associated coiled coil-containing protein kinase
RVD	regulatory volume decrease
SDS-PAGE	sodium dodecyl sulfate-polyacrylamide gel electrophoresis
siRNA	small interference RNA
SPA-luc	*Staphylococcus* protein A-fused luciferase
SNARE	soluble N-ethylmaleimide-sensitive factor attachment protein receptor
TRPV4	transient receptor potential vanilloid 4
VAMP8	vesicle associated membrane protein 8
VDAC	voltage-dependent anion conductance
WD-HBE cells	well-differentiated primary human bronchial epithelial cells

CHAPTER I

Introduction

1. Mucociliary clearance in health and disease

The airway epithelium, with the combined function of mucin-secreting goblet cells and ciliated cells, is responsible for maintaining efficient mucociliary clearance (MCC), the primary innate defense mechanism against inhaled bacteria, viruses, and other noxious particles (1).

Essential to MCC is the composition and hydration state of the airway surface liquid (ASL) that lines the airway epithelium. The ASL is composed of two distinct layers: a periciliary liquid (PCL) layer and a mucus layer (2-3). The PCL layer is in close contact with the cells and provides a low viscosity solution where cilia beat, facilitating mucus transport towards the upper airways (4). The length of the outstretched cilia, i.e., 7 µM, defines PCL height. The mucus layer varies in height from 0.1 µM to 50 µM, and is composed of mucins, e.g., MUC5AC and MUC5B, secreted from goblet cells of the superficial epithelia and submucosal glands (5-6), and is responsible for trapping of inhaled particles. As discussed below, the hydration state of ASL reflects the balance between Cl^- secretion and Na^+ absorption activities (7). Cl^- secretion is mediated primarily by the cyclic AMP (cAMP) regulated cystic fibrosis transmembrane conductance regulator (CFTR) Cl^- channel and to some extent by a calcium-activated chloride channel (CaCC), while Na^+ absorption is exclusively mediated by the epithelial sodium channel (ENaC).

The mucus layer acts as a fluid reservoir, accepting or donating liquid to maintain apposition of the mucus layer inner surface with the tips of the cilia. Thus, when liquid is added to the airways luminal surface, mucus swells and clearance accelerates (8). Conversely, under conditions of relative dehydration, mucus donates water to preserve PCL layer hydration. In chronic lung diseases, where the airway surfaces become severely dehydrated,

2

the ability of the mucus layer to donate water is exhausted. The PCL layer collapses, resulting in mucus adhesion and diminished MCC (7). Concentrated mucus plaques and plugs form, which lead to airway obstruction and serve as a niche for infection, contributing to the pathogenesis of chronic lung diseases, e.g., cystic fibrosis (CF), asthma, and chronic obstructive pulmonary disease (COPD) (9).

Efficient MCC activities, i.e., ion transport, mucin secretion, and ciliary beat frequency, are crucial for maintaining healthy lungs. Therefore, it is necessary for these activities to be precisely regulated. This role is fulfilled, at least in part, by extracellular nucleosides (i.e., adenosine) and nucleotides (e.g., ATP) acting on cell surface purinergic receptors.

2. Purinergic receptors in the airways

Extracellular nucleosides/nucleotides accomplish autocrine and paracrine functions via activation of three widely distributed families of purinergic receptors: P2Y receptors (P2Y-R), P2X receptors (P2X-R), and P1 receptors. P2Y-R are G protein-coupled receptors (GPCRs) activated by uridine and adenine nucleotides, and nucleotide sugars. Molecular cloning and functional studies have identified eight human P2Y-R subtypes: $P2Y_1$, $P2Y_2$, $P2Y_4$, $P2Y_6$, $P2Y_{11}$, $P2Y_{12}$, $P2Y_{13}$, and $P2Y_{14}$. P2X-Rs comprise seven species ($P2X_1$ – $P2X_7$) of ligand-gated ion channels selectively activated by ATP. ATP binding to P2X-R induces opening of the channel, allowing cations (e.g., calcium and sodium) to enter the cell. The P1 receptor family is constituted by four adenosine-activated GPCRs: A_1, A_{2a}, A_{2b}, and A_3 receptors. The agonist selectivity and signaling properties of purinergic receptors are summarized in **Table 1.1**. As discussed below, A_{2b}-R, $P2Y_2$-R, and $P2Y_6$-R are expressed on airway epithelial cells.

Purinergic signaling on the airway surfaces is modulated by the actions of a host of ectoenzymes that dephosphorylate or transphosphorylate nucleotides within the extracellular milieu, hence, terminating or modifying purinergic receptor stimulation. These ectoenzymes include ecto-nucleoside triphosphate diphosphohydrolases (E-NTPDases), nucleotide pyrophosphatases/phosphodiesterases (E-NPPs), alkaline phosphatases, 5'-nucleotidase (5'-NT), and the nucleotide converting enzymes nucleoside diphosphokinase (NDPK) and adenylate kinase (AK) (10-16). E-NTPDases 1 and 3, as well as an unidentified E-NPP, dephosphorylate ATP. Once ATP is metabolized to AMP, the actions of 5'-NT and alkaline phosphatase result in adenosine formation. Adenosine levels are controlled by adenosine deaminase 1 (ADA1) and nucleoside transporters (14, 17). The reactions catalyzed by airway nucleotide/nucleoside metabolizing ectoenzymes are described in **Table 1.2**.

A_{2b}-R, $P2Y_2$-R, and $P2Y_6$-R are expressed on the apical surface of human airway epithelial cells (10, 18-22), suggesting that adenosine and adenine/uridine nucleotides are endogenous modulators of airway functions. Indeed, *in vivo* and *in vitro* studies indicate that adenosine, ATP, UTP, and UDP are present in physiologically relevant concentrations in ASL (11, 23-26). A_{2b}-R promotes cAMP-regulated CFTR activity and increases ciliary beat frequency (27-28). $P2Y_2$-R is the predominant nucleotide-sensing receptor in the airways and it is activated to a similar extent and equipotently by ATP and UTP (29). $P2Y_2$-R activation promotes mucin secretion, enhanced ciliary beat frequency, inhibition of ENaC, and activation of CaCC (9, 18, 21, 30-35). Ca^{2+}-mediated CaCC responses also occur in response to $P2Y_6$-R stimulation, but they are smaller than $P2Y_2$-R-mediated responses, likely reflecting a less abundant expression of $P2Y_6$-R relative to $P2Y_2$-R (10, 29).

Of note, P2X$_4$-R has been proposed to promote CaCC activities (36); however, the physiological relevance of P2X-R expression is not clear, since UTP and ATP exerted similar potency and efficacy in the regulation of ion transport and intracellular calcium mobilization (18). Furthermore, in P2Y$_2$-R$^{-/-}$ mouse airway epithelial cells residual ATP-mediated Ca^{2+}-responses were minor and not affected by removal of extracellular Ca^{2+}, arguing against a major role of P2X-Rs in the control of CaCC activities in the airway epithelia (29, 37). **Figure 1.1** illustrates a model that represents how ASL nucleosides and nucleotides regulate MCC activities.

2.1. Purinergic regulation of ion transport

The notion that purinergic receptors regulate airway epithelial ion transport, and hence the hydration state of ASL, derived from studies indicating that ATP, UTP and adenosine administered to the surface of human airway epithelial cells promoted Cl$^-$ secretion and inhibition of Na$^+$ absorption (18-19, 38-39). These observations were further supported by *in vivo* measurements of nasal transepithelial potential differences in response to topical UTP or ATP (40-41).

CFTR is the primary regulator of chloride secretion in airway epithelia. Defective CFTR activity leads to CF, the most common lethal genetic disease in Caucasian populations, which pathognomonic feature in the lung is ASL depletion. CFTR activity is controlled by extracellular adenosine. Adenosine levels within the ASL are in the 100-400 nM range, enough to promote A$_{2b}$-R activation (25), thereby inducing formation of cAMP and activation of protein kinase A (PKA) (8, 22, 27-28, 41-42), leading to phosphorylation and activation of CFTR (43-44). The role of endogenous adenosine in ASL hydration regulation has been elucidated by studies in well-differentiated primary human bronchial epithelial (WD-HBE)

cell cultures showing that ASL volume is depleted in the presence of ADA or A_{2b}-R antagonists. Indeed, PCL height on ADA-treated normal HBE cultures decreased from ~7 μm to < 4 μm, indicating that normal cultures behave as CF cultures when A_{2b}-R activation is impaired (7, 25). In addition to A_{2b}-R/PKA-promoted CFTR phosphorylation and activation, $P2Y_2$-R-induced protein kinase C (PKC) activation enhances CFTR activity. Two scenarios have been proposed for the effect of $P2Y_2$-R on CFTR: (i) phosphorylation of CFTR by PKC facilitates subsequent PKA-mediated activation (45-46) and (ii) PKC enhances apical expression of CFTR due to inhibition of endocytosis (47).

A CFTR-independent chloride channel, CaCC, is also present on the apical surface of airway epithelial cells, which is activated by Ca^{2+}, hence, by $P2Y_2$-R-activation. Recently, three independent groups identified TMEM16A, also known as Ano1, as a CaCC (48-50). Bioelectric measurements in mouse tracheas, which display low CFTR- and high CaCC-activity relative to those of humans, indicated that TMEM16A CaCC-mediated Cl^- secretion is necessary for ASL homeostasis (35). Specifically, newborn Tmem16a$^{-/-}$ mice displayed ~ 60% diminished UTP-promoted CaCC activity compared to WT littermates. Furthermore, Tmem16a$^{-/-}$ mice tracheas exhibited intraluminal mucus accumulation, likely, secondary to diminished Cl^- secretion and depleted ASL volume. Thus, the importance of CaCC relies on the fact that it may serve to protect tissues with a defective CFTR, i.e., providing an alternative route for Cl^- secretion.

ENaC is the major contributor to sodium absorption in the airway epithelia. ENaC is constitutively activated by proteolytic cleavage, and it is inhibited by CFTR and $P2Y_2$-R activation. The identity of the endogenous protease that cleaves ENaC on the airway epithelial cell surface has not been fully elucidated, but prostasin and other members of the

6

channel-activating protein (CAP) family are likely involved (51-53). ENaC is inhibited by CFTR. This concept derived from two main observations (i) CF airway epithelia absorb Na^+ at two to three times the normal rate, and (ii) stimuli that raise intracellular cAMP further stimulate the already elevated rate of Na^+ absorption in CF cells (54-55). However, the molecular basis of CFTR inhibition of ENaC remains to be elucidated. $P2Y_2$-R stimulation promotes ENaC inhibition (56); this inhibition is not mediated by Ca^{2+}-mobilization or PKC activation but requires depletion of phosphatidylinositol 4, 5-bisphosphate (PIP_2) (34, 57). The notion that ENaC activity depends on PIP_2 levels is supported by studies indicating that (i) ATP-promoted inhibition of Na^+ absorption was suppressed by neomycin, which binds to PIP_2 and inhibits PLC-catalyzed PIP_2 hydrolysis and by inhibitors of PIP kinase (57) ; (ii) co-expression of $P2Y_2$-R and α,β,γ-ENaC in *Xenopus* oocytes resulted in ATP-promoted ENaC inhibition (57) ; (iii) PIP_2 co-immunoprecipitated with the β-subunit of ENaC (57); and (iv) the open probability of ENaC increased by binding of PIP_2 to its β-subunit (34). Additional support to the concept that $P2Y_2$-R regulates ENaC activity through PIP_2 depletion has been recently provided (58-61).

2.2. Purinergic regulation of mucin secretion

Secretory mucins are stored in granules localized at the apical sub-domain of airway epithelial goblet cells, ready for release via Ca^{2+}-regulated exocytosis. Therefore, it has been suggested that mucin secretion can be stimulated by Ca^{2+}-mobilizing GPCRs, e.g., leukotriene receptors, and PARs (62-64). However, the major mucin secretagogues identified in the airways are ATP and UTP acting on $P2Y_2$-R (30, 65-67).

In addition to Ca^{2+}-triggered mucin secretion, diacylglycerol (DAG) induces mucin granule exocytosis by two mechanisms (i) activating the priming protein Munc13-2 (68), and

(ii) activating protein kinase C (PKC) (31, 69-72). PKC is a key regulator of the myristoylated alanine-rich C kinase substrate (MARCKS), which binds to the membranes of the mucin granule (73) facilitating its recruitment and insertion to the plasma membrane via the contractile cytoskeleton (74-75).

2.3. Purinergic regulation of ciliary beat frequency

In normal airways, motile cilia are tightly packed on the surface of the epithelium, and hence, the room required for a single cilium to beat greatly exceeds the space between neighboring cilia. Therefore, a high degree of synchronization between beating cilia is required for efficient MCC. The rate of MCC is determined by the ciliary beat frequency (CBF), which is regulated by changing the phosphorylation state of the cilium components and/or intracellular Ca^{2+} concentrations (76-77). The strongest extracellular signals that raise CBF are extracellular ATP and adenosine, i.e., acting on $P2Y_2$-R and A_{2b}-R, respectively.

$P2Y_2$-R-promoted CBF is a calcium-dependent process. $P2Y_2$-R stimulation induces a peak release of Ca^{2+} from inositol 1,4,5-triphosphate ($InsP_3$)-sensitive stores and a sustained Ca^{2+} influx via plasma membrane Ca^{2+}-channels (78-80). The raise in intracellular Ca^{2+} triggers an initial, rapid increase in CBF (81), and the sustained Ca^{2+} influx prolongs the elevation in CBF. It has been proposed that the initial response of CBF to rising Ca^{2+} is caused by a direct action of Ca^{2+} on the axoneme, i.e., a detergent-resistant cilium devoid of membranes.

A_{2b}-R-mediated changes in CBF rely on cAMP formation and PKA activation (21). Although the target for PKA phosphorylation that regulates CBF has not been identified, PKA-mediated phosphorylation of axonemal proteins (e.g., dynein light chain) may regulate CBF (82-85).

3. ATP release from airway epithelial cells

Realization of the regulatory effects that extracellular nucleotides (18, 30, 39) and nucleosides (86) exert on MCC activities suggested that these molecules naturally occur within ASL. Initial evidence supporting this concept emerged from studies that measured ATP concentrations in the bathing media of airway epithelial cell cultures, using the highly sensitive luciferin/luciferase assay (87-88). These observations were verified in studies using samples derived from nasal turbinate lavages (11), bronchoalveolar lavages, breath condensates, and sputa (24), and in studies using primary cultures of WD-HBE cells grown on an air/liquid interface to maintain cilia and a pseudostratified epithelial structure, thereby providing an *in vivo*-like model (4, 24, 26, 89).

The presence of ATP within ASL, coupled to the realization that ecto-ATPases convert released ATP to adenosine, suggests a link among nucleotide release, metabolism, and receptor activation, i.e., extracellular adenosine is an important regulator of MCC activities. A number of studies have tested this hypothesis. Huang *et al.*, combining electrophysiological measurements with high performance liquid chromatography (HPLC) analysis (see below) of ASL purines in Calu-3 cells, a cell line that endogenously expresses CFTR and lacks ATP receptors, observed that (i) CFTR activity is sensitive to the adenosine-degrading enzyme ADA and to inhibitors of the A_{2b}-R, (ii) enhanced ATP release increases CFTR activity, and (iii) ATP-induced CFTR activity decreases in the presence of 5'NT inhibitors, suggesting that ATP release and metabolism is necessary for generating adenosine at the cell surface, which acts on A_{2b}-R, regulating CFTR activity (27).

These observations were further investigated in primary cultures of human bronchial epithelial cells. Lazarowski *et al.* noticed that extracellular ATP was metabolized within

seconds within the ASL, as measured by the degradation of exogenously added [γ-^{32}P] ATP, and steady-state ATP levels were found in the 5-20 nM range (25). These concentrations are far below the EC_{50} value for P2Y$_2$-R stimulation, and therefore, it is unlikely that ATP accumulating on resting airways will promote MCC activities via P2Y$_2$-R activation. In this context, it was hypothesized that the concerted actions of NTPDases, which dephosphorylate ATP and ADP, and 5'NT, which dephosphorylates AMP, result in the formation of a sufficient amount of adenosine to promote MCC activities. This hypothesis was validated using the chloroacetaldehyde derivatization technique, a sensitive assay for the quantification of adenine-nucleotide and -nucleoside mass. The chloroacetaldehyde derivatization technique consists in the quantitative conversion of the adenine ring of adenosine and its nucleotides into fluorescent 1, N6-etheno (ε)-adenine derivatives, i.e., ε-adenosine, ε-AMP, ε-ADP, and ε-ATP. (ε)-adenyl purines are separated by HPLC and readily quantified with nanomolar sensitivity. Using this technique, adenosine levels on resting cells were found in the 180-350 nM range high enough to promote A$_{2b}$-R mediated MCC activities (25). Furthermore, this study and others demonstrated that adenosine removal or inhibition of adenosine receptors in WD-HBE cell cultures impaired ASL volume regulation (7, 25). Collectively, these studies indicate that constitutive release of ATP results in sufficient formation of adenosine formation to activate A$_{2b}$-R. Thus, A$_{2b}$-R is the major regulator of MCC activities in resting airways, whereas P2Y$_2$-R is relatively inactive.

The observations that (i) mechanical forces acting on epithelial cells promote robust ATP release (87-88), and (ii) the airways are continuously exposed to physiological mechanical stimuli, such as shear stress generated by airflow during tidal breathing, suggested that *in vivo* ATP may reach physiological concentrations within the ASL to promote P2Y$_2$-R

10

mediated MCC activities. This hypothesis was tested by Tarran *et al.* recapitulating *in vitro* the shear stress associated with breathing (7). The authors observed that shear stress increased ATP release (~ 100 nM) onto the apical surface of the epithelium (but not to the basolateral side), which was sufficient to regulate ASL volume. ASL volume regulation was sensitive to the ATP metabolizing enzyme apyrase (ATP → ADP → AMP), suggesting that *in vivo* extracellular ATP is necessary for ASL homeostasis.

Expression of the uridine nucleotide-activated $P2Y_2$, and $P2Y_6$ receptors on the airway epithelial cell surface suggested that extracellular UTP and its product of metabolism UDP, in addition to ATP and adenosine, are important extracellular signaling molecules within the ASL. To investigate whether UTP was released from airway epithelial cells, Lazarowski *et al.* developed a method based on the high selectivity of UDP-glucose pyrophosphorylase for UTP as a co-substrate for the conversion of glucose-1P to UDP-glucose (90). The authors observations' that (i) a similar ratio of UTP to ATP was present in the cell bathing media relative to the cell content, and (ii) both ATP and UTP release was enhanced by mechanical perturbations, suggests the existence of a common mechanism/pathway for nucleotide release from airway epithelial cells.

4. Mechanisms and pathways of nucleotide release

While remarkable progress has been made in understanding how MCC functions are regulated by purinergic receptors, we have only recently begun to understand how ATP reaches the airway surface to accomplish extracellular signaling.

In secretory cells, as in neurons and neuro-endocrine cells, Ca^{2+}-regulated exocytosis of ATP containing granules/vesicles is a major mechanism involved in ATP release (91-93). In

cells of non-neuronal origin, such as endothelial or epithelial cells, there is not a clearly defined mechanism.

In airway epithelia, the complex cellular composition, i.e., ciliated cells and mucin secreting goblet cells, suggests that several mechanisms and pathways are involved in ATP release. Recent studies from our laboratory and others indicated the presence of three major scenarios for nucleotide release, i.e., (i) constitutive release from vesicles, (ii) Ca^{2+}-regulated exocytosis of mucin granules, (iii) receptor- and mechanically-induced release from non-mucous cells via connexons/pannexons [discussed below and in **Chapters III-VI**].

4.1. Constitutive release from vesicles

In the airways, steady-state nucleotide concentrations reflect a balance between release and metabolism. Under resting conditions, ASL ATP concentrations are in the low nanomolar range. However, following addition of ecto-ATPase inhibitors, ASL ATP levels increase steadily at a rate of 300-500 fmol/min cm^2 (25-26). This constant ATP accumulation, suggested that airway epithelial cells release ATP is constitutively, i.e., in the absence of external stimuli.

The fact that UDP-sugars participate in glycosylation reactions within the secretory pathway suggested that these molecules are released as cargo molecules during the export of glycoconjugates to the plasma membrane. This concept, coupled to the observation that in most cells constitutive ATP release is accompanied by the release of UDP-sugars, suggested that the secretory pathway participates in the constitutive release of nucleotides from non-excitatory cells.

The vesicular origin of extracellular UDP-sugar species was assessed by correlating UDP-*N*-acetylglucosamine (UDP-GlcNAc) transporter expression in the ER/Golgi with the cellular release of its cognate substrate, i.e., UDP-GlcNAc (94). Using a yeast model system that exhibits constitutive (but glucose-dependent) release of UDP-sugars and ATP, Sesma *et al.* demonstrated that yeast mutants that lack the ER/Golgi-resident UDP-GlcNAc transporter Yea4 displayed impaired UDP-GlcNAc release. Yea4-defficient cells complemented with Yea4 showed UDP-GlcNAc release rates similar to wild type cells. Furthermore, by overexpressing HFRC1, a human Golgi-resident UDP-GlcNAc/UMP translocator in human bronchial epithelial 16HBE14o⁻ cells, the authors observed enhanced apical release of UDP-GlcNAc, which correlated with enhanced expression of GlcNAc-containing glycans (94). The data strongly suggest that Golgi-derived vesicles contribute to the constitutive release of nucleotide-sugars from airway epithelial cells. Similar to UDP-sugar transporters, ATP/AMP antiporters translocate ATP to the ER and Golgi. Therefore, an appealing explanation for constitutive release of nucleotide-sugars and ATP is that it may reflect the continuous and exocytotic release of these cargo molecules during constitutive export of proteins and glycoconjugates to the apical plasma membrane.

4.2. Ca^{2+}-regulated exocytosis of mucin granules

Evidence from our laboratory and others has recently emerged supporting the notion that Ca^{2+}-dependent release of nucleotides from non-excitatory cells involves an exocytotic mechanism. Inhibition of vesicular trafficking between the ER and Golgi with brefeldin A, or depletion of ATP storage granules with bafilomycin A_1, effectively diminished ATP release in response to various stimuli in numerous cell systems, including astrocytes, hepatocytes, epithelial, and endothelial cells (71, 95-98)

Relevant to airway epithelia, Kreda *et al.* identified subapical electron-translucent granules that resemble mucin granules of goblet cells in Calu-3 cells (99). Real-time confocal microscopic analyses revealed that these subapical granules were competent for Ca^{2+}-regulated exocytosis. Immunostaining and slot blot analysis indicated that the mucin MUC5AC was a major component in these granules. Ca^{2+}-promoted mucin secretion was accompanied by enhanced ATP release into the apical bath. The kinetics of Ca^{2+}-elicited ATP release and mucin-granule secretion were similar and affected by conditions that inhibit granule exocytosis, suggesting that nucleotides are stored within and released from mucin granules. Consistent with the possibility that a vesicular/granular ATP pool contributed to Ca^{2+}-stimulated ATP release, bafilomycin A_1 markedly impaired ionomycin-promoted ATP release from Calu-3 cells. These observations are in good agreement with a recently proposed mathematical model predicting that a vesicular pool of ADP/AMP/adenosine contributes to ASL adenosine levels (100). Based on these observations, **Chapter IV** tests the hypothesis that ATP is released from mucin granules of airway epithelial goblet cells. A corollary of this hypothesis would be that ATP release, concomitantly with mucin secretion, is a mechanism by which mucin-secreting goblet cells produce paracrine signals for mucin hydration within ASL.

4.3. Mechanically- and receptor-triggered nucleotide release from non-mucous cells via connexons/pannexons

The airways are under continuous exposure to mechanical forces that promote MCC activities. During normal tidal breathing shear stress is imparted by airflow (101), and it varies little throughout the branching airway anatomy. Cyclic compressive (transmural) pressure also contributes to the overall magnitude of cellular shear stress. During each

breathing cycle, the pressure gradient fluctuates below and above atmospheric pressure (102). In addition, glands secrete their hypotonic content onto airway surfaces, promoting transient cell swelling (103). Shear stress, cyclic pressure, and hypotonic challenge have been replicated *in vitro* in order to study stress-regulated MCC activities. Shear, compressive, and hypotonic stresses promote robust, non- lytic ATP release from WD-HBE cells, which results in $P2Y_2$-R mediated MCC activities (7, 26, 87-88, 104-105).

In non-mucous lung epithelial cell lines and WD-HBE cell cultures, which consist mostly of ciliated cells, Ca^{2+}-mobilizing agents, such as UTP and the calcium ionophore ionomycin, promote only minor nucleotide release, relative to ATP released in response to mechanical stimuli. For example, Tatur *et al.* observed that ionomycin- and hypotonicity-promoted ATP release from lung epithelial A549 cells shared similar kinetics; however, the concentration of extracellular ATP induced by ionomycin was only a fraction of that promoted by hypotonicity (106). Similarly, we observed that UTP and ionomycin promoted negligible ATP release compared to hypotonic challenge in WD-HBE and A549 cells, respectively. Collectively, the data suggest that signals in addition or alternative to Ca^{2+} are involved in hypotonic stress-induced ATP release.

It is noteworthy to mention that different mechanical stimuli acting on airway epithelial cells share some features between them, but also differ in some aspects. For example, shear stress acts at the apical cell surface to deform cells in the direction of flow, transmural pressure tends to deform cells in all directions (107), and hypotonic challenge produces cell swelling-imparted membrane stretch. In addition, hypotonic stress dilutes the cytosolic contents (26, 108) and promotes compensatory ion transport. Thus, it is possible that stress-

specific elements contribute to airway epithelial ATP release and, therefore, caution should be taken on generalizing conclusions from studies with one type of stress.

Cell-swelling activated anion conductance channels

Most cells react to cellular swelling with the activation of volume-sensitive anion channels (109), which, coupled to the fact that hypotonicity-induced cellular swelling promotes robust ATP release (110-114), lead to the proposal that a large electrochemical outwardly directed ATP gradient (cytosolic concentration of ATP is 3–10 mM, while the steady-state extracellular ATP is 5-20 nM) facilitates ATP release via volume-sensitive anion channels.

Three discernible types of anion conductance are known to be activated by cellular swelling: (i) ClC-2 channels, (ii) the volume-sensitive organic osmolyte-anion channel (VSOAC; synonyms: VRAC, VSOR) (109), and (iii) a 'maxi' or large anion conductance. Although ClC channels are widely expressed in epithelia, analysis of the crystal structure and electrophysiological data from ClC channels clearly exclude permeation of the large organic ion ATP through these pores (115).

Whereas the molecular nature of VSOAC remains undefined, it has been suggested that the maxi-anion conductance is identical to the mitochondrial voltage-dependent anion conductance (VDAC) channel and is also present at the plasma membrane (109). In contrast to ClC channels, the maxi-anion channel shows broad selective conductance, allowing different small organic anions and osmolytes to pass. Due to the net positive charge within the channel, anions such as ATP and ADP are favored (116-117). It has been proposed that VDAC is present in the plasma membrane as a specific splice variant (pl-VDAC-1) (118). Consistent with this theory, studies suggested that the maxi-anion conductance VDAC-like

channel is a plasma membrane ATP-conductive pore in mammary cancer cells (111) and in macula densa cells (119). Furthermore, hypotonicity-stimulated ATP release decreased in VDAC-1 knockout mouse tissue, and increased when pl-VDAC-1 was overexpressed in fibroblasts (114). Although these observations suggest a role of VDAC in ATP release, mechanically-induced ATP release continues to be present in the absence of pl-VDAC-1 (114). Furthermore, genomic analysis indicated absence of a pl-VDAC splice variant in humans (120). Collectively, these studies indicate that it is unlikely that VDAC acts as an ATP release pathway in human airway epithelial cells.

The hypothesis that pl-VDAC acts as a maxi-anion channel has been also argued by Sabirov *et al.* After deleting all known VDAC isoforms in mouse fibroblasts individually and collectively, the authors found that the maxi-anion channel activity remained unaltered (120). Furthermore, single-channel properties, such as anionic permeability and pore size, differed significantly between VDAC and the maxi-anion channel, indicating that they are unrelated proteins (121) Thus, while VDAC is unlikely to mediate ATP release, whether the maxi-anion channel is an ATP release pathway in the airway epithelia remains to be defined.

CFTR

It was also suggested that the CFTR chloride channel either conducts ATP or modulates a related ATP-conductive pore (122-126). This concept derived in part from initial observations suggesting that the multi-drug resistance (MDR) P-glycoprotein, which like CFTR is a member of the ATP-binding cassette (ABC) family of transporters, functions as an ATP channel (127). Despite these initial observations, a number of studies consistently have failed to detect differences in extracellular ATP concentrations in normal and CFTR-deficient epithelial tissues. For example, Reddy *et al.* found that ATP was not conducted

17

through CFTR in intact organs, polarized human lung cell lines, stably transfected mammalian cell lines, or planar lipid bilayers reconstituted with CFTR protein (128). Watt *et al.*, carefully controlling for mechanically-induced ATP release, reported that ATP accumulation on the surface of resting normal human nasal epithelial cells was not affected after incubating the cells with agents that promoted elevation of intracellular cAMP and CFTR activation (87). Subsequently, Okada *et al*., using cell-attached luciferase to assess ATP release *in situ*, in real-time, demonstrated that ATP concentrations at the cell surface and ATP release rates were comparable in cell cultures from CF and normal donors, and that CFTR inhibition did not affect ATP release from hypotonically-stimulated WD-HBE cell cultures (26). Lastly, Lazarowski *et al.* demonstrated that not only ATP, but also ADP, AMP, and adenosine concentrations were similar in the ASL from normal and CF donors (25). In summary, current evidence indicates that CFTR is not involved in regulated ATP release from airway epithelial cells.

Connexin and pannexin hemichannels

Connexin and pannexin hemichannels have been proposed as ATP release pathways in a broad range of tissues and cell types. Pannexins and connexins share a similar structure of four transmembrane domains with the amino- and carboxy-termini residing on the cytoplasmic side, and two extracellular loops (129). **Figure 1.2** illustrates the predicted amino acid sequence and transmembrane structure of pannexin 1. Six subunits form a hemichannel. Hemichannel assemblies composed of connexin subunits are known as connexons, whereas those composed of pannexins are called pannexons. Both homomeric and heteromeric connexons are expressed in different tissues. Similarly, homomeric pannexons are found in several cell types; however, naturally occurring heteromeric

pannexons have not been described (130). Depending on both subunit composition and cell type, connexons or pannexons may be predominantly trafficked to the plasma membrane or retained within intracellular membrane pools (131).

Some connexons (but not pannexons) are gated by external divalent cations. It has been postulated that Ca^{2+} induces a conformational change of connexons (132) via direct interaction with a site in the external portion of the pore (133). Furthermore, it has been proposed that the Ca^{2+} binding site that accounts for both pore occlusion and blockage of gating is formed by a ring of 12 aspartate residues (two per subunit, between the first and third cysteines of the second extracellular loop) (133). Therefore, lowering extracellular Ca^{2+} concentrations is a widely-used maneuver to increase the open state probability of the connexin hemichannel (134-139). Indeed, most experimentally obtained evidence indicating that connexins participate in ATP release relies heavily on the effect of extracellular Ca^{2+} concentrations (140-141).

Connexin subunits are the building blocks of gap junctions formed at sites of direct cell-cell contact. The apposed connexin hemichannels from adjacent cells readily dock together to form a transcellular gap junction channel. Consistent with their role in metabolic coupling, gap junction channels are permeable to cytosolic metabolites, including ATP. Thus, it has been speculated that connexons localize at the plasma membrane as non-junctional hemichannels and may form a regulated exit pathway for ATP. Indeed, using gap junction-deficient cell lines, Cotrina *et al.* reported a 5- to 15-fold increase in ATP release after expressing different connexins (Cx43, Cx32, Cx26) and removing extracellular Ca^{2+}, suggesting that connexins were involved in ATP release (140). Hofer *et al.*, using confocal and electron microscopy studies, confirmed the presence of connexin hemichannels in

astrocytes. In addition, consistent with the notion that connexin hemichannels are permeable to small molecules, lowering extracellular Ca^{2+} allowed the uptake of small fluid phase fluorophores, which was blocked by antibodies against connexins (142). Arcuino *et al.* observed that lowering extracellular Ca^{2+} concentrations resulted in increased ATP release from HBE16o$^-$ and other cell lines, which was associated with the uptake of the small dye propidium iodide. In Cx43-expressing C6 glioma or astrocytoma cells, ATP release from a point source cell was imaged. Light emissions resulting from the addition of a luciferase/luciferin mixture to the cell culture were observed at the single-cell level in real time. Furthermore, entry of propidium iodide into the cells in the point-source of light emission was shown (141). Altogether, these results support the notion that connexin hemichannels can be stimulated to open, thus allowing ATP release.

There are, however, several shortcomings in the hypothesis of connexin-mediated ATP release under physiological conditions. Most studies on connexin-mediated ATP release are based on protocols that remove or diminish extracellular divalent cations, to promote connexin hemichannel activation, a situation unlikely to be found under physiological $[Ca^{2+}]ex$ concentrations(140-142). In addition, very large, unphysiological depolarization protocols (> 80 mV) are necessary for the opening of most connexin hemichannels (143-146). While connexons have been shown to be functionally present in the plasma membrane and, as predicted from their hypothetical structure, could allow the exit of ATP, unequivocal proof is lacking as to whether they may open and release ATP under physiological conditions.

In contrast to connexons, plasma membrane pannexons do not readily assemble into the plaque-like ensembles that typify gap junctions (147-149). Although initial studies indicated

20

that functional gap junctions could be formed by overexpression of pannexin 1 in *Xenopus* oocytes or in human prostate carcinoma cells, no data available support an *in vivo* role for pannexin 1 as a component of physiologically relevant gap junction channels. On the contrary, studies overexpressing murine or rat pannexin 1 report that pannexin 1 is exported to the cell surface as a glycosylated protein, and that pannexin glycosylation prevents the docking between pannexons on adjacent cells (147, 149). In addition, immunohistochemical and electrophysiological studies indicate that pannexin 1 is highly expressed in cells that do not form gap junctions, such as erythrocytes (150). Thus, non-junctional pannexons comprise the predominant structural state and are presumed to be functional.

Several properties associated with pannexin 1 make this protein an appealing candidate for an ATP-releasing channel in airway epithelial cells. Namely, pannexin 1 can be activated (i) by physiological membrane depolarizations (-20 mV to + 20 mV), allowing enhanced release of small molecules, including ATP (130, 151-152), (ii) at physiological $[Ca^{2+}]$ex concentrations (151), and (iii) by mechanical perturbations, as indicated by studies in whole oocytes overexpressing pannexin 1 or excised membrane patches (152). These properties strongly suggest that pannexins may be physiologically relevant conductive pores for ATP release. Studies in **Chapter III** and **Chapter V** provide further evidence that pannexin 1 mediates ATP release from receptor- and mechanically-activated airway epithelial cells.

Receptor-promoted ATP release

While it is recognized that mechanical stimuli promote cellular ATP release without involving cell death or damage (26, 87, 105, 153), it is not known how mechanical stresses are transduced into biochemical signaling, and hence, delineating a systematic strategy for

identifying signaling elements regulating ATP release in response to mechanical stresses in airway epithelial cells has proven problematic.

A few studies from our and other labs reported that Ca^{2+}-mobilizing GPCR agonists promote ATP release from astrocytes, endothelial, MDCK, and other cell types (95, 154-156). Thus, to identify mechanistic components upstream of ATP release from airway epithelial cells, our strategy was to investigate the effect of selected GPCR activation on ATP release. Initially, we performed a systematic screening of GPCR expression in WD-HBE cell cultures. We verified the expression of apical $P2Y_2$-Rs and identified basolateral protease activated receptors (PARs), and demonstrated that PAR activation results in robust ATP release to ASL relative to $P2Y_2$-R activation. In **Chapter III**, we discussed the nature of these observations and defined signaling elements downstream of PAR that participate in ATP release.

5. Statement of purpose

The series of studies included in this dissertation provide the first model of receptor-promoted ATP release from airway epithelia. These studies also demonstrate that PAR-elicited ATP release occurs via two mechanisms: 1) pannexin/connexin hemichannel opening from non-mucus secreting cells [discussed in **Chapter III**], and 2) mucin granule secretion from goblet cells [discussed in detail in **Chapter IV**]. In addition, compelling evidence is provided indicating that Rho GTPases, and consequently Rho kinase and myosin light chain kinase (MLCK) are key regulators of receptor-induced ATP release from WD-HBE cells.

Based on our findings with receptor-activated WD-HBE cells, the role of pannexin 1 and RhoA signaling was assessed in mechanically-stimulated airway epithelia; these studies are

discussed in **Chapter V**. **Figure 1.3** illustrates a model summarizing our current knowledge about ATP release mechanisms in the airway epithelia.

For studying airway epithelial ATP release mechanisms, I have used a combination of techniques, including (1) tissue culture, (2) molecular biology, (3) radioisotopic- and HPLC-based assays, (4) bioluminescent assays, (5) immunoblotting, and (6) confocal microscopy.

The knowledge gained from this research has provided novel insights into purinergic regulation of airway epithelial cell functions and, ultimately, will provide new therapeutic targets to improve MCC in chronic lung diseases.

Table 1.1. Purinergic receptors, agonists, and signaling properties.

	Agonist (human)	Signaling pathways
Adenosine receptors		
A_1, A_3	Adenosine	$G_i \rightarrow \downarrow AC/\downarrow cAMP$
A_{2a}, A_{2b}	Adenosine	$G_s \rightarrow AC/cAMP$
P2Y receptors		
$P2Y_1$	ADP	$G_q/PLC\beta \rightarrow Ca^{2+}/PKC$
$P2Y_2$	ATP = UTP	$G_q/PLC\beta \rightarrow Ca^{2+}/PKC$
$P2Y_4$	UTP	$G_q/PLC\beta \rightarrow Ca^{2+}/PKC$
$P2Y_6$	UDP	$G_q/PLC\beta \rightarrow Ca^{2+}/PKC$
$P2Y_{11}$	ATP	$G_q/PLC\beta \rightarrow Ca^{2+}/PKC$ $G_s \rightarrow AC/cAMP$
$P2Y_{12}$	ADP	$G_i \rightarrow \downarrow AC/\downarrow cAMP$
$P2Y_{13}$	ADP	$G_i \rightarrow \downarrow AC/\downarrow cAMP$
$P2Y_{14}$	UDP-glucose	$G_i \rightarrow \downarrow AC/\downarrow cAMP$
P2X receptors		
$P2X_1$-$P2X_7$	ATP	ATP-gated cation channel

Table 1.2. Nucleotide/nucleoside metabolizing ectoenzymes, substrates, and reactions in the human airways.

Reaction	Enzymes
ATP → ADP + Pi	NTPDase 1 NTPDase 3 Alkaline phosphatase
ADP → AMP + Pi	NTPDase 1 NTPDase 3 Alkaline phosphatase
AMP → ADO + Pi	5'-NT Alkaline phosphatase
ATP→ AMP + PPi	E-NPPs
ATP + NDP ⇆ NTP + ADP	NDPK
ATP + AMP ⇆ 2ADP	AK
ADO → INO	ADA1

Figure 1.1. Purinergic regulation of MCC activities. In the airways, P2Y$_2$-R stimulation by extracellular ATP promotes Gq/PLCβ signaling, which results in DAG and InsP$_3$ formation, leading to the activation of PKC and Ca^{2+}-mobilization, respectively. In ciliated cells, P2Y$_2$-R activation results in activation of CaCC, inhibition of the epithelial sodium channel ENaC, and enhanced CBF. The P2Y$_2$-R expressed on goblet cells promotes Ca^{2+}-regulated exocytosis of mucin granules. ATP metabolism results in adenosine (ADO) accumulation. A$_{2b}$-R activation elicits the formation of cAMP and PKA-mediated phosphorylation and activation of CFTR. CFTR inhibits ENaC by mechanisms that are not well defined.
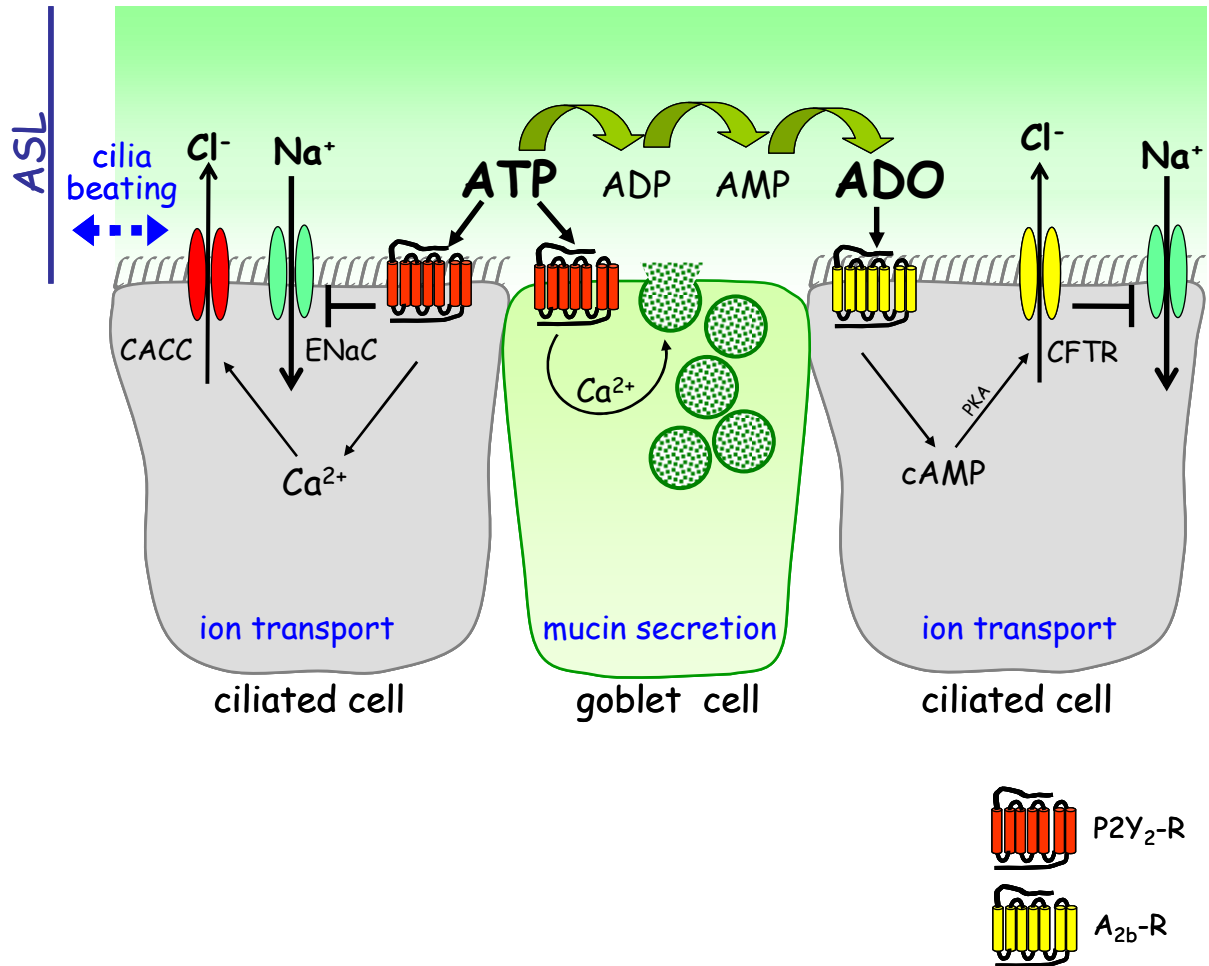
Figure 1.2. Predicted amino acid sequence and transmembrane domain structure of human pannexin 1. Red and grey circles indicate predicted sites for N-glycosylation and phosphorylation, respectively.
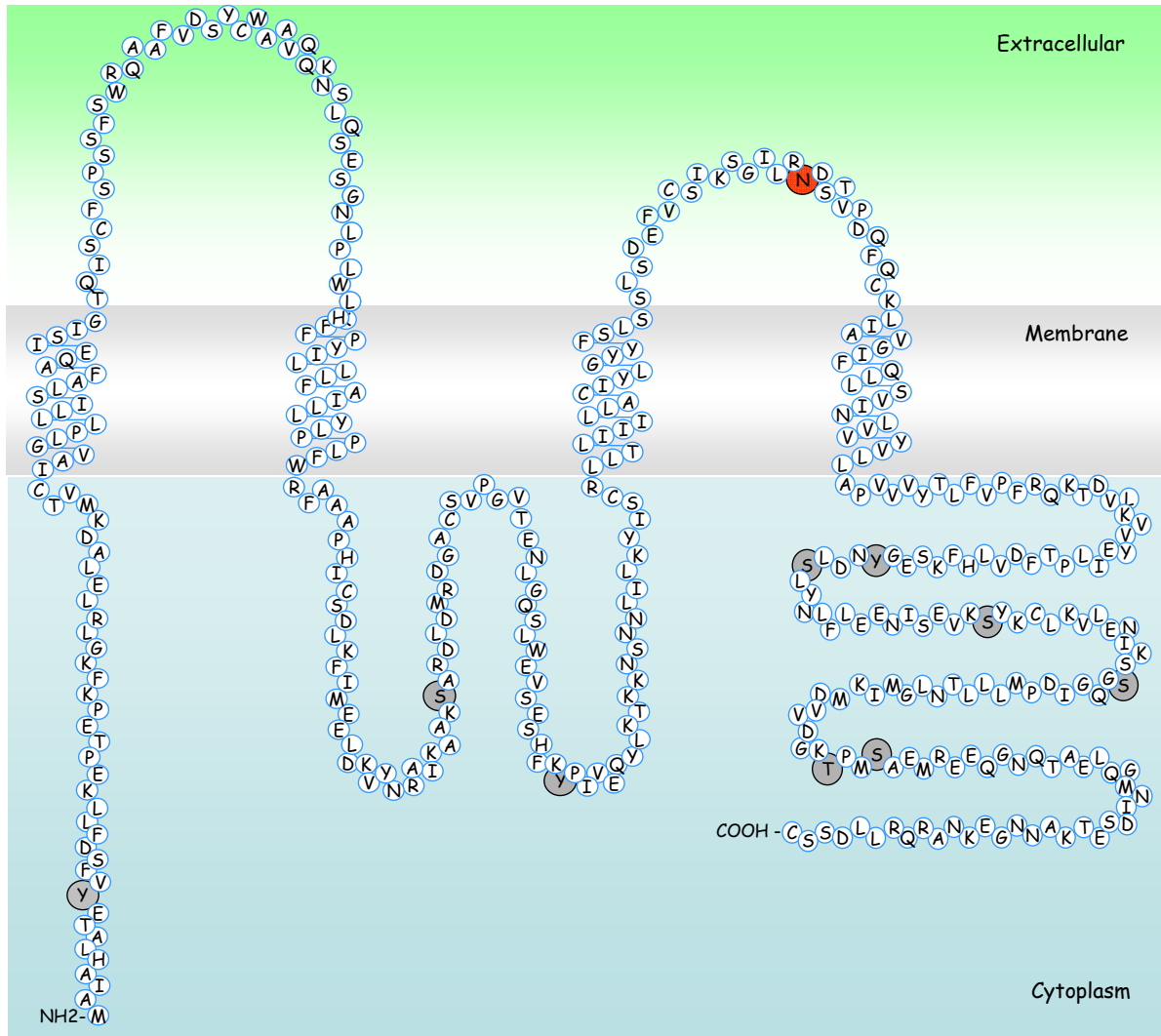
Figure 1.3. Model of ATP release mechanisms in airway epithelia. This dissertation provides new insights into the mechanisms of ATP release from airway epithelial cells, demonstrating that (i) pannexin 1 (Panx1) channels act as ATP release pathways or pathway regulators in non-secretory cells, (ii) Rho GTPases, Rho kinase, and myosin light chain kinase are key regulators of receptor- and mechanically-induced ATP release, and (i) mucin granules containing ATP, ADP and AMP are competent for Ca^{2+}-regulated exocytosis.
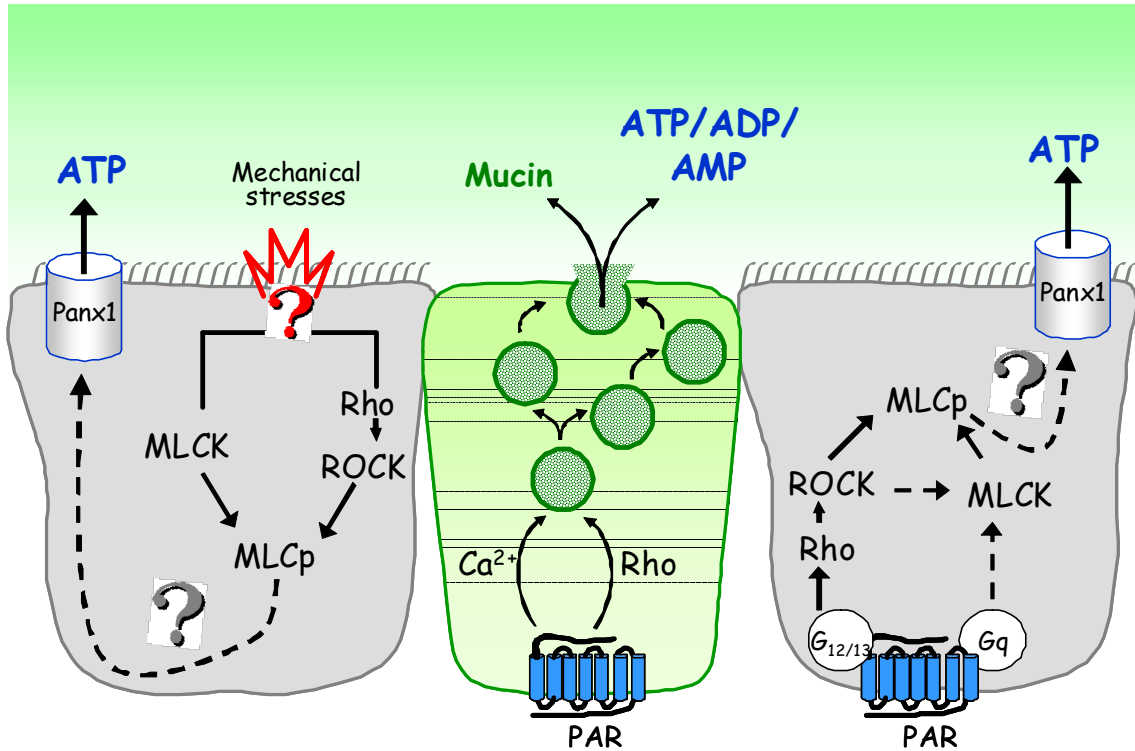
CHAPTER II

Assessment of Extracellular ATP Concentrations

1. Introduction

Extracellular ATP plays important signaling roles by activating a score of broadly distributed cell surface purinergic receptors. ATP concentrations at the cell surface, and consequently the magnitude of purinergic receptor stimulation, reflect a well-controlled balance between rates of ATP release and extracellular metabolism.

Given the physiological importance of purinergic signaling, there is an increased interest in assessing nucleotide concentrations on the surface of cells and tissues, and in understanding the mechanisms of cellular ATP release. Numerous approaches have been developed in recent years to assess extracellular levels of ATP and other nucleotides [reviewed in (157)]. Several factors complicate the accurate measurement of extracellular ATP concentrations. For example, it is difficult to assess ATP concentrations in the physiologically relevant unstirred film covering the cell surface. Moreover, robust ATP release occurs in response to mechanical stress; thus, experimental maneuvers (cell wash, sampling, transporting the cell dishes) often result in artifacts. Finally, rapid hydrolysis of released ATP may compromise the relevance of ATP measurements.

In this chapter, it is discussed the use of the luciferin/luciferase-based reaction to measure extracellular ATP concentrations with high sensitivity. Protocols are adapted to assess ATP levels either in sampled extracellular fluids or *in situ* at the cell surface (**Fig. 2.1**). Although our focus is on studies of ATP release from epithelial cells, protocols described here are applicable to practically all cell types.

2. Measuring ATP concentrations in sampled fluids: Off-line bioluminescence detection.

This section describes a protocol that uses the luciferin/luciferase-based reaction (see Note 1) to quantify ATP concentrations in samples obtained from cell culture conditioned media. Briefly, samples are collected gently to minimize unwanted mechanical release of ATP, heat-inactivated to abolish ATPase activities potentially present in the extracellular solution, and transported to the dark chamber of a luminometer. The luciferase/luciferin cocktail is added by an automatic injector, and the resulting luminescence is recorded (**Figure 2.1A**).

The methodology described here is applicable to ATP measurements in tissue extracts, biological fluids, bacterial cultures, *in vitro* enzymatic reactions, etc.

2.1. Materials

All reagents should be of the highest purity available, and maintained free of bacterial contamination to avoid ATP degradation. De-ionized water should be used, preferably HPLC grade water. Use of aerosol-protected tips is strongly recommended to avoid reagent cross-contamination.

2.1.1. Cell culture

Experiments described in this section were performed with A549 cells (ATCC # CCL-185) seeded on 24-well multiwell plastic plates (BD Falcon). Cells were grown on Dulbecco's modified eagle's medium (DMEM) with high glucose (Gibco), supplemented with 10% fetal bovine serum (FBS), 60 µg/ml (100 IU/ml) penicillin and 100 µg/ml streptomycin.

2.1.2. Reagents to stimulate ATP release

In epithelial and endothelial cells, robust ATP release can be triggered by mechanical stimuli such as shear stress, stretch, compression, and hypotonicity-induced cell swelling (26, 96, 105, 153). Reagents to stimulate ATP release by hypotonic stress-induced cell swelling are as follow:

1) Hypotonic solution: 1.2 mM $CaCl_2$, 1.8 mM $MgCl_2$, and 25 mM 4-(2-hydroxyethyl)-1-piperazine ethanesulfonic acid (HEPES), pH 7.4. Store at 4°C.

2) Control (isotonic) solution: 154 mM NaCl (0.9% NaCl solution), 1.2 mM $CaCl_2$, 1.8 mM $MgCl_2$, and 25 mM HEPES, pH 7.4. Store at 4°C.

2.1.3. Reagents to inhibit ATP metabolism

Commonly used inhibitors of ecto-nucleotidase activities are β,γ-methyleneadenosine 5′-triphosphate (β,γ-metATP), 6-*N*-*N*-diethyl-β,γ-dibromomethylene-D-ATP (ARL-67156), and 2-phenyl-1,2-benzisoselenazol-3(2H)-one (ebselen) (26, 71, 95, 105, 156). Levamizole has been used to inhibit alkaline phosphatase activity present on epithelial cells (26). In A549 cell cultures, we obtain maximal inhibition of ATP metabolism by using a cocktail containing 300 µM β,γ-metATP and 30 µM ebselen (See **Fig. 2.3**).

1) Ebselen: 10 mM in dimethyl sulfoxide (DMSO), aliquoted, and stored at -20°C.

2) β,γ-metATP: 100 mM in water, aliquoted, and stored at -20°C.

2.1.4. Luminometry reagents

Several commercial brands of luminometers are available. The protocol described below was adapted for a Berthold AutoLumat luminometer, which is configured to process 180 test tubes at a time (See Note 2).

1) 4X LUMI solution: 6.25 mM $MgCl_2$, 0.63 mM ethylenedinitrilotetraacetic acid (EDTA), 75 µM dithiothreitol (DTT), 1mg/ml bovine serum albumin (BSA), and 25 mM HEPES, pH 7.8. Filter and store sterile at 4° C.

2) Luciferase from *Photinus pyralis* (Sigma, L9506) is dissolved at 0.5 mg/ml in 4X LUMI solution and stored in 30 µl aliquots at -20° C.

3) Luciferin (BD PharMingen) is dissolved at 10 mg/ml in water and stored in 100 µl aliquots, protected from light, at -20° C.

4) Hank's balanced salt solution (HBSS) supplemented with 1.2 mM $CaCl_2$ and 1.8 mM $MgCl_2$ (HBSS+). HBSS+ is filtered sterile and stored at 4° C. 25 mM HEPES, pH 7.4, is added freshly prior to experiments (See Note 3).

5) Clear 5 ml polystyrene or glass test tubes (e.g., Sarstedt).

6) ATP stock solution (e.g., 100 mM, GE Healthcare, 27-2056-01) stored at -20° C.

2.2. Methods

2.2.1. Preparation of samples

1) Grow lung epithelial A549 cells in 24-well plastic plates (surface area of 2 cm^2) until confluence (See Note 4).

2) Rinse gently confluent cultures with HBSS+ twice to remove cell debris and serum components present in the medium.

3) Pre-incubate cells in HBSS+ for 1 h at 37 °C and 5% CO_2 in a tissue culture incubator. To minimize unwanted mechanically-induced ATP release during sampling, cell cultures should be covered sufficiently with media (e.g., 250 µl for one well of a 24-well plate).

4) Expose cell cultures to reagents and/or stimuli, as described in **Fig. 2.3**.

5) Collect up to 100 µl of the cell bathing medium into 1.5-ml Eppendorf tubes placed on ice.

6) Heat samples for 2 min at 98°C to inactivate potential nucleotidase activities.

7) Store samples at -20°C until bioluminescence measurements.

2.2.2. Quantification of ATP (**Figs. 2.2 and 2.3**)

This protocol assumes the use of a LB953 AutoLumat luminometer (Berthold, Wildbad, Germany), but can be modified to other luminometers by following the manufacturer's instructions.

1) Prepare the luciferin/luciferase cocktail freshly by adding one aliquot of luciferase and luciferin stock solutions (described in Materials) to 12.5 ml 4X LUMI solutions, at room temperature (RT), protected from light. Final luciferin and luciferase concentrations in 4X LUMI are 265 µM and 1.2 µg/ml, respectively.

2) Place the luciferin/luciferase solution in the injector port of the luminometer. Prime the injector line following the manufacturer's instructions.

3) Prepare an ATP calibration curve (e.g., up to 1000 nM ATP, see Note 5) in the same solution/media used for incubations with cells.

4) Add 30 µl of each sample to a 5 ml test tube containing 300 µl H_2O (See Note 6).

5) Transfer the test tubes to the dark chamber of the luminometer and proceed with the luciferin/luciferase injection and bioluminescence recording, i.e., arbitrary light units (ALUs), as instructed by the manufacturer.

6) Determine ATP concentration in the sample by intersecting sample ALU values with the calibration curve ALU values (See Notes 7 and 8).

Notes

1. Firefly luciferase catalyzes the following reaction:

D-luciferin + ATP + luciferase (L) $\rightarrow$ L(luciferyl-adenylate) + pyrophosphate

L(luciferyl-adenylate) + O_2 $\rightarrow$ L(oxyluciferin*; AMP) + CO_2

L(oxyluciferin*; AMP) $\rightarrow$ L(oxyluciferin; AMP) + photon

L(oxyluciferin; AMP) $\rightarrow$ L + oxyluciferin + AMP
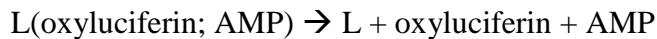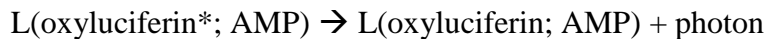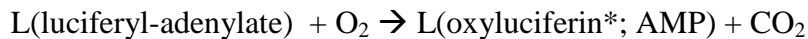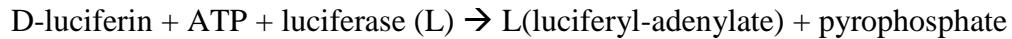
2. Many luminometers are configured as micro-plate readers. Sample volume and luciferase-luciferin cocktail should be modified to fit the volume of an individual well, following the manufacturer's instructions.

3. Minimum essential medium (MEM), DMEM, or several other culture media (without serum) are equally effective as HBSS+ and could be used as an alternative in the sample preparation assay. Avoid using media supplemented with ATP, such as Medium 199.

4. Seeding density of 1 x 10^5 A549 cells/well will provide confluent cultures at 24 h.

5. Under the conditions described a linear ATP concentration: luminescence relationship is observed in the range of 0.1–1000 nM ATP. This ATP concentration range covers ATP concentrations detected in the bulk extracellular medium of most cell cultures.

6. Media or other saline-based solutions (e.g., 0.9% NaCl or PBS) contain anions that interfere with the luciferase reaction [**Fig. 2.2A** and (158-159)], decreasing the sensitivity of

the assay. Therefore, we recommend using water as the diluting agent to achieve the highest sensitivity in the assay.

7. The luciferase reaction is inhibited by components present in cell culture media, e.g., anions (**Fig. 2.2B**). Moreover, phosphatases and other components present in FBS-supplemented and hormone-supplemented media (e.g., BEGM or SAGM, Lonza Walkersville, MD) affect ATP availability for the luciferase reaction. Albumin-bound ATP can be dissociated by heating the sample at 95°C for 2 min (**Fig. 2.2B**).

8. All test drugs added to the cells should be tested for potential interference with luciferase activity [**Fig. 2.3** and (159)].

3.   Real-time, cell-surface measurement of extracellular ATP

In this section, we will describe methods for real-time measurement of ATP by using cell surface-bound luciferase (**Fig. 2.1C**), and will compare this method with measurements obtained with soluble luciferase (**Fig. 2.1B**). The protocols below are designed for measuring luminal ATP concentrations on polarized epithelial cells; however, they are also applicable to measuring extracellular ATP concentrations of non-polarized cells grown on culture plates. Cell surface-binding luciferase can be engineered by fusing luciferase to cell surface binding constructs, e.g., *Staphylococcus* protein A (26, 156, 160), biotin, or lectins, and allows the assessment of ATP concentrations near the cell surface. Soluble luciferase assesses the average ATP concentrations in the medium (from the cell surface to the surface of the bathing solution) and, when used in a small volume, reflects near-cell surface ATP concentrations (**Figs. 2.4 and 2.5**). For real-time assessment of ATP concentrations, cultures (either non-polarized or polarized) are placed directly in the luminometer [e.g., TD-20/20 (Turner Biosystems)].

3.1. Materials

3.1.1. Cell culture

Cells can be grown on plastic dishes (for non-polarized cells) or Transwells (for polarized cells) 3.5 cm or less in diameter.

3.1.2. Luminometry reagents

1) Luciferin (BD PharMingen)

2) Luciferase (Sigma, L9506)

3) *Staphylococcus* protein A-fused luciferase [SPA-luc; see Note 1 and (26) for purification protocols]

4) Buffer: HBSS+ buffered with 10 mM HEPES (HBSS/HEPES). HBSS+ can be replaced with other nutrient-containing solutions (e.g., DMEM, MEM, F12).

3.1.3. Luminometer

Luminometer with a real-time measurement function, e.g., TD-20/20 (Turner, Sunnyvale, CA).

3.2. Methods

3.2.1. Attachment of Staphylococcus protein A-fused luciferase (SPA-luc) to cell surface (see Note 2)

1) Wash the surface (apical, if polarized cells are used) of cell cultures with phosphate buffered saline (PBS), 3x.

2) Incubate the (apical) surface with 50 μl (for cultures of 12 mm diameter) of a blocking solution [PBS containing 1% BSA (PBS/BSA)] for 30 min on ice. If polarized cells are used, keep the basolateral surface immersed in medium.

3) Replace the blocking solution with a solution containing the designated primary antibody (Note 3). For primary airway epithelial cells, use 50 μl of 10 μg/ml (i.e., 1:300) anti-keratan sulfate antibody (mouse IgG2b, Chemicon, Temecula, CA) in PBS/BSA. Incubate for 1 h on ice.

4) Wash 3x with PBS.

5) Incubate with 0.5 mg/ml purified SPA-luc (Note 1) for 1 h at 4°C in the dark. SPA-luc will bind to the Fc domain of the antibody attached to the cells, as indicated in 1.3.

6) Wash carefully 3x with PBS. Replenish the apical surface with ATP assay solution (e.g., HBSS/HEPES). Keep cultures in the dark at RT for 30 min to equilibrate the extracellular ATP concentrations.

3.2.2. Measurement of cell surface ATP concentrations using SPA-luc

1) Place a SPA-luc-bound cell culture in the Turner TD-20/20, add soluble luciferin (150 μM final, to the apical solution for polarized cultures) and close the lid. When a Transwell is used, place it in a chamber (or a dish) containing HBSS/HEPES to cover the basolateral side (**Figs. 2.1B and 2.1C**). Assays are typically performed at RT (Note 4).

2) Record baseline luminescence (arbitrary light unit, ALU) every minute with 5-10 s integration time, according to manufacturer's instructions. Monitor ALU until baseline luminescence is achieved (see Note 5). Baseline luminescence is usually achieved within 5 to 30 min and represents basal ATP concentrations (see **Fig. 2.4**).

3) To assess stimulated ATP release, add stimuli (e.g., pharmacological reagents, hypotonic challenge, etc.) and record the ALU. ALU integration time needs to be optimized, as well as the frequency of recording, for each experiment. For example, when airway epithelial cells are challenged with 33% hypotonicity, H_2O (a half volume of the initial luminal volume) is added to the luminal solution at t = 0. The ALU is recorded for 5 min; every 0.2 s for the first minute, then every 10 s (with 4 s integration time) for the next 4 min. A typical time-course of ATP concentrations is shown in **Fig. 2.5**.

4) At the end of each assay, an ATP-luminescence relationship (calibration curve) is generated to calculate ATP concentrations. Known concentrations of ATP are added to the luminal liquid in a stepwise manner (e.g., 1 nM added twice, 10 nM added twice, then 100 nM added twice - for the accuracy of the calibration curve, adding each concentration twice is recommended), and increases in ALUs recorded each time (see Note 6).

3.2.3. Measurement of cell surface ATP concentrations using soluble luciferase

1) Wash the surface of cultures with PBS, 3x.

2) Add HBSS/HEPES (0.5-1 ml for non-polarized 3.5 cm cultures. Bilaterally for polarized cultures- 1 cc and 25-500 µl to luminal and serosal side, respectively, when 12 mm Transwell is used). Equilibrate the cultures in an incubator (37°C and 5% CO_2) for 1 h.

3) Add luciferase (~0.8 µg/cm^2 culture surface) and luciferin (150 µM) to the luminal buffer, and start the measurement as described in Methods 3.2.2.

Notes

1. SPA-luc fused to a hexa-histidine (6 x His) tag is purified over a Ni^{2+}-chelating column. The 6 x His tag is cleaved by Tobacco-Etch virus (TEV) protease after purification. For the detailed purification protocols, see (26).

2. The principle of SPA-luc attachment to cell surface is as follows. First, bind an antibody to cell-surface molecules; next, attach protein A (of SPA-luc) to the Fc domain of the antibody. It is important to choose an antibody that protein A is capable of binding; for example, protein A strongly binds to total IgG, IgG_{2a}, IgG_{2b} and Ig_3, but exhibit weak or no binding to IgG_1, which is the most common class of monoclonal antibodies.

3. For primary human airway cells, lectins and monoclonal antibodies against keratan sulfate or MUC1 served as SPA-luc attachment molecules (26). For mouse Bac-1.2F5 macrophages, monoclonal antibodies against CD45.2 or $H-2K^d$ major histocompatibility complex (MHC) class I; for human platelets, monoclonal antibodies against CD41 or anti-HLA-ABC served as SPA-luc attachment molecules (160). For cell types in which finding an endogenous antigen on the cell surface for sufficient antibody attachment is difficult, antigens can be over-expressed [e.g., CD14 (156)]. However, the effect of antigen over-expression on ATP release and metabolism needs to be addressed.

4. Though it is ideal to perform ATP release assays at a physiological temperature (37ºC), luciferase activity is dramatically decreased above 30˚C (161). Being aware that some ATP release pathways (e.g. exocytosis) might be suppressed at low temperatures, assays can be carried out at RT. It is critical to maintain pH of the assay solution on cells (which contains luciferin and luciferase) at 7.0 to 7.4 (161) by including 25 mM HEPES (pH 7.4).

5. Experimental maneuvers, such as changing and adding luminal solutions and transferring Transwells, cause robust ATP release from cells. Baseline ATP concentrations are achieved after such artifactually released ATP is hydrolyzed by endogenous ecto-ATPases, usually within 5 to 30 min of incubation.

6. The sensitivity of luciferin-luciferase reactions may vary among assays; thus, an ATP-ALU relationship should be generated for each assay. The end products of luciferin-luciferase reaction (e.g., pyrophosphate, oxyluciferin) inhibit the luciferase reaction. However, when sufficient amounts of luciferin and luciferase are included at the beginning of the assay, the assay sensitivity is typically maintained for at least 30 min on cells.

Figure 2.1. Off-line and real-time approaches to measure extracellular ATP concentrations. Extracellular ATP concentrations can be measured by off-line luminometry of sampled extracellular fluids (A), or on-line luminometry using either soluble luciferase dissolved in medium covering the cells (B) or cell-surface attached luciferase (C). ATP concentrations detected by each method in different volumes are compared in Figs. 2.4 and 2.5.
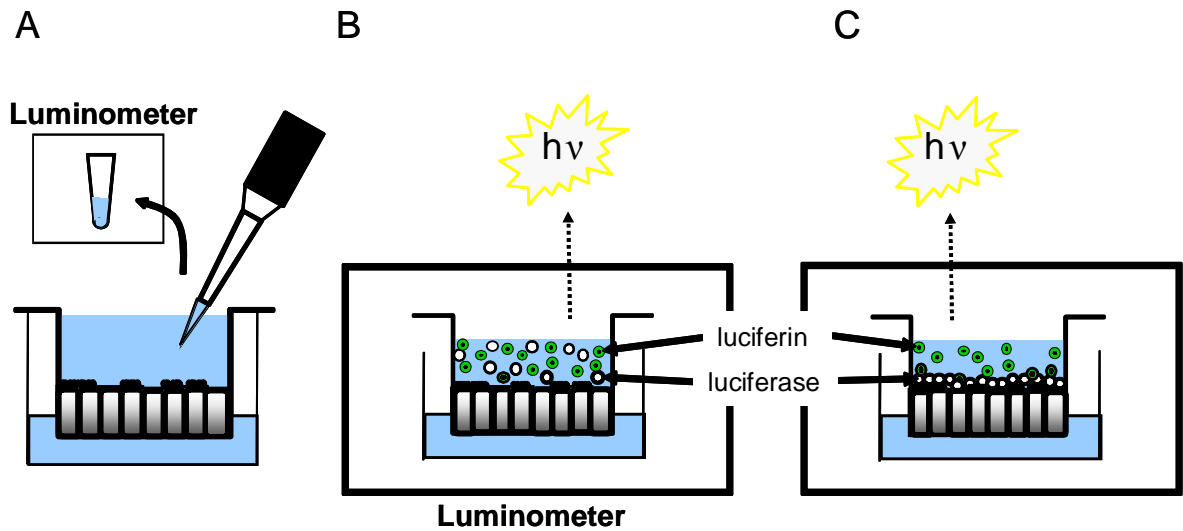
Figure 2.2. Quantification of ATP using luciferin/luciferase. *(A) Anions greatly interfere with the luciferase reaction.* Calibration curves of ATP were performed by adding 30 µl of the indicated ATP concentrations to a 5 ml test tube containing 300 µl H_2O or 154 mM NaCl. Values are the mean ± SEM of two separate experiments, n = 3. * indicates significant difference (p < 0.05) against control (H_2O). *(B) Serum components decrease ATP detection.* ATP was diluted at the indicated concentrations in H_2O, HBSS+, MEM, or MEM supplemented with 10% FBS. A 30 µl aliquot was collected and added to a 5 ml test tube containing 300 µl of water. Values are the mean ± SEM of two separate experiments, n = 4. *(C) Albumin and other serum components affect ATP detection.* 100 nM ATP was prepared in MEM, MEM supplemented with 10% FBS, or MEM supplemented with 4 g/dl human albumin, and incubated at RT for 10 min. Samples were heated at 98 °C for 2 min (except non-heated controls) prior to ATP measurements.
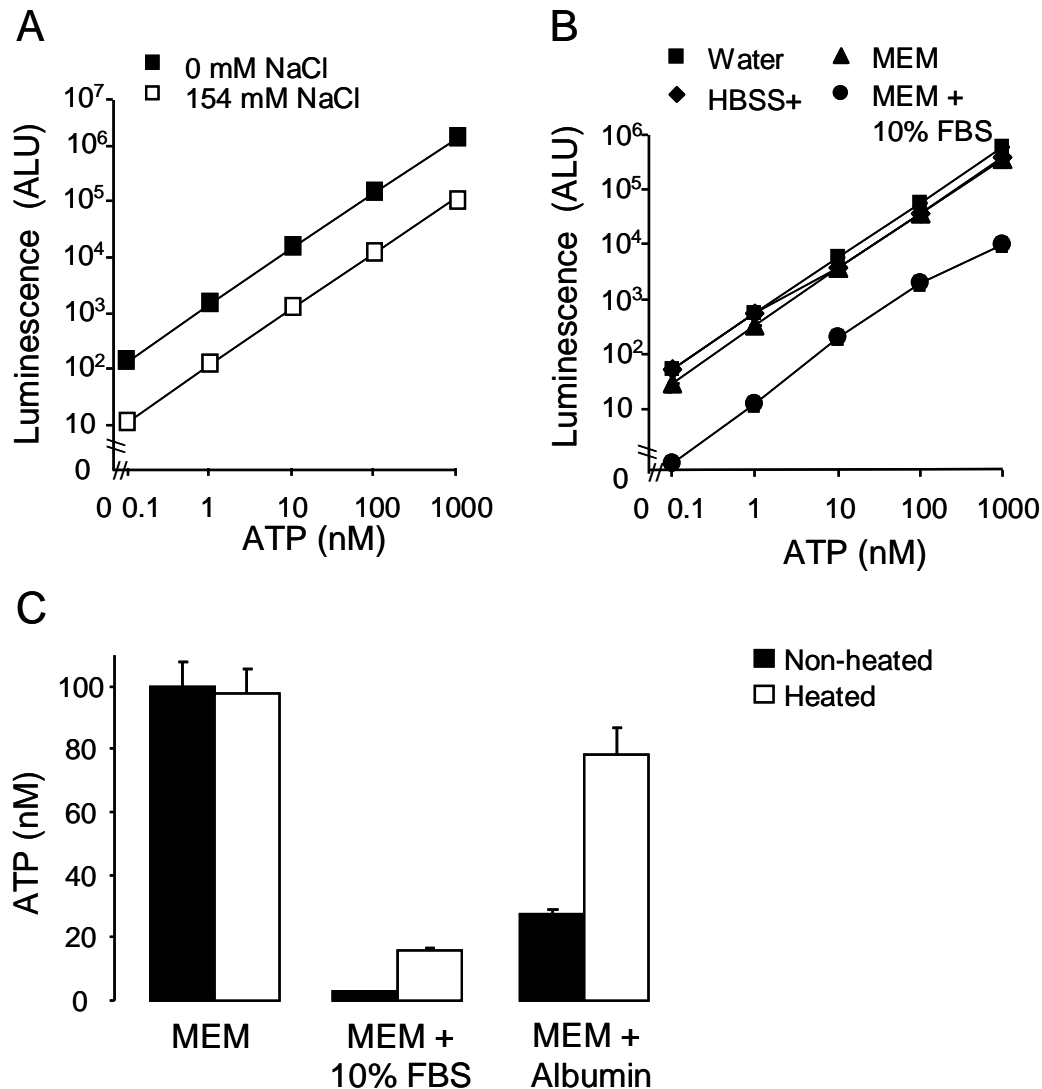
Figure 2.3. Effect of pharmacological reagents on ATP detection. *A, Luciferase activity is not affected by ATPase inhibitors, but decreases in the presence of some purinoceptor antagonists.* Calibration curves of ATP were performed in HBSS+ alone, or supplemented with 300 µM β,γ-metATP, or 30 µM ebselen. *Inset:* 100 nM ATP was prepared in HBSS+ alone, or containing 100 µM pyridoxal-phosphate-6-azophenyl-2',4'-disulfonic acid (PPADS), 100 µM reactive blue 2 (RB2), or 100 µM suramin. Values are the mean ± SEM of three separate experiments, n = 3. *B, Effect of ecto-ATPase inhibitors on ATP hydrolysis in A549 cells.* Cells were incubated for the indicated times at 37°C with 300 µl HBSS+ containing 100 nM ATP (vehicle), 100 nM ATP and 300 µM β,γ-metATP, 100 nM ATP and 30 µM ebselen, or 100 nM ATP and β,γ-metATP and ebselen. Samples were collected and luminescence recorded. Values are the mean ± SEM of two separate experiments, n = 4. *C, Measurements of extracellular ATP concentrations are underestimated in the absence of ecto-ATPase inhibitors.* A549 cells were incubated at 37°C for 5 min with 300 µl HBSS+ in the absence (control) or in the presence of 300 µM β,γ-metATP and 30 µM ebselen, and treated for 5 min with isotonic solution (Iso) or 33% hypotonic challenge (Hypo). Samples were collected and luminescence recorded. Values are the mean ± SEM of 2 separate experiments, n = 6.
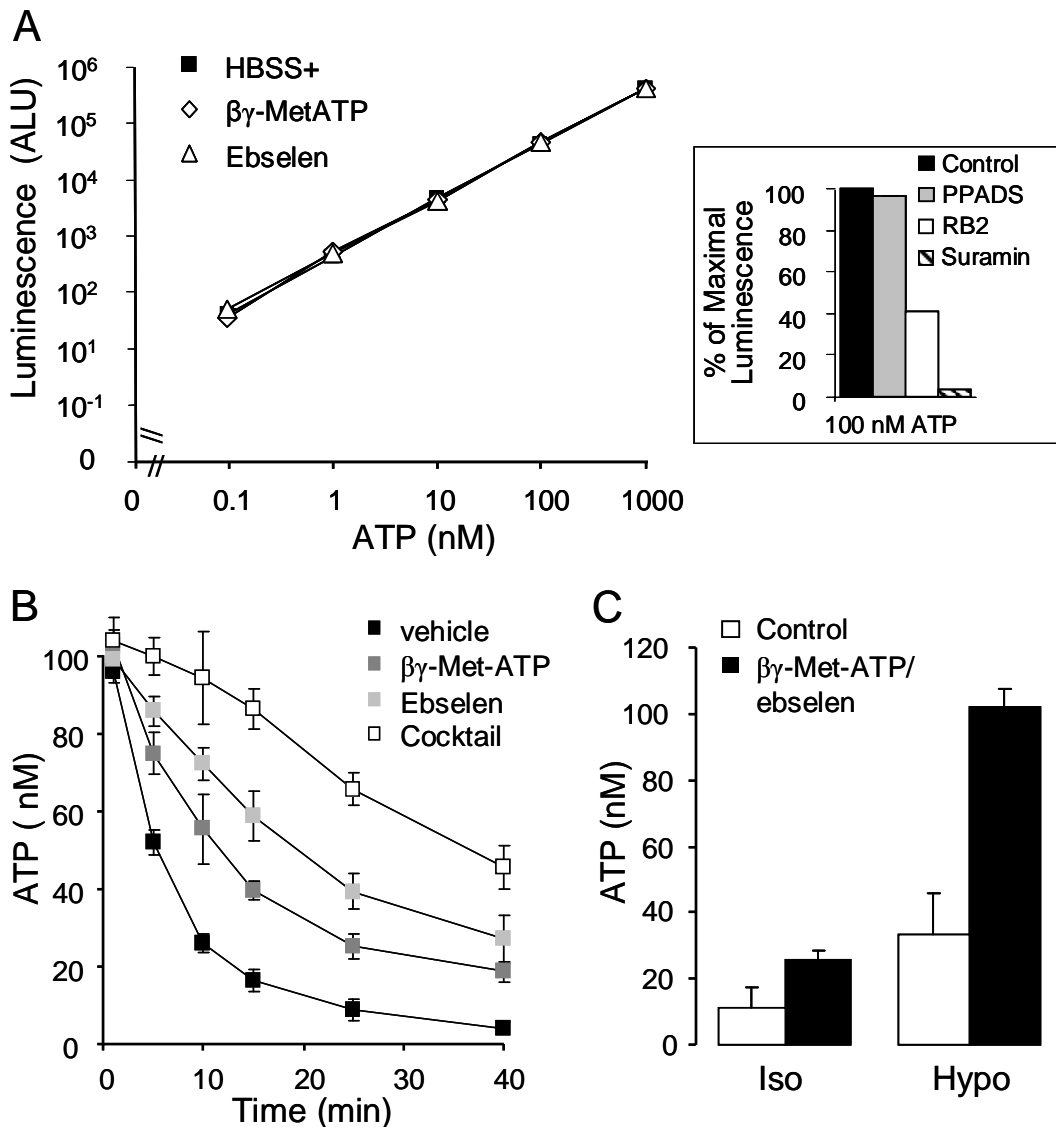
Figure 2.4. Basal ATP concentrations on the cell surface. ATP concentrations in varied luminal volumes on resting human bronchial cells were measured by off-line luminometry (as in Fig. 2.1A, grey triangle), or by real-time measurement with luciferase dissolved in bulk (as in Fig. 2.1B, open circle), and attached to the cell surface (as in Fig. 2.1 C, solid diamond). Values are mean ± SEM of 4 Transwells/subject established from 3 different subjects. No major differences in basal ATP concentrations were observed with these approaches.
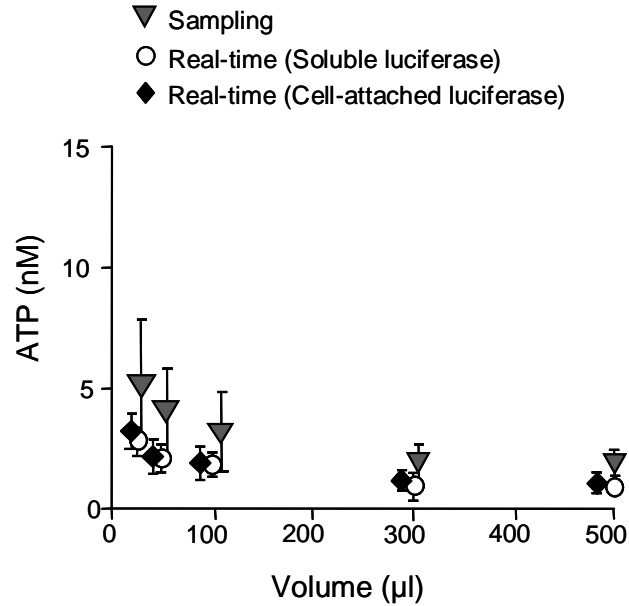
Figure 2.5. Hypotonicity-induced ATP release. Primary human bronchial epithelial cultures were exposed to luminal 33% hypotonic challenge at t = 0. ATP concentrations were measured by off-line luminometry (A), real-time luminometry with soluble luciferase (B), and real-time luminometry with cell surface-attached luciferase (C). Varied luminal volumes were applied on 12 mm Transwells, as indicated. D: Summary data illustrating peak ATP concentrations as measured by soluble luciferase (open circle) and cell-attached luciferase (solid diamond) in varied luminal volumes. In A-C, values are mean ± SEM of 3-4 Transwells/subject established from 3 different subjects. In diluted solutions (100-500 µl), ATP concentrations measured at the cell surface (C) are higher than those measured in bulk (B) or by sampling (A). However, ATP concentrations in small volumes (25-50 µl) were similar between cell-attached luciferase detection and soluble luciferase detection (D).

CHAPTER III

Thrombin promotes release of ATP from lung epithelial cells through coordinated activation of Rho- and Ca^{2+}-dependent signaling pathways

1. Introduction

Nucleotides and nucleosides within the airway surface liquid regulate mucociliary clearance activities, the primary innate defense mechanism that removes foreign particles and pathogens from the airways (7, 25, 32, 105). ATP activates the G_q-coupled $P2Y_2$ receptor ($P2Y_2$-R) present on the airway epithelial cell surface, promoting mucin secretion and ciliary beat frequency, and inhibiting the epithelial Na^+ channel (21, 32, 45, 56-57, 61, 162). In addition, ATP induces activation of CaCC, via $P2Y_2$-R and, possibly, the ATP-gated ion channel $P2X_4$-R (18, 29, 163). Adenosine, generated from the hydrolysis of ATP in airway surface liquid, activates the G_s-coupled A_{2b}-R, promoting cyclic AMP-regulated CFTR Cl^- channel activity (164) and increasing cilia beat frequency (21). In the distal lung, ATP and/or adenosine (mainly via $P2Y_2$-R and A_{2b}-R, respectively) stimulate type II cell surfactant secretion (165), regulate alveolar ion transport and fluid clearance (166), and contribute to alveolar remodeling and inflammation (167-168). While it is recognized that ATP and adenosine are naturally occurring extracellular signals that regulate key physiological components of lung function (15, 25), the origin of these signals in the extracellular milieu is poorly understood.

Lung epithelia exhibit a complex cellular composition, and thus, several mechanisms and pathways likely are involved in the release of nucleotides into the airways and bronchoalveolar space. Circumstantial evidence supports the involvement of both secretory pathways and plasma membrane channels or transporters in the cellular release of nucleotides from non-excitatory tissues. However, unambiguous evidence for either vesicular or conductive/transport mechanisms in the airways and in most non-neural tissues is lacking. Moreover, the regulatory processes involved in ATP release is largely unknown (169).

48

While most studies with airway- or alveolar-derived epithelial cells have relied on the use of mechanical and/or osmotic stimuli to promote ATP release, biochemical signals regulating ATP release are less well-defined. Recent data suggest that ATP release in hypotonically-swollen lung epithelial A549 cells depends on the availability of intracellular Ca^{2+} (106, 153, 170). However, Ca^{2+}-mobilizing agents (e.g., ionomycin, UTP) promoted only minor release of ATP from these cells, relative to hypotonic shock (106, 170), suggesting that signals in addition to Ca^{2+} are required up-stream of ATP release. This conclusion was not restricted to epithelial cells. For example, studies from our laboratory and those of others reported that Ca^{2+} is necessary but not sufficient to impart maximal ATP release from 1321N1 human astrocytoma cells (95, 156). In these cells, the serine-protease thrombin promoted robust Ca^{2+}-dependent nucleotide release via protease-activated receptor-1 (PAR1), and recent evidence indicates that Rho signaling was involved in this response (171).

Since thrombin receptors are expressed in lung epithelial cells (172), we reasoned that PAR activation might physiologically mediate regulated ATP release from these cells. In the present study, we demonstrated that thrombin promotes robust release of ATP from A549 lung epithelial cells via PAR3 activation. We also investigated signaling mechanisms and pathways involved in thrombin-evoked ATP release from A549 cells as well as from physiologically relevant primary cultures of WD-HBE cells.

2. Methods

Reagents- Human α-thrombin was purchased from Enzyme Research Laboratories (South Bend, IN). 2-Phenyl-1,2-benzisoselenazol-3(2H)-one (ebselen), β,γ-methylene ATP (β,γ-metATP), arachidonylethanolamide (anandamide), flufenamic acid, carbenoxolone, and luciferase from *Photinus pyralis* were obtained from Sigma (St. Louis, MO). Fura-2

acetoxymethyl-ester (Fura 2-AM), 1,2-bis(o-aminophenoxy)ethane-N,N,N',N'-tetraacetic acid-acetoxymethyl-ester (BAPTA-AM) and thapsigargin were purchased from Molecular Probes (Eugene, OR). Luciferin was obtained from BD PharMingen (Franklin Lakes, NJ). The Rho Activation Assay Biochem Kit was purchased from Cytoskeleton (Denver, CO). Propidium iodide was purchased from Invitrogen Corp. Carlsbad, CA.The PAR1-activating peptide TFLLRNPNDK-amide and the PAR4-activating peptide AYPGKF-amide, respectively (hereafter referred to as PAR1-AP and PAR4-AP, respectively) were synthesized at the UNC Microprotein Sequencing and Peptide Synthesis Facility. *myo-*[^{3}H]Inositol (20 Ci/mmol) was obtained from Amersham Pharmacia Biotech (Piscataway, NJ). Other chemicals were from sources reported previously (25, 95).

Cell culture- A549 lung epithelial cells were obtained from the UNC Tissue Culture Facility and grown to confluence in Dulbecco's modified Eagle's medium (DMEM) supplemented with 10 % calf serum (HyClone, Ogden, UT), 60 µg/ml (100 IU/ml) penicillin and 100 µg/ml streptomycin (Gibco). Cells were grown on 35-mm plastic dishes for real-time ATP measurements and on 24-well plastic plates for off-line ATP assays, cyclic AMP formation, and inositol phosphate measurements. RhoA pulldown assays and confocal microscopy studies were performed with cells grown on 100-mm Falcon plastic dishes and 8-well Lab-Tek II glass chamber slides (Nalge Nunc Int., Naperville, IL), respectively. Since a gradual decline in thrombin-promoted responses was noted with passages, A549 cells were used within passages 3 to 14. Polarized cultures of WD-HBE cells (provided by the UNC Cystic Fibrosis Center Center Tissue Culture Core Lab) were grown on 12-mm Transwell supports (Costar) and maintained at an air–liquid interface that mimics the *in vivo* environment of the airway epithelia, as previously described (25-26).

Measurement of ATP release and hydrolysis- A549 ells were washed twice with HBSS supplemented with 1.6 mM $CaCl_2$, 1.6 mM $MgCl_2$, and 25 mM HEPES pH 7.4 (HBSS+), and incubated for 1 hour at 37˚C in HBSS+. For real-time ATP measurements in thin film (**Fig. 3.1B**), cultures were transferred to a Turner TD-20/20 luminometer (Turner Biosystems, Sunnyvale, CA). Luciferase (15-30 x 10^6 light units mg^{-1}) and luciferin (60 µM) were added and luminescence monitored, as previously described (26). Off-line ATP measurements were performed via a LB953 AutoLumat luminometer (Berthold), as previously described (173). Calibration curves using known concentrations of ATP were generated at the end of each experiment. None of the reagents used during ATP release measurements interfered with the luciferase reaction. To assess ATP hydrolysis, 100 nM ATP was added to cells in the absence or presence of 30 µM ebselen and 300 µM βγ-metATP, two previously characterized ATP hydrolysis inhibitors (26, 173-175). Samples were collected at various times, and the resulting ATP concentration measured as indicated above. WD-HBE cells were rinsed and incubated with 300 µl mucosal and 500 µl basolateral HBSS, and ATP release was measured off-line, as described above.

Inositol phosphate formation- A549 cells were labeled overnight in inositol-free DMEM containing 2 µCi/ml *myo*-[³H]inositol (S.A., 20 Ci/mmol). WD-HBE cells were labeled for three days in 500 µl basolateral and 100 µl mucosal medium containing 10 µCi/ml *myo*-[³H]inositol. At the time of assay, 10 mM LiCl was added to the cells for 10 min, followed by 20 min incubation in the presence of drugs. Incubations were terminated by the addition of 0.75 ml 50 mM formic acid and 0.25 ml 150 mM ammonium hydroxide. [³H]Inositol phosphates were separated on Dowex anion exchange columns and quantified as previously described (157).

Calcium mobilization- A549 cells grown on glass coverslips were loaded with Fura 2-AM for 30 min. Cells were washed, mounted on a platform of a fluorometer-coupled microscope, and fluorescence from 30–40 cells was acquired alternately at 340 and 380 nm. Other details were as previously described (26).

Cyclic AMP quantification- Cells were rinsed, pre-incubated for 10 min in HBSS containing 200 µM 3-isobutyl-1-methylxanthine (IBMX), and subsequently challenged for an additional 10 min with 30 µM forskolin and the indicated concentration of thrombin. The conversion of ATP to cyclic AMP was quantified by HPLC analysis of $1,N^6$-ethenoadenine derivatives, as previously described (25).

RT-PCR analysis- Total RNA was prepared using the RNeasy Mini Kit (Qiagen, Inc., Valencia, CA) and reverse-transcribed using SuperScript III reverse transcriptase (RT; Invitrogen Corporation, Carlsbad, CA). RT-PCR was performed using the following cycling conditions: 4 min/94°C, 1 min/72°C, 45 s/94°C, 1 min/55°C, and 1 min/72°C; 36 cycles. PAR1 (GenBank M62424), PAR2 (GenBank U34038), PAR3 (GenBank U92972), PAR4 (GenBank AF080214) primers were 5'-CAGTTTGGGTCTGAATTGTGTCG-3', 5'-TGCACGAGCTTATGCTGCTGAC-3', 5'-TGGATGAGTTTTCTGCATCTGTCC-3', 5'-CGTGATGTTCAGGGCAGGAATG-3', 5'-TCCCCTTTTCTGCCTTGGAAG-3', 5'-AAACTGTTGCCCACACCAGTCCAC-3', 5'-AACCTCTATGGTGCCTACGTGC-3', 5'-CCAAGCCCAGCTAATTTTTG-3', respectively. Amplified products were sequenced at the UNC Genome Analysis Facility.

Semi-quantitative PCR was performed in a Lightcycler PCR machine® thermal cycler (10 min/95ºC; 5 s/55ºC, 8 s/72ºC; 45 cycles), using the Lightcycler Fast start DNA master SYBER Green I kit (Roche Applied Science, Indianapolis, IN). Melting curve analysis was

performed by heating the reactions from 65ºC to 95ºC at 0.11ºC intervals, and a fluorescence threshold (Ct) was determined using the LightCycler Software (version 4.0). Ct values were adjusted for differences in amplification efficiencies. Glyceraldehyde 3-phosphate dehydrogenase (GAPDH) served as a housekeeping gene for normalization between samples, and was included in each cycling run. The melting temperature of the PCR product for each reaction was monitored to ensure that only a single product of the correct size was amplified. Primer pairs for PAR3 were as above. Primers for GAPDH were 5'-GAAGTTGAAGGTCGGAGTCA-3', and 5'-GATCTCGCTCCTGGAAGATG-3'. The average crossover point was determined using the Roche software. The relative expression levels of PAR3 were calculated from the efficiency of the PCR reaction and the crossing point, and normalized to the expression of the reference gene, as previously described (94).

Overexpression of PAR3 and dominant negative mutants of RhoGEF and RhoA- A549 cells were transfected with pcDNA3.1 empty vector, pmaxFP-Green-C GFP-expressing vector, or vector containing the desired insert, using FuGENE HD (Roche). pcDNA3.1 vectors expressing p115RGS and RhoA(T19N), and pBJ1 vector expressing HA-tagged PAR3, were kindly provided by Dr. T. K. Harden (176-177) and Dr. S. R. Coughlin (178), respectively. A transfection efficiency of 70-80% was achieved, as assessed with the GFP-expressing pmaxFP-Green-C vector.

Small interference RNA (siRNA)- Oligonucleotides targeting human PAR3 and scrambled control (5'-GGCATTCTTTGGATTCTTA-3' and 5'-GTGAGTTCGTTCTCTATTA-3', respectively) were purchased from Dharmacon, Inc. A549 cells were transfected with 1 µg oligonucleotide, using the Amaxa Nucleofector Device™ and Cell Line Nucleofector® Kit T (Amaxa Biosystems, Gaithersburg, MD), following the

manufacturer's instructions. Transfected cells were grown in serum-supplemented DMEM for at least 24 h, prior to assays.

Site-directed mutagenesis of PAR3- The QuikChange II XL® Site-directed Mutagenesis Kit (Stratagene, La Jolla, CA) was used to generate a PAR3 mutant isoform (PAR3$^{\otimes}$) resistant to siRNA oligonucleotide knockdown. The sequence 5'-GGCATTCTTTGGATTCTTA-3' was mutated to 5'-GGCATTTTTTGGGTTCTTA-3'. Nucleotide changes and sequence integrity of the expression vector were confirmed by sequencing. A549 cells were co-transfected with a pBJ1 expression vector bearing PAR3$^{\otimes}$ (100 ng) and the indicated siRNA oligonucleotide, using the Amaxa system, as described above.

RhoA pulldown assay- Measurements of GTP-bound RhoA were performed using the Rho Activation Assay Biochem Kit (Rhoketin assay), according to the manufacturer's instructions. Cell lysates and pulldowns were resolved by sodium dodecyl sulfate-polyacrylamide gel electrophoresis (SDS-PAGE) and transferred to polyvinyldifluoride membranes. RhoA was detected by Western blot, using monoclonal anti-RhoA antibody (1:500) provided by the manufacturer and IRdye®800 conjugated affinity purified goat anti-mouse IgG (Rockland Immunochemicals, Philadelphia, PA). Immunoblots were revealed and quantified using the Odissey® Infrared Imaging System (LI-COR Biosciences, Lincoln, NE).

MLC phosphorylation- Proteins were resolved by SDS-PAGE and duplicated membranes were separately blotted with anti-phospho-MLC(Ser19) antibody (1:500) or anti-MLC (1:1000) antibodies (Cell Signaling Technology Inc. Danvers, MA) by goat anti-rabbit Alexa Fluor®680 secondary antibody (Invitrogen, Eugene, Oregon). Blots were quantified as indicated above.

Uptake of propidium iodide- Cells were rinsed and challenged with agonist for 5 min, in the presence of 20 µM propidium iodide. At the end of the incubation, the bathing solution was replaced with HBSS+ containing 4% paraformaldehyde. Confocal images of nuclear staining and differential interference contrast (DIC) were acquired in a Leica SP5 confocal microscope, using a 561 nm laser and a 20x Leica lens (Leica, Germany). The number of nuclei stained with propidium iodide was calculated using Adobe Photoshop.

Data Analysis- Differences between means were determined by unpaired Student's t-test and were considered significant when $p < 0.05$.

3. Results

Thrombin promotes ATP release from A549 cells. The paucity of pharmacological approaches to trigger regulated nucleotide release poses a problem for studying the mechanism of ATP release from lung epithelial cells. Quantification of ATP release is further complicated by the presence of cell surface ecto-ATPases that rapidly hydrolyze released ATP. By implementing a protocol that quantifies ATP release in real-time in a thin film near the cell surface (26), we investigated the action of GPCR agonists on ATP release from lung epithelial cells.

Our initial screening revealed that the serine protease thrombin promoted robust ATP release from lung carcinoma A549 cells (**Fig. 3.1**). However, thrombin-evoked ATP release was evident only when ATP hydrolysis was inhibited. Specifically, in the absence of drugs, ATP levels on resting cells stabilized around ~9 ± 2 nM and reached a level of 12 ± 4 nM after the addition of thrombin (30 nM, 10 min). In contrast, in the presence of ecto-ATPase inhibitors [30 µM ebselen and 300 µM β,γ-metATP (26)], extracellular ATP levels on resting cells increased modestly to 22 ± 7 nM in 10 min, likely reflecting constitutive nucleotide

release (26, 156, 173). Addition of thrombin in the presence of ebselen and β,γ-metATP resulted in robust increase of extracellular ATP, which reached a concentration of 113 ± 15 nM after 10 min (**Fig. 3.1A**). Based on these results, subsequent measurements of agonist-promoted ATP release were performed in the presence of 30 µM ebselen and 300 µM β,γ-metATP.

PAR3 mediates thrombin-promoted ATP release in A549 cells. Thrombin and other serine-proteases activate a family of four G-protein-coupled receptors, referred as to protease-activated receptors (PAR1-PAR4). Thrombin activates PAR1, PAR3, and PAR4. The remaining member of the PAR family, PAR2, is activated by trysin and other proteases but not by thrombin [reviewed in (179-180)]. To gain an insight into the PAR subtype(s) present in A549 cells, RT-PCR studies were conducted. **Figure 3.1B** illustrates that PAR3 but not PAR1, PAR2, or PAR4 transcripts could be amplified from A549 cells.

PARs are activated by proteolytic cleavage of the amino-terminal exodomain of the receptor. This cleavage generates a new amino terminus that functions as a tethered ligand, which binds to the body of the receptor and promotes signaling (179-180). Synthetic peptides representing the newly formed amino-terminus selectively activate PAR1, PAR2, and PAR4, independent of receptor cleavage. Human PAR3 is not activated by PAR3-mimicking peptides, which suggests that PAR3 activation requires proteolytic cleavage at the amino terminal exodomain (178). **Figure 3.1C** shows that thrombin, but not PAR1- and PAR4-activating peptides (PAR1-AP and PAR4-AP, respectively), elicited ATP release in a concentration-dependent manner. Enhanced ATP release was readily observed in response to 1 nM thrombin and was maximal with 30 nM thrombin ($EC_{50} = 7$ nM).

Since activation of thrombin receptors results in phospholipase C activation (178, 181-182), we investigated the effect of thrombin and PAR-APs on inositol phosphate formation, using [^{3}H]inositol-labeled A549 cells. **Figure 3.1D** shows that thrombin promoted [^{3}H]inositol phosphate formation with a potency ($EC_{50} = 6.3$ nM) similar to that observed for ATP release. PAR1-AP or PAR4-AP promoted negligible [^{3}H]inositol phosphate formation (**Fig. 3.1D**). Altogether, the data in **Figure 3.1** suggest that PAR3 in the only thrombin receptor present in A549 cells.

To more definitively assess the involvement of PAR3 in thrombin-elicited ATP release, the effect of PAR3 overexpression/suppression was examined. Overexpression of PAR3 conferred enhanced thrombin-elicited ATP release and inositol phosphate formation to A549 cells, relative to vector-transfected cells (**Fig. 3.2**). Gain in thrombin-promoted ATP release was noted in cells transfected with as low as 10 ng PAR3 cDNA/well and was robust with 100-300 ng cDNA/well (**Fig. 3.2A**). The potency of thrombin in eliciting ATP release and inositol phosphate formation increased by ~5 fold ($EC_{50} = 1.1$ nM) and ~7 fold ($EC50 = 1.2$ nM), respectively, in cells transfected with 100 ng PAR3 cDNA, relative to vector-transfected cells (**Fig. 3.2B and C**).

The contribution of PAR3 to ATP release from A549 cells was directly examined by targeting the endogenous PAR3 via siRNA. Transfection of A549 cells with a PAR3-selective (but not its scramble) siRNA oligonucleotide resulted in ~60% decrease of PAR3 transcripts, as judged by quantitative PCR (**Fig. 3.3A**). This manipulation also resulted in ~50% inhibition of thrombin-evoked inositol phosphate formation (**Fig. 3.3B**) and ATP release (**Fig. 3.3C**). The PAR3 siRNA approach had no effect on GPCR (other than PAR3)-mediated signaling, since UTP-evoked inositol phosphate formation was unaffected in PAR3

siRNA-transfected cells (vehicle, 1155 ± 178 cpm; UTP 5430 ± 177 cpm; PAR siRNA-transfected cells: vehicle, 1195 ± 164, UTP 5869 ± 257; mean $\pm$ SD, n = 4). To verify that the siRNA approach did not knock down downstream effectors of PAR3, cells were co-transfected with PAR3$^{\otimes}$, a PAR3 cDNA mutant resistant to the PAR3 siRNA oligonucleotide. PAR3$^{\otimes}$-mediated ATP release was not affected by PAR3 siRNA (**Fig. 3.3D**). Altogether, these results indicate that PAR3 is the major contributor to thrombin-evoked ATP release in A549 cells.

Ca^{2+} is necessary but not sufficient for agonist-evoked ATP release. Cytosolic Ca^{2+} is an important regulator of ATP release in many cells. For example, in excitatory tissues, ATP is released from ATP storage granules via Ca^{2+}-regulated exocytosis (157). Ca^{2+}-dependent ATP release has been also reported in cells lacking specialized ATP storage granules (71, 99, 106, 153, 170). Pre-incubation of A549 cells with 10 µM BAPTA-AM or 1 µM thapsigargin resulted in major inhibition of thrombin-promoted ATP release (**Fig. 3.4A**), suggesting that Ca^{2+} is required for ATP release from thrombin-stimulated A549 cells.

Since thrombin-elicited ATP release requires a Ca^{2+}-dependent step, we asked whether Ca^{2+}-mobilizing receptors other than PARs (e.g., P2Y$_2$-R) promote ATP release from these cells. Incubation of A549 cells with 100 µM UTP resulted in enhanced extracellular ATP concentrations, but the effect of UTP on ATP levels was modest, relative to thrombin (**Fig. 3.4B**). To investigate whether differences in UTP- vs. thrombin-elicited second messenger signaling have accounted for the observed differences in agonist-promoted ATP release, UTP-promoted phosphoinositide breakdown was examined. UTP promoted inositol phosphate formation responses that were greater than thrombin responses. Nucleotide-evoked inositol phosphate formation, with potency order UTP = ATP >> ADP, UDP, was consistent

58

with P2Y$_2$ receptor expression (**Fig. 3.4C**). RT-PCR analysis confirmed the expression of P2Y$_2$ receptor transcripts in A549 cells (not shown). Importantly, UTP promoted Ca^{2+} mobilization responses in Fura 2-loaded A549 cells that were similar or greater in magnitude than thrombin (**Fig. 3.4D**). Altogether, the results suggest that receptor-promoted Gq/phospholipase-β activation/Ca^{2+} mobilization alone was not sufficient to elicit ATP release from A549 cells.

Thrombin-induced ATP release is independent of Gi activation. It has been established that PAR1 interacts with G$_q$, G$_i$ and G$_{12/13}$ families of G proteins (179, 183). Unlike PAR1, the G protein coupling of PAR3 is poorly defined. The fact that thrombin promotes phosphoinositide breakdown in a PAR3-dependent manner in A549 cells (**Figs. 3.2 and 3.3**), as well as in PAR3-transfected COS-7 cells (178), suggests that PAR3 couples to G$_q$. However, as mentioned above, signaling in addition to G$_q$/phospholipase C/Ca^{2+} is likely involved in thrombin-evoked ATP release from A549 cells. To assess G$_i$ activation in thrombin-stimulated A549 cells, thrombin-promoted inhibition of cyclic AMP formation was examined. Addition of 30 µM forskolin (in the presence of the phosphodiesterase inhibitor IBMX) markedly enhanced cyclic AMP formation in A549 cells (control, 8 ± 2 pmoles/well; forskolin, 103 ± 6 pmoles/well), which was inhibited (27% maximal inhibition) by thrombin, in a dose-dependent manner (**Fig. 3.5A**). Pertussis toxin, which ADP-ribosylates and inhibits G$_{\alpha i}$ proteins, reversed the inhibitory effect of thrombin on forskolin-elicited cyclic AMP formation (**Fig. 3.5A**). Pertussis toxin failed to inhibit thrombin-promoted ATP release (**Fig. 3.5B**). Thus, while these results illustrated the presence of a G$_i$-coupled thrombin receptor in A549 cells, ATP release was not regulated by G$_i$ activation. Consistent with these results, pre-incubation of cells with the PI 3-kinase inhibitor wortmannin (200 nM/15 min) had no

effect on thrombin-elicited ATP release (**Fig. 3.5B**). Thus, PI 3-kinase, known to be activated by β/γ subunits of G_i proteins downstream of PAR activation (184), was not involved in thrombin-promoted ATP release in A549 cells.

Thrombin promotes ATP release via $G_{12/13}$-mediated RhoGEF/RhoA activation. Rho GTPases are well-known downstream effectors of $G_{12/13}$, via $G_{\alpha 12/13}$ activation of guanine nucleotide exchange factors (GEF) of Rho (RhoGEF) [reviewed in (185)]. Addition of thrombin to A549 cells caused a rapid and robust activation of RhoA, measured by the RhoA pulldown assay. RhoA activation was observed as early as 30 s post-thrombin addition and was robust after 90 s (**Fig. 3.6A**). Thrombin-elicited RhoA activation increased considerably in cells transfected with PAR3 (**Fig. 3.6A**) and was reduced by PAR3 siRNA (**Fig. 3.6B**).

To examine the possibility that PAR3-elicited ATP release involved activation of $G_{12/13}$/RhoGEF/Rho, A549 cells were transfected with dominant negative mutants of RhoGEF and RhoA. Transfection of A549 cells with p115RGS, a $G_{12/13}$-inhibitory protein derived from the RGS domain of p115-RhoGEF (177), impaired thrombin-promoted ATP release (**Fig. 3.7A**). Similarly, transfection of cells with the RhoA mutant RhoA(T19N), which tightly binds to RhoGEF but does not promote downstream effector activation (186), markedly inhibited thrombin-elicited ATP release (**Fig. 3.7A**). Control experiments indicated that thrombin-promoted inositol phosphate formation was not significantly affected by p115RGS or RhoA(T19N) transfections (**Table 3.1**).

ROCKs are important effectors of Rho (187). Pre-incubation of A549 cells with the ROCK inhibitor Y27632 resulted in dose-dependent inhibition of thrombin-promoted ATP release, with maximal inhibition observed with 1 μM Y27632 (**Fig. 3.7B and D**). H1152, a more potent and selective ROCK inhibitor than Y27632 (188), also reduced ATP release in

response to thrombin (**Fig. 3.7B**). ROCK activation is known to promote MLC phosphorylation, e.g., by phosphorylating and inactivating MLC phosphatase (189). Consistent with the possibility that MLC is an effector of ROCK upstream of ATP release, thrombin-promoted MLC phosphorylation was observed and was inhibited by 100 nM H1152 (**Fig. 3.7C**). Further, ML-7 (1 µM), an inhibitor of the Ca^{2+}/calmodulin-dependent MLCK (190), reduced MLC phosphorylation (**Fig. 3.7C**) and impaired ATP release (**Fig. 3.7D**) in thrombin-stimulated A549 cells. None of these inhibitors affected the ability of thrombin to promote inositol phosphate formation (**Table 3.1**).

Altogether, the data indicate that Rho activation is necessary for PAR3-promoted ATP release in A549 cells. The data also suggest that Rho actions are mediated, at least in part, by ROCK activation, likely facilitating MLC phosphorylation by MLCK.

ATP release requires the coordinated action of Ca^{2+}- and Rho-dependent pathways. Since P2Y$_2$-R stimulation has been linked to RhoA activation in endothelial cells (191), we asked whether UTP promotes RhoA activation in A549 cells and, if so, whether such activation differed from that of thrombin. **Figure 3.8A** shows that incubation of A549 cells with 100 µM UTP resulted in RhoA activation that was similar in magnitude to thrombin. However, unlike the rapid effect of thrombin, UTP-promoted RhoA activation was observed only after 15 min. Thus, while thrombin promoted RhoA activation and Ca^{2+} mobilization (**Figs. 3.4, 3.6, and 3.8**) with overlapping time-frames (30-90 s), UTP-induced RhoA activation was dissociated in time from Ca^{2+} responses (**Fig. 3.4 and 3.8**).

We hypothesized that Rho activation and Ca^{2+} mobilization must be temporally coordinated to promote ATP release. To assess this hypothesis, cells were pre-incubated for 15 min with 100 µM UTP (to achieve robust RhoA activation), followed by a 5 min

61

challenge with the Ca^{2+} ionophore ionomycin. As a control, cells were pre-incubated with vehicle. **Figure 3.8B** illustrates that addition of ionomycin (either alone or in combination with UTP) to untreated cells resulted in negligible ATP release. In contrast, addition of ionomycin to cells that were pre-incubated for 15 min with UTP resulted in robust release of ATP (**Fig. 3.8B**). The simplest interpretation of these results is that maximal ATP release requires synchronized activation of Rho and Ca^{2+} signaling.

Thrombin promotes opening of connexin-like hemichannels in a Ca^{2+} and ROCK-dependent manner. Connexin and pannexin hemichannels have been proposed as a electrodiffusive pathway for the release of ATP under various experimental conditions (192-193). Connexin (but not pannexin) hemichannels close at millimolar extracellular Ca^{2+} ($[Ca^{2+}]_{ex}$) and open when $[Ca^{2+}]_{ex}$ is lowered. Exposure to lowered extracellular divalent ion conditions is a well-known procedure to potentiate or trigger the opening of connexin hemichannels, leading to ATP release (194-195). In addition, both pannexins and connexins have been reported to release ATP at physiologically relevant $[Ca^{2+}]_{ex}$ (192-193).

While investigating the role of calcium in PAR-stimulated responses, we observed that removal of $[Ca^{2+}]_{ex}$ resulted in enhanced ATP release from resting and thrombin-stimulated A549 cells (**Fig. 3.9A**), suggesting that connexin hemichannels are present on the A549 cell surface. This observation led us to investigate the possibility that hemichannels were involved in the release of ATP from thrombin-stimulated A549 cells, under normal $[Ca^{2+}]_{ex}$ conditions. **Figure 3.9B** illustrates that thrombin-induced ATP release, assessed in the presence of 1.6 mM $[Ca^{2+}]_{ex}$, was markedly inhibited by non selective-connexin/pannexin inhibitors (100 µM anandamide, 100 µM flufenamic acid, and 10 µM carbenoxolone).

Control experiments indicated that none of the hemichannel inhibitors affected thrombin-evoked inositol phosphate formation (**Table 3.1**).

To further assess the possibility that thrombin promoted connexin/pannexin hemichannel opening, the uptake of the hemichannel-permeable reporter dye propidium iodide was investigated. Propidium iodide displays low intrinsic fluorescence, but its fluorescence increases 20- to 30- fold upon binding to nucleic acids. Under resting conditions, a small population (<4%) of A549 cell nuclei were labeled with propidium iodide, but dye uptake increased markedly (3-4 fold) following a 5 min incubation of the cells with 30 nM thrombin (**Fig. 3.9C**). Unlike propidium iodide, which has a relatively small molecular weight (668.4 Da), the endocytosis marker fluorescein Dextran (3000-10000 Da) was not taken up by thrombin-stimulated A549 cells (not shown). Consistent with connexin/pannexin hemichannel involvement in agonist-promoted dye uptake, carbenoxolone inhibited the effect of thrombin on nucleus-associated fluorescence (**Fig. 3.9D**). Particularly relevant to our present study was the observation that thrombin-induced dye uptake was markedly inhibited by ROCK (Y26632 and H1152) or MLCK inhibitors (ML-7), and BAPTA-AM (**Fig. 3.9D**). Unlike thrombin, UTP (100 µM) and ATP (1 mM) promoted no changes in dye uptake (**Fig. 3.9D**), indicating that $P2Y_2$-R activation did not suffice to induce hemichannel opening. Moreover, lack of effect of 1 mM ATP on propidium iodide uptake argues against the possibility that the pore forming $P2X_7$-R (196) is expressed in these cells. Altogether, the data suggest that thrombin promoted Ca^{2+}- and Rho-regulated ATP release via connexin/pannexin hemichannels in A549 cells.

Thrombin promotes mucosal ATP release from primary cultures of WD-HBE cells. Having identified mechanistic components involved in ATP release in A549 cells, we asked

whether observations made with these cells apply to physiologically relevant airway epithelia. Therefore, we examined the effect of thrombin on ATP release from polarized cultures of WD-HBE cells. Addition of 30 nM thrombin to the mucosal compartment had no effect on ATP release (not shown). In contrast, thrombin added to the basolateral compartment of WD-HBE cultures resulted in a robust release of ATP through the apical (but not basolateral) surface (**Fig. 3.10A**). The data are in agreement with previous observations indicating that (i) ATP release occurs through elements that segregate to the apical domain after cell polarization (25, 94), and (ii) PARs are expressed at the basolateral membrane of polarized lung epithelial cells (33, 197-198). The identity of the PAR evoking ATP release in WD-HBE cells remains to be elucidated. As in A549 cells, the effect of thrombin on ATP release was markedly reduced in WD-HBE cells that were pre-incubated with the ROCK inhibitor H1152, the MLCK inhibitor ML-7, or the connexin/pannexin hemichannel blocker carbenoxolone (**Fig. 3.10B**). Unlike thrombin, mucosal UTP caused no ATP release from WD-HBE cells (**Fig. 3.10A**), despite the well-established presence of $P2Y_2$ receptors on these cells [(10, 199) and see **Fig. 3.10C**].

Regardless the lack of effect of UTP on ATP release (**Fig. 3.10A**), the presence of phospholipase C-activating $P2Y_2$ receptors on the apical surface of WD-HBE cells (10, 199) suggests that ATP released onto the thin liquid film covering the mucosal airway epithelial cell surface contributed, at least in part, to PAR-evoked signaling. To test this possibility, the effect of the ATPase enzyme apyrase on thrombin-elicited [^{3}H]inositol phosphate formation was assessed. To minimize dilution of released ATP, the mucosal surface liquid volume was reduced to 100 µl/well (83 µl/cm^2 culture). Inclusion of 5 U apyrase in this thin airway surface liquid resulted in small (21%) but reproducible decrease of [^{3}H]inositol phosphate

formation in response to basolateral addition of thrombin (**Fig. 3.10C**). As expected, (mucosal) UTP promoted [^{3}H]inositol phosphate formation, which was nearly abolished in the presence of apyrase (**Fig. 3.10C**)

4. Discussion

By examining the effects of PAR and P2Y-R agonists, we demonstrated that Rho/Rho kinases, in concert with cytosolic Ca^{2+}, are important regulators of ATP release. We also demonstrated that connexin/pannexin hemichannels are likely effectors of Rho/ROCK and Ca^{2+} signaling pathways that mediate ATP release from lung epithelial cells. An additional novel finding was that thrombin actions on A549 cells are mediated by PAR3, a poorly characterized thrombin receptor subtype.

Our data, indicating that BAPTA and thapsigargin impaired ATP release from thrombin-stimulated A549 cells, are consistent with the notion that Ca^{2+} mobilization is necessary for ATP release. However, ATP release in response to Ca^{2+}-mobilizing agents (e.g., UTP, ionomycin) represented a minor fraction relative to that observed with thrombin stimulation (**Fig. 3.4**). Thrombin-promoted ATP release decreased in cells transfected with dominant negative mutants of p115-RhoGEF and RhoA as well as in cells exposed to ROCK inhibitors (**Fig. 3.7**). Thus, Rho GTPases are key regulators of PAR-elicited ATP release. Importantly, Rho activation itself promoted no ATP release when temporarily dissociated from Ca^{2+} mobilization. Therefore, Rho signaling is an obligatory partner of Ca^{2+} mobilization upstream of ATP release in A549 cells.

Our present results are also consistent with previous studies implicating Rho as modulator of ATP release. Ito and coworkers reported that Y26632 impaired lysophosphatidic acid (LPA)- and/or hypotonic challenge-promoted ATP release in human umbilical vein and

bovine aortic endothelial cells (200-201). In a recent report, Blum *et al.* reported that inactivation of RhoGTPases with Clostridium botulinum C3 exoenzyme impaired thrombin- and LPA-promoted Ca^{2+}-dependent ATP release from 1321N1 astrocytoma cells (171). However, Y26632 and ML-7 had no effect on ATP release in these cells, suggesting that Rho regulation of ATP release in 1321N1 astrocytoma cells occurred independently of ROCK and MLC phosphorylation. Unlike 1321N1 cells, Y26632, H1152, and ML-7 impaired thrombin-evoked ATP release in A549 cells. While Rho activation may utilize downstream effectors in addition to ROCK (202), our results suggest that ROCK is an important regulator of ATP release from A549 cells. Moreover, our data suggest that Ca^{2+}- and Rho/ROCK-dependent ATP release from thrombin-stimulated A549 cells occurs via connexin or pannexin hemichannels, a pathway that appeared not competent for ATP release in 1321N1 astrocytoma cells (171). Specifically, in A549 cells: (i) thrombin-promoted ATP release was inhibited by connexin/pannexin inhibitors, (ii) thrombin promoted the uptake of propidium iodide, an indicator of non-selective pore opening, which was inhibited by connexin/pannexin inhibitors, and (iii) thrombin-elicited dye uptake was inhibited by ROCK and MLCK inhibitors and by BAPTA-AM.

Our study did not address the identity of the putative hemichannel involved in ATP release. Based on the effect of $[Ca^{2+}]_{ex}$, connexin hemichannels likely are expressed at the plasma membrane of A549 cells. However, whether a connexin or pannexin hemichannel was responsible for the release of ATP in physiologically relevant $[Ca^{2+}]_{ex}$, as well as the mechanism potentially involved in hemichannel activation, remain to be investigated.

A surprising finding in our study was that thrombin actions in A549 cells could not be associated with PAR1. While we have recently reported that the PAR1 peptide

TFLLRNPNDK promoted nucleotide release and inositol phosphate formation in 1321N1 human astrocytoma cells (95), TFLLRNPNDK failed to promote these responses in A549 cells. Moreover, A549 cells used in the current study do not express PAR1 transcripts (**Fig. 3.1**). Our data also suggest that PAR4 is not expressed in A549 cells (**Fig. 3.1**). The finding that thrombin actions on A549 cells were not mediated by PAR1 or PAR4 was striking since the ability of PAR3 (the other member of the thrombin receptor family) to generate intracellular signaling has been questioned (178). The finding that murine PAR3 functions as a cofactor for proteolytic activation of PAR4 in platelets has reinforced the assumption that PAR3 does not signal by itself. However, this observation may also reflect cell type and species specific functions for distinct PARs [reviewed in (183)]. Expression of human PAR3 (but not empty vector) in COS-7 cells resulted in thrombin-evoked inositol phosphate formation (178), likely via G_q-mediated phospholipase C activation. In addition, co-expression of $G_{\alpha 16}$ (a G protein endogenously expressed in hematopoietic cells that promiscuously transduces GPCR activation into phospholipase C activation) also conferred enhanced and potent thrombin-promoted inositol phosphate formation to PAR3-transfected COS-7 cells (178).

Unlike other PARs, evidence that natively-expressed PAR3 promotes cellular responses by its own is scarce. For example, Ostrowska and Reiser recently reported that thrombin, but not a PAR1 peptide, promoted IL-8 secretion from both lung epithelial and astrocytoma cells, and that silencing PAR1 and PAR3 simultaneously (but not PAR1 alone) resulted in reduced IL-8 production in astrocytoma cells. The authors suggested thrombin actions were mediated by PAR3 (203). McLaughlin et al. reported that thrombin-elicited transendothelial electrical resistance (TER) was mediated in part by PAR3, which (together with PAR1) is

67

endogenously expressed in human endothelial cells. PAR3 suppression resulted in ~50% reduction of TER, while PAR1 suppression completely reduced TER in response to thrombin. Based on bioluminescent resonance energy transfer-2 (BRET^2) measurements, the authors concluded that PAR3 dimerizes with and regulates PAR1 signaling (204). Our data, illustrating that (i) PAR1-AP and PAR4-AP fail to promote cellular responses in A549 cells, (ii) PAR3 is the only PAR transcript present in these cells, and (iii) PAR3 siRNA decreased thrombin-evoked responses, indicate that PAR3 is the major thrombin receptor functionally present in these cells. Moreover, the observation that PAR3 over-expression enhanced thrombin-elicited inositol phosphate formation, RhoA activation, and ATP release, strongly suggest that PAR3 is capable of triggering signaling.

Collectively, our results demonstrate that thrombin actions on A549 cells are mediated by PAR3-promoted Ca^{2+} mobilization and Rho activation, and that these signaling cascades must be temporally coordinated to allow ATP release via connexin/pannexin hemichannel opening.

Key observations obtained with A549 cells were expanded to physiologically relevant primary cultures of WD-HBE cells. In these cultures, basolateral addition of thrombin resulted in robust mucosal ATP release, which was inhibited by ROCK and MLCK inhibitors as well as by connexin/pannexin hemichannel blockers (**Fig. 3.10A and B**). In addition, measurements of [^{3}H]inositol phosphate formation in thrombin-stimulated WD-HBE cells suggested a previously unnoticed autocrine action of released ATP, i.e., as a contributor to PAR-evoked signalling (**Fig. 3.10C**). In summary, our study is the first to demonstrate the occurrence of robust ATP release in GPCR agonist-stimulated human airway epithelial cells

and to implicate the participation of ROCK and MLCK as potential upstream effectors of

ATP release via connexin/pannexin hemichannels.

Table 3.1. Thrombin-promoted inositol phosphate formation is not affected by Ca^{2+}, Rho, or connexin/pannexin inhibitors. *myo*-[^{3}H]inositol-labeled A549 cells were challenged for 20 min with 30 nM thrombin, and the resulting inositol phosphates were quantified as indicated in Experimental Procedures. Transfections and pre-incubations with pharmacological inhibitors were as described in Methods.

	Inhibitor	Mean ± SD (cpm)	n
Control	-	1638 ± 296	8
Thrombin	-	3187 ± 516	8
Thrombin	P115-RGS	3516 ± 251	4
Thrombin	RhoA(T19N)	2680 ± 82	4
Thrombin	1 µM H1152	3536 ± 496	8
Thrombin	10 µM Y27632	3269 ± 202	8
Thrombin	1 µM ML-7	2924 ± 227	4
Thrombin	100 µM Anandamide	3361 ± 235	4
Thrombin	100 µM Flufenamic Acid	3076 ± 467	4
Thrombin	10 µM Carbenoxolone	3316 ± 289	8

Figure 3.1. Thrombin-promoted ATP release and inositol phosphate formation in a PAR1- and PAR4-independnet manner. A, extracellular ATP concentrations were measured on real-time, in the absence or presence of 30 μM ebselen and 300 μM β,γ-metATP (added at t = 0), as described in Methods. Thrombin (30 nM) was added at t = 10 min. Values are the mean ± SEM of eight independent measurements. B, PAR mRNA expression in A549 cells was determined by RT-PCR analysis. Plasmids expressing the indicated PAR were used as positive controls (Ctrl). Results are representative of nine independent A549 cell RNA preparations. C, cells were stimulated for 5 min with thrombin, PAR1-AP, or PAR4-AP, and extracellular ATP measured off-line, as described in Methods. Values are the mean ± SEM of three independent measurements performed in sextuplate. D, myo-[³H]inositol-labeled cells were incubated for 20 min with the indicated agonist, and the resulting [³H]inositol phosphates were separated and quantified, as described in Methods. Results are from three independent experiments performed with quadruplicate samples.
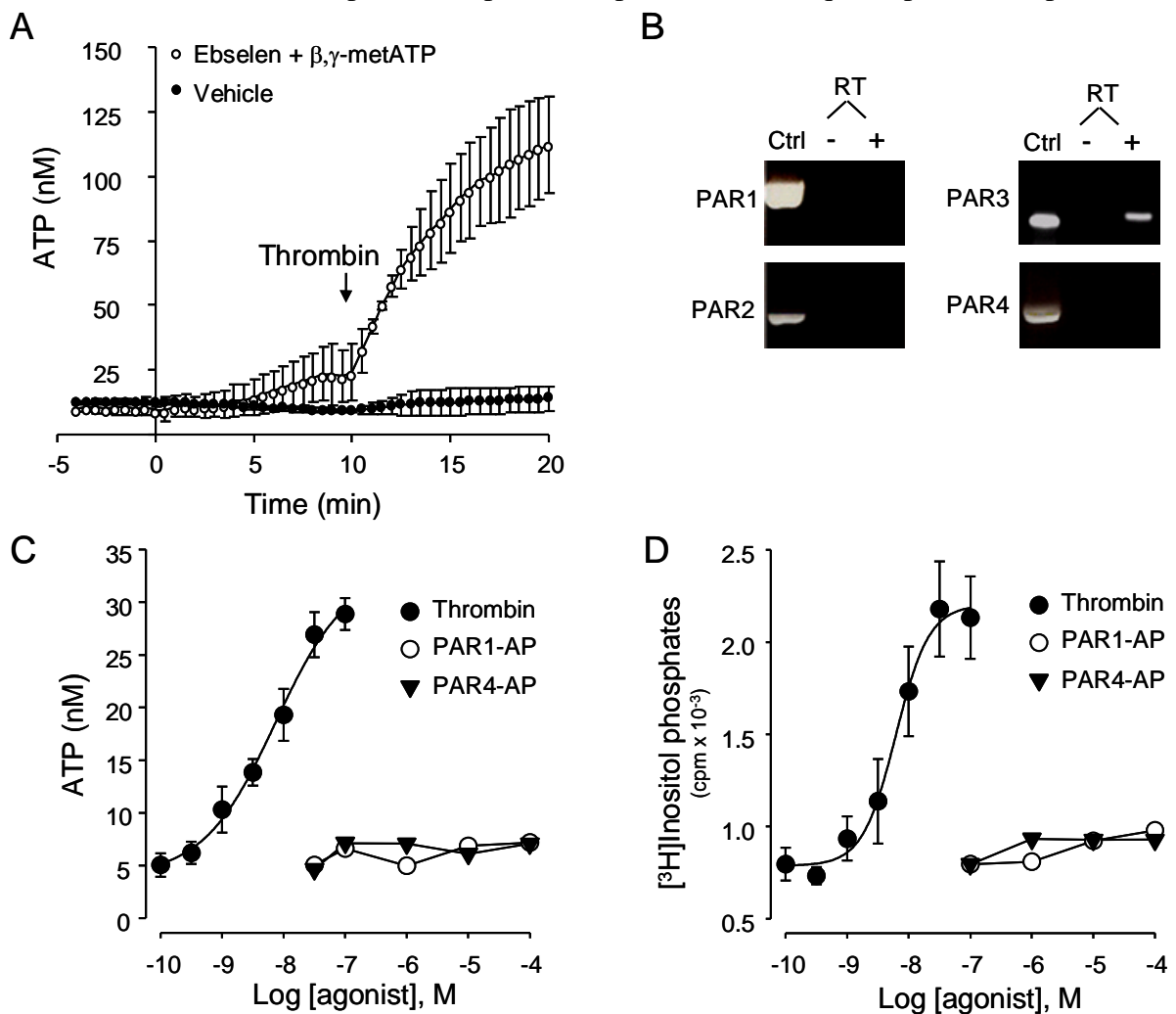
Figure 3.2. PAR3 overexpression enhances thrombin-elicited ATP release and inositol phosphate formation in A549 cells. A, cells were transfected with the indicated amount of cDNA. Forty eight hours post transfection, cells were pre-incubated with ebselen and β,γ-metATP as in Figure 3.1 and incubated for 5 min with 30 nM thrombin or vehicle. B and C, cells transfected with 100 ng PAR3 cDNA were stimulated for 5 min (B) or 20 min (C) with the indicated concentration of thrombin, and ATP release and inositol phosphate formation were measured as described in Figure 3.1C and D, respectively. The data represent the mean ± SEM of at least three independent experiments performed in quadruplicate.
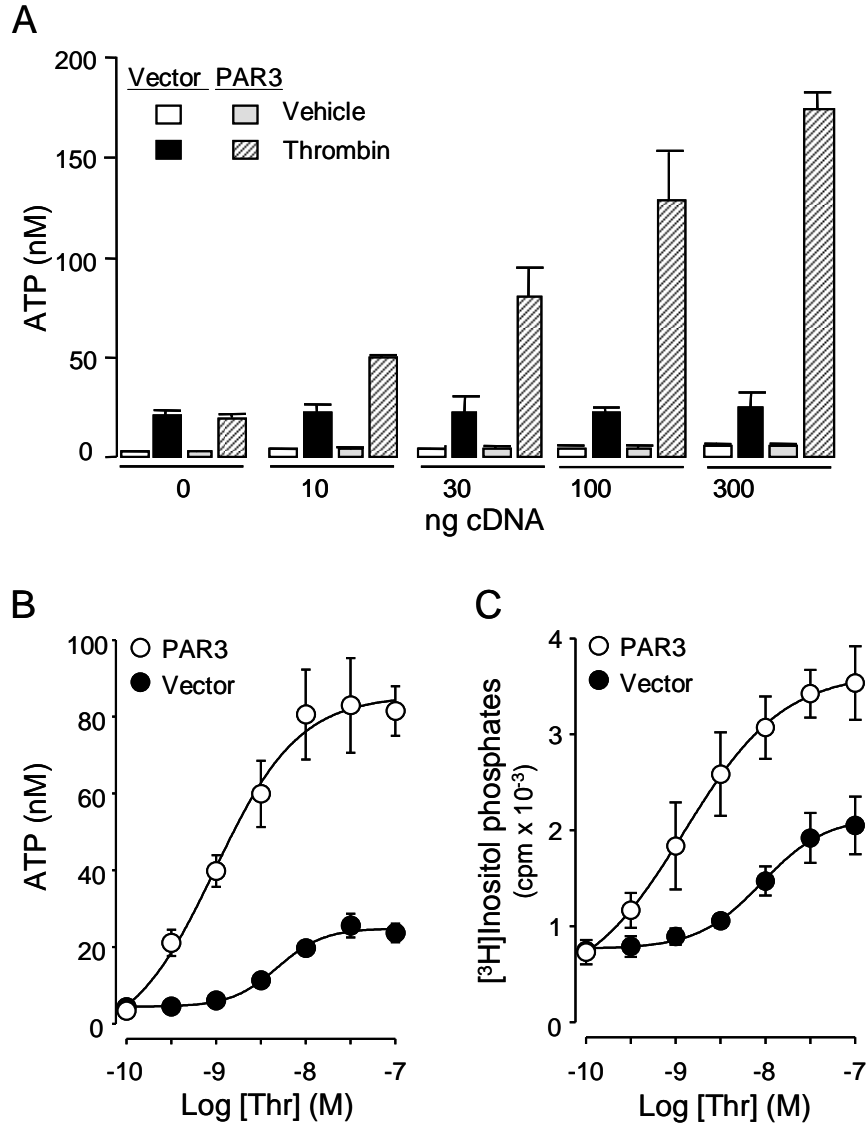
Figure 3.3. PAR3 mediates thrombin-elicited ATP release and inositol phosphate formation in A549 cells. A, PAR siRNA reduces PAR3 mRNA expression. B, effect of PAR3 siRNA on thrombin (30 nM)-promoted inositol phosphate formation. C, ATP release was measured in cells transfected with either PAR3 siRNA or its scramble oligonucleotide. D, cells transfected as above were co-transfected with empty-vector or siRNA-resistant PAR3[⊗] cDNA. ATP was measured off-line, 5 min after the addition of vehicle or 30 nM thrombin, in the presence of 30 µM ebselen and 300 µM β,γ-metATP. The data represent the mean ± SEM of three separate experiments performed in triplicate; $p < 0.05$.
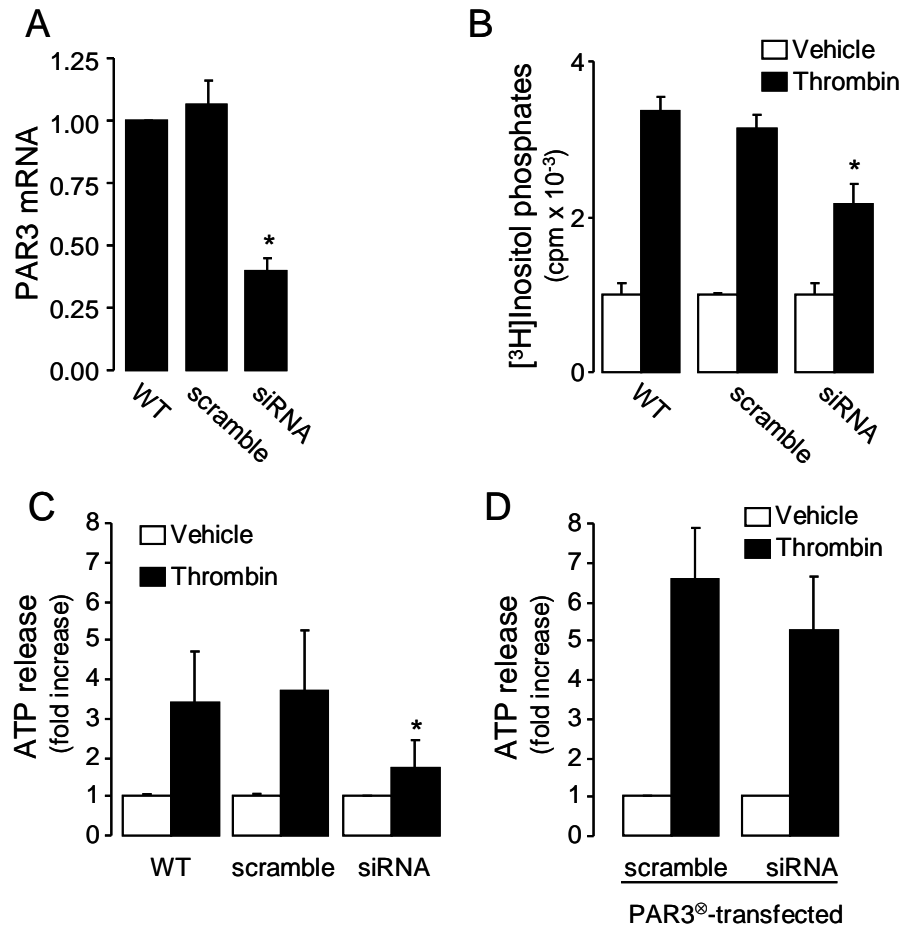
Figure 3.4. Ca^{2+}is necessary but not sufficient by itself for agonist-evoked ATP release. A, cells were pre-incubated for 20 min with vehicle (Ctrl), 1 μM tapsigargin (Tg), or 10 μM BAPTA-AM (BAPTA) and ATP concentrations were measured off-line, 5 min following the addition of vehicle or 30 nM thrombin. Ebselen (30 μM) and β,γ-metATP (300 μM) were added to cells 5-10 min prior addition of vehicle/thrombin. The data represent the mean ± SEM of at least six separate experiments performed in quadruplicate. B, cells were incubated with vehicle, 30 nM thrombin, or 100 μM UTP, and ATP concentrations were measured as above. C, *myo*-[³H]inositol-labeled cells were incubated for 20 min with the indicated drugs, and the resulting [³H]inositol phosphates were separated and quantified as in Figure 3.1D. Results are from four independent experiments performed with quadruplicate samples. D, cells were loaded with Fura 2-AM for 30 min, and stimulated with 30 nM thrombin or 100 μM UTP. Fluorescence from ~40 cells was acquired as described in Methods. Representative tracings are illustrated; similar results were obtained in six independent experiments.
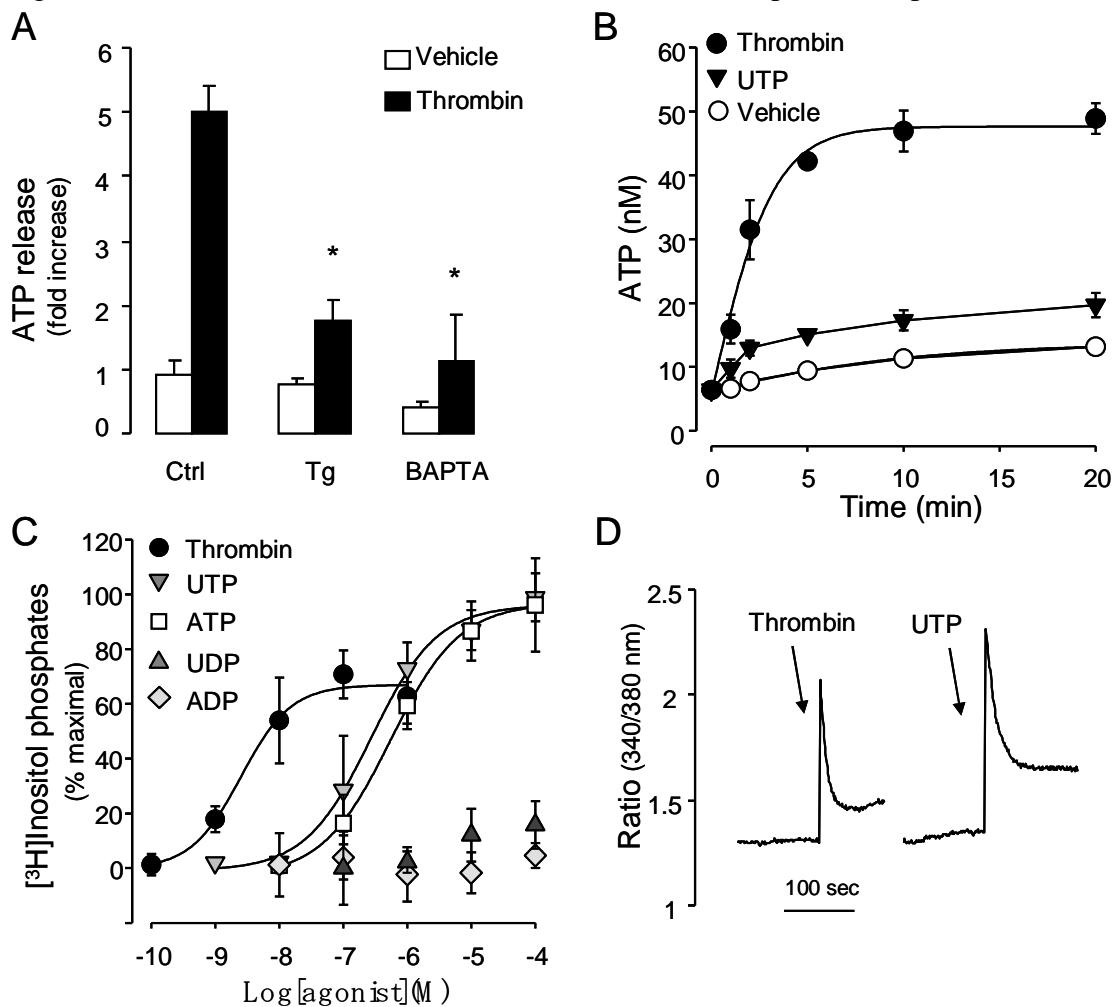
Figure 3.5. Thrombin-promoted ATP release is independent of Gi activation. A, cyclic AMP (cAMP) was measured in cells pre-incubated 18 h with 50 ng/ml pertussis toxin (PTX) or vehicle, and stimulated for 5 min with 30 μM forskolin and the indicated concentrations of thrombin. Values are the mean ± SEM of two independent experiments performed in triplicate. B, cells were preincubated with vehicle, PTX (50 ng/ml, 18 h) or wortmannin (Wortm, 200 nM, 15 min), and incubated for 5 min with 30 nM thrombin or vehicle. Values are the mean ± SEM of four independent experiments performed in quadruplicate.
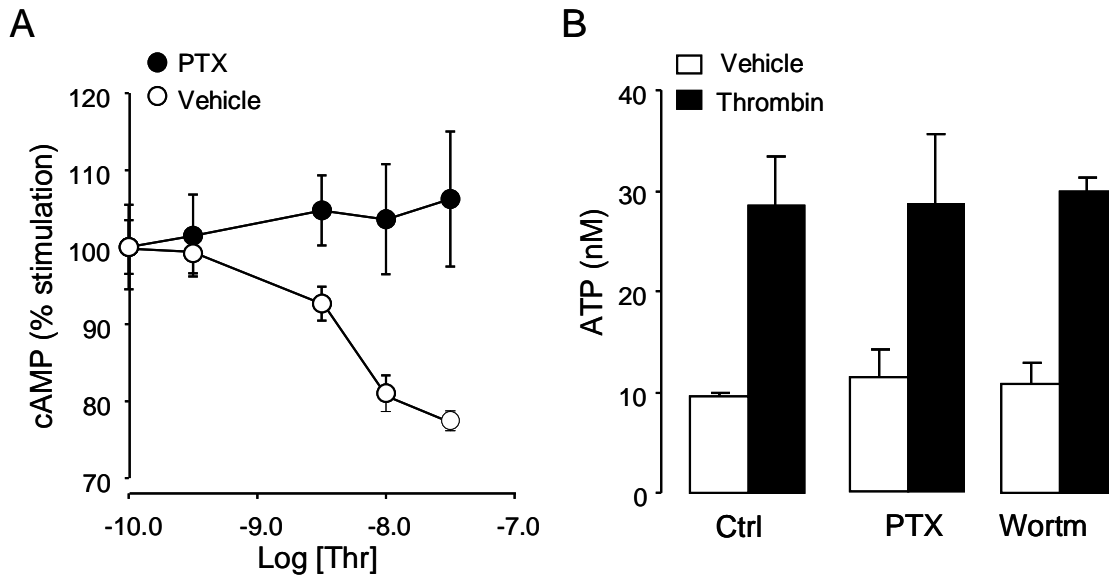
Figure 3.6. PAR3 promotes RhoA activation. A, total RhoA and RhoA-GTP were measured in A549 cells transfected with 100 ng empty vector or PAR3 cDNA, as in Figure 3.2. RhoA activation was visualized by the pulldown assay (left), as described in Experimental Procedures. RhoA activation is expressed as fold increase over control (vector, t = 0); values are the mean ± SEM of ten independent experiments (right). B, PAR3 siRNA reduced thrombin (30 nM, 5 min)-promoted RhoA activation. The Western blot (left) is representative of four experiments performed under similar conditions. Values (right) are expressed as fold increase over vehicle in scramble-transfected cells (mean ± difference to mean, n = 4).
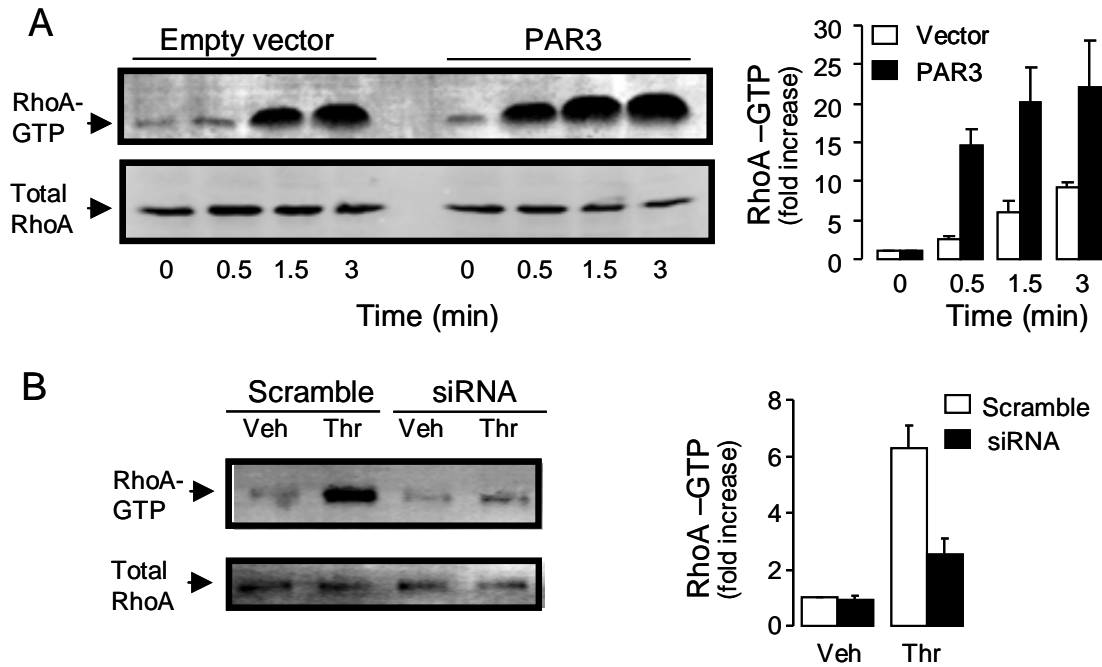
Figure 3.7. Thrombin-elicited ATP release is mediated by $G_{12/13}$/RhoA/ROCK. A, ATP release was quantified in P115-RGS-, or RhoA(T19N)- transfected cells, after 5 min incubation with 30 nM thrombin or vehicle. Values are the mean ± SEM of four independent experiments performed in quadruplicate. B, cells were pre-incubated for 1 h with the indicated concentrations of H1152 or Y27632, and ATP release was measured after 5 min incubation with 30 nM thrombin or vehicle. The data are plotted as the percent of stimulation observed with 30 nM thrombin, in the absence of inhibitors. Values the mean ± SEM from five separate experiments performed in quadruplicate. C, the effect of 100 nM H1152 or 1 μM ML-7 on thrombin-promoted MLC phosphorylation is illustrated by a Western blot (top). Quantification of p-MLC is indicated in the bottom; mean ± SD, n= 3. D, effect of 1 μM ML-7 on thrombin-promoted ATP release. Values are the mean ± SD from at least three independent experiments performed in quadruplicate. (*) indicates significant inhibition of thrombin responses, $p < 0.05$. ATP measurements were performed in the presence of ebselen and β,γ-metATP as indicated in previous Figures.
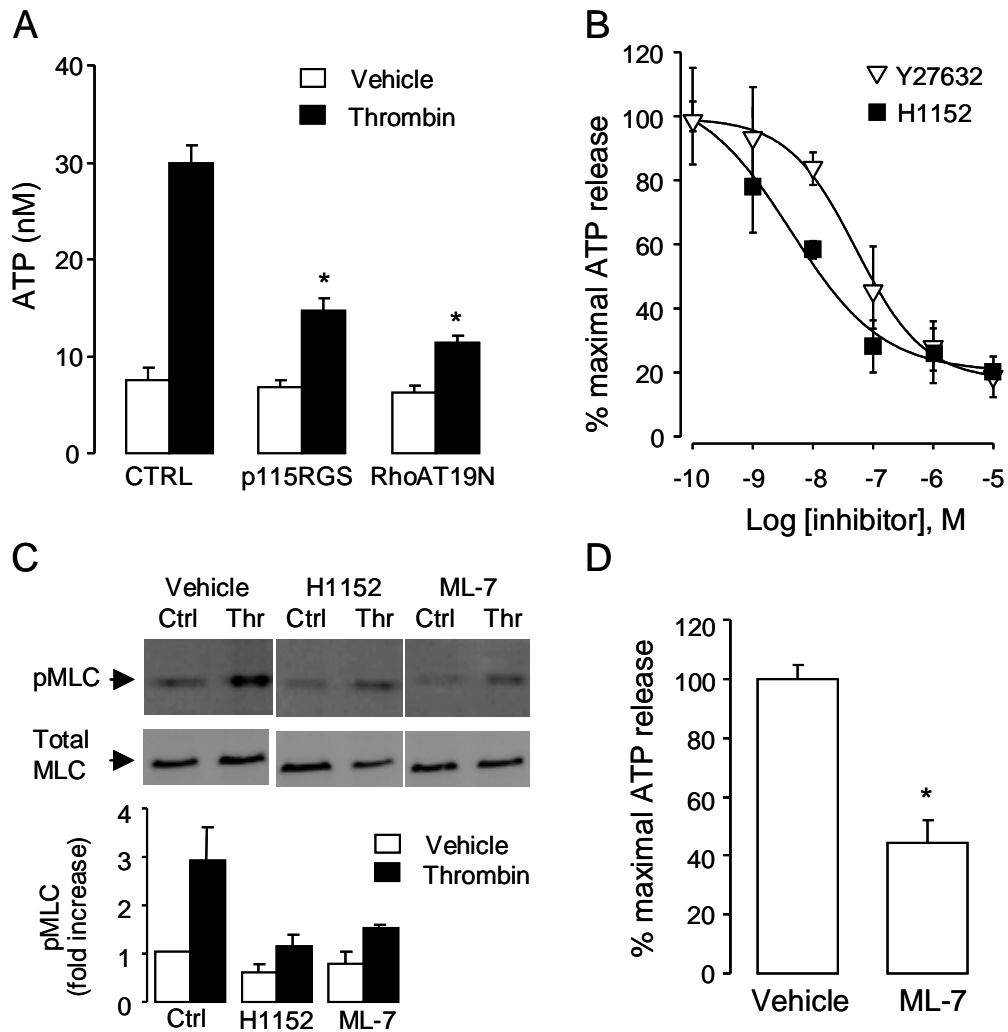
Figure 3.8. RhoA-activation and Ca^{2+} mobilization act in concert to promote ATP release. A, RhoA activation was measured and quantified in A549 cells stimulated for the indicated times with 30 nM thrombin or 100 μM UTP. The results (fold increase relative to untreated cells) represent the mean ± SEM of five separate experiments. B, ATP release was measured in cells pre-incubated with vehicle or 100 μM UTP for 15 min, and challenged for additional 5 min with the indicated drugs. The data represent the mean ± SEM of three separate experiments performed in quadruplicate. Ebselen and β,γ-metATP were added as indicated in previous Figures.
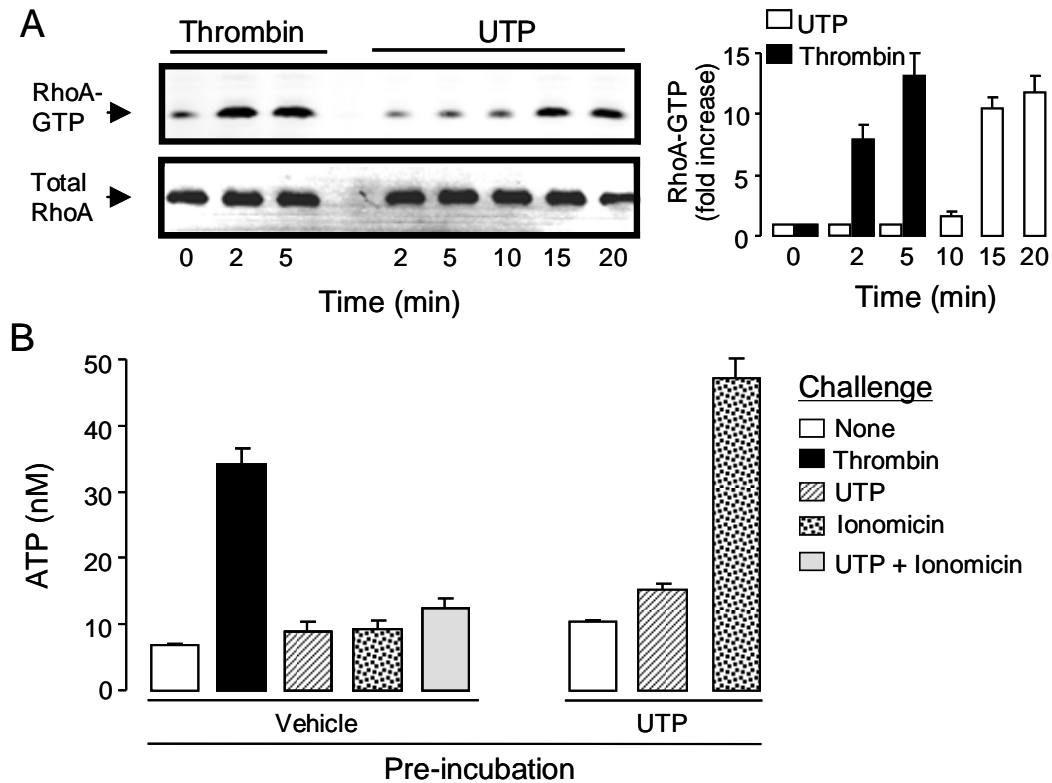
Figure 3.9. Involvement of connexin/pannexin hemichannels in thrombin-promoted ATP release from A549 cells. A, cells were pre-incubated for 2 min in EGTA/Ca^{2+}-buffered solutions and extracellular ATP measured after an additional 5 min incubation with vehicle or 30 nM thrombin. The data represent the mean ± SEM of three separate experiments performed in quadruplicate. B, changes in ATP concentrations were measured in cells pre-incubated for 15 min with 100 µM anandamide, 100 µM flufenamic acid (FFA), or 10 µM carbenoxolone (CBX), and challenged for 5 min with vehicle or 30 nM thrombin. Values represent the mean ± SEM of at least six separate experiments performed in quadruplicate. C, uptake of cells propidium iodide (PI) was assessed after 5 min incubation with vehicle or 30 nM thrombin. The images represent an overlay of propidium iodide (red)-associated nuclear fluorescence and DIC. D, A549 cells were pre-incubated with vehicle or with 10 µM carbenoxolone (CBX, 15 min), 10 µM Y27632 (45 min), 1 µM H1152 (45 min), 10 µM BAPTA-AM (20 min), or with 1 µM ML-7 (45 min), and challenged for 5 min with no agonist (Ctrl), 30 nM thrombin, 100 µM UTP, or 1 mM ATP in the presence of propidium iodide. Cells were fixed and images taken and analyzed by confocal microscopy. Dye uptake is expressed as the percent of nuclei displaying red fluorescence. The data are the mean ± SEM, n = 4. Similar results were obtained in at least three separate experiments performed in quadruplicate. Bar, 100 µm. (*). $p < 0.05$.
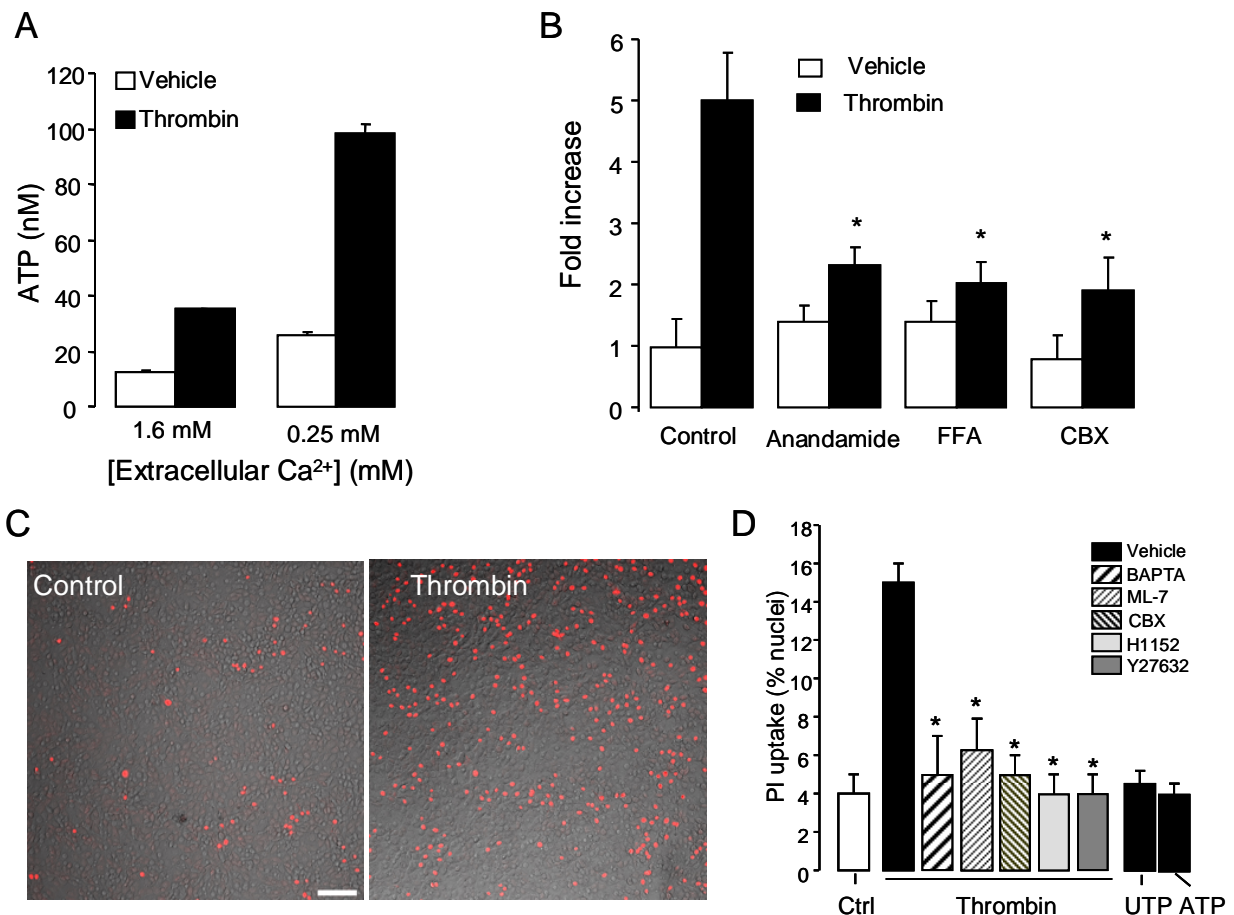
Figure 3.10. Thrombin-promoted ATP release and inositol phosphate formation in WD-HBE cells. A, WD-HBE cells were incubated for 5 min with 30 nM thrombin (basolateral), 100 µM UTP (apical), or vehicle; ATP released to the apical or basolateral (BL) medium was quantified, as indicated in Methods. B, WD-HBE cells were pre-incubated bilaterally (1 h) with 1 µM H1152, 10 µM ML-7 or1 µM CBX, and apical ATP release was measured after 5 min incubation with 30 nM thrombin (basolateral addition) or vehicle. C, [^{3}H]inositol-labeled WD-HBE cells were incubated for 20 min in the presence of vehicle, 30 nM thrombin (basolateral addition), 100 µM UTP (apical addition), and in the absence or presence of 5 U/ml apyrase (apical addition). The resulting [^{3}H]inositol phosphates were quantified as indicated in Methods. The data (mean ± SD) represent the net increase in counts above background, and they are representative of two separate experiments with independent cultures performed each with quadruplicate samples. (*) indicates significant difference between apyrase-treated vs. non-treated cultures, $p < 0.01$.

80
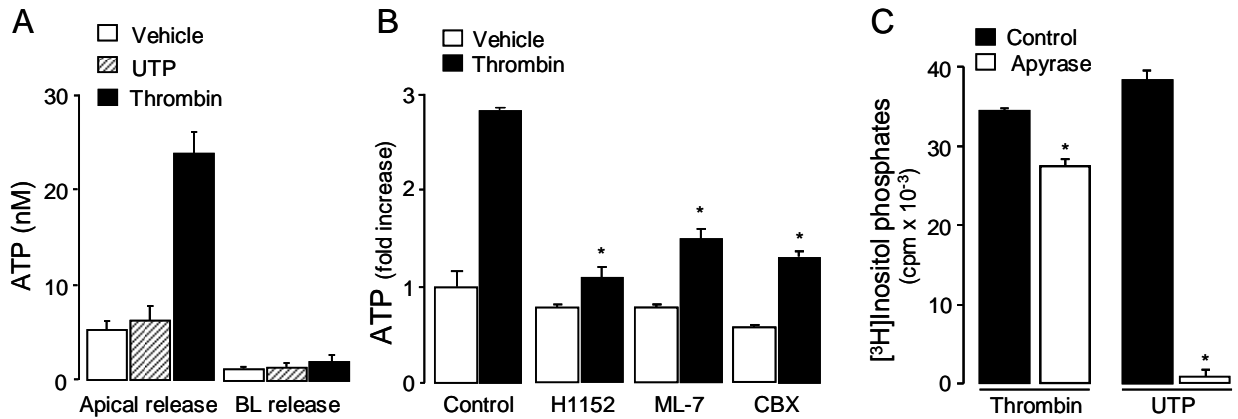
CHAPTER IV

Receptor-promoted exocytosis of airway epithelial mucin granules containing a spectrum of adenine nucleotides

1. Introduction

The airway MCC system is crucial for innate lung defense. The major components of MCC are ciliary beating, mucin secretion and electrolyte / fluid transport. The balance amongst these components ensures the rapid removal of inhaled foreign materials. Failure in this balance may lead to airway obstructive and inflammatory diseases. For example, cystic fibrosis results from aberrant ion transport activities and impaired hydration of ASL, mucus accumulation, and ultimately chronic obstructive pulmonary disease (205). Thus, a key physiological component of lung defense involves mucin hydration and clearance.

However, mucin secretion and ASL hydration / clearance functions reside in distinct cell types, i.e., goblet and ciliated cells, respectively, and thus, coordination of these activities is required for effective mucus clearance. A body of evidence suggests that ATP release from airway epithelial cells provides a mechanism for the control of MCC functions [reviewed in (206)]. Extracellular ATP and its metabolite adenosine activate subsets of purinergic receptors expressed on the mucosal surface of airway epithelial cells. The predominant nucleotide-sensing receptor in the airways is the G_q-coupled $P2Y_2$ receptor, which is activated by ATP and UTP. $P2Y_2$ receptor activation promotes mucin secretion and ciliary beating, inhibition of the epithelial Na^+ channel ENaC, and activation of CFTR and the Ca^{2+}-activated Cl^- channel. Extracellular ATP hydrolysis results in formation of adenosine, which activates the G_s-coupled A_{2b} receptor, promoting cyclic AMP-regulated CFTR Cl^- channel activity and thus, fluid secretion (206). Functional and biochemical evidence suggest that adenosine / A_{2b} receptor is the major regulator of CFTR activity in airway epithelium (25). ATP and adenosine are naturally occurring components of ASL (25), but the cellular pathways that yield these extracellular molecules are poorly defined.

Given the complex cellular composition of airway epithelia, multiple mechanisms and pathways likely participate in the release of nucleotides into ASL. Nucleotide release from airway epithelial cells has been proposed to occur via different mechanisms: (i) tonic release from vesicles via a constitutive pathway in non-mucous cells (94); (ii) a conductive mechanism likely involving pannexin hemichannels, potentially localised within ciliated cells [(207) and **Chapter III**]; and (iii) ATP release associated with Ca^{2+}-regulated exocytosis (153).

We recently demonstrated that ATP release from goblet cell-like Calu-3 cells was associated with Ca^{2+}-promoted mucin secretion (71). An attractive hypothesis derived from this observation is that mucin granules store ATP, and likely, other purine nucleotides. Relevant to this hypothesis, a recent mathematical model of nucleotide regulation in the ASL predicts the release of AMP and ADP accompanying ATP from a vesicular pool (100). Thus, a mix of nucleotides released upon mucin granule exocytosis could provide paracrine signalling to ciliated cells to increase ion and water secretion to support mucin hydration and ultimately mucus clearance. However, the contribution of mucin granule exocytosis to ASL nucleotides has awaited quantification of nucleotide concentration within mucin granules.

Recently, we discovered that the serine protease thrombin elicited robust ATP release from WD-HBE cell cultures [discussed in **Chapter III**]. Thrombin-promoted ATP release was mediated via activation of cognate G-protein coupled PARs. The family of PARs includes four members (PAR1, PAR2, PAR3, and PAR4). Thrombin is the physiological activator of PAR1, PAR3, and PAR4; however, other proteases can cleave these receptors and may contribute to their function *in vivo* (208). PAR2 is activated by multiple serine proteases including trypsin and tryptase, but not by thrombin (208). Relevant to our studies,

activation of PARs has been described to induce mucin secretion from gastrointestinal and airway epithelial cells (209-210). Thus, PAR activation of airway goblet cells may provide a useful model to investigate the potential coordination between ATP release and mucin secretion.

In the present study, we used WD-HBE and airway goblet-like Calu-3 cells to investigate (i) whether PAR agonist-elicited mucin exocytotic secretion is associated with enhanced nucleotide release, and (ii) whether mucin granules purified from airway goblet cells contain ATP and possibly other adenyl nucleotide species.

2. Methods

Reagents - Bafilomycin A$_1$, cytochalasin D, ionomycin, H-1152, ML7, and Y27632 were purchased from Calbiochem (San Diego, CA). 2-Phenyl-1,2-benzisoselenazol-3(2H)-one (ebselen), β, γ -methylene ATP, luciferase from Photinus pyralis, Percoll®, and quinacrine were purchased from Sigma (St Louis, MO). BAPTA AM, Fluorescently-labelled phalloidin, Fura-2 AM, and antibodies against cytochrome oxidase subunit III and IV and ATP-synthase α-subunit were purchased from Molecular Probes (Eugene, OR). [^{3}H]ATP (20 Ci / mmol) was purchased from Amersham Biosciences (Piscataway, NJ). MUC5AC and MUC1 antibodies were purchased from LabVision (Fremont, CA). VAMP-8 antibodies were from Abcam (USA) and Synaptic Systems (Germany). Luciferin and antibodies against GM 130, p230 antibodies, protein disulfide isomerase, and LAMP-1 were from BD Biosciences Pharmingen (San Jose, CA). Secondary antibodies were from Jackson ImmunoResearch Labs (West Grove, PA) and LI-COR (Lincoln, NE). Human alpha-thrombin was purchased from Enzyme Research Laboratories (South Bend, IN). The PAR1-activating peptide TFLLRNPNDK and the PAR2-activating peptide SLIGKV were synthesized at Tufts

University Peptide Synthesis Core Facility. Other chemicals were of the highest purity available and from sources previously reported.

Cell culture – Airway epithelial Calu-3 cells are derived from pleural effusion associated with human lung adenocarcinoma (211). Unless otherwise indicated, Calu-3 cells were grown on 12-mm Transwell supports and maintained at air-liquid interface for at least two weeks, as described previously (71). Well-differentiated human bronchial epithelial cells were grown on collagen-coated 12-mm Transwell supports and maintained at air-liquid interface for at least four weeks, as described previously (212). Human tissue specimens for cell culture production and mRNA expression analyses were collected according to the guidelines of the Institutional Review Board for Protection of Human Rights at the University of North Carolina at Chapel Hill.

RT-PCR Analysis – Total RNA was prepared using the RNeasy Mini Kit (Qiagen) and reverse-transcribed using Super- Script III reverse transcriptase (RT, Invitrogen). RT-PCR analyses were performed at the UNC-CH Cystic Fibrosis Center Molecular Biology Core Lab using standardized protocols. Amplified PCR products were identified by sequence analysis at the UNC-CH DNA sequencing facility. Primers used to amplify human PAR1, PAR2, PAR3, and PAR4 were prepared according to Chapter III. A fragment between bp 71 and 339 of human VAMP-8 was amplified with forward primer (F) 5'-AGGTGGAGGAAATGATCGTG and reverse primer (R) 5'-TGGCAAAGAGCACAATGAAG.

Quantification of ATP with the luciferin-luciferase assay – To measure ATP release, WD-HBE and Calu-3 cell cultures were rinsed and pre-incubated in 0.4 ml basolateral, 0.25 ml mucosal Hank's Balanced Salt Solution with 20 mM HEPES and 1.6 mM Ca^{2+} and 1.8

mM Mg^{2+} (HBSS). ATP hydrolysis inhibitors (30 µM ebselen and 300 µM β, γ -methylene ATP) were added for 5 min prior to stimuli. At the end of the incubation, aliquots of the extracellular baths were removed, and heated to $95^{o}C$ to inactivate nucleotidases, as described in **Chapter III**. The luciferin-luciferase reaction mix was added to tubes and luminescence recorded in an Auto-Lumat LB953 luminometer (173). An ATP standard curve was performed in parallel. None of the reagents used during ATP release measurements interfered with the luciferase reaction.

Mucin secretion - MUC5AC release by WD-HBE and Calu-3 cells was determined by immuno-slot blot analysis of the extracellular media, as previously described (71). Slot blots were scanned and quantified in a LI-COR Odyssey system (Lincoln, NE).

Intracellular calcium measurements - Calu-3 cells grown on glass coverslips were loaded with Fura-2 AM for 15-30 min. Cells were washed, mounted on a platform of a fluorometer-coupled Nikon microscope, and fluorescence from 30–40 cells was acquired alternately at 340 and 380 nm. Other details were as previously described in Chapter III.

Immunofluorescence and confocal microscopy – Cell cultures were fixed in 4% paraformaldehyde, permeabilized in 0.1 % Triton X-100 for 10 min, and subjected to immunofluorescence staining and confocal microscopic analysis, as previously described (71).

Quinacrine associated granule fluorescence – Calu-3 cell secretory granules were pre-labelled with 10 µM quinacrine, as previously described (71). Cells were mounted on the stage of the confocal microscope and real-time recording was performed every 10 and 30 s in the xy axes. The fluorescence intensity of all the pixels contained within granules of 1-2 µm diameter were measured at each time point, normalized to basal values (time = 0), and

averaged using Leica software. To confirm the cellular location of quinacrine-loaded granules, y-stacks were generated at the end of each experiment.

Mucin granule isolation – Calu-3 cells were grown in four 75 cm^2 culture flasks for at least 10 days. Cells were detached using Varsene solution. In some experiments, cells were loaded with quinacrine for 15 min prior to detaching from the flask. Cells were pelleted at 500 x g and re-suspended in 4 ml of ice-cold lysis buffer (PIPES 20 mM pH=6.8, 130 mM K glutamate, 3 mM MgCl$_2$, 0.1 mM CaCl$_2$, and 3 mM EGTA). Cells were disrupted by cavitation (800-1000 psi, 30 min on ice). Lysate was centrifuged for 3 min at 500 x g and the supernatant pelleted at 5000 rpm for 3 min. The resulting pellet was resuspended in isotonic 50% Percoll® suspension prepared in lysis buffer and centrifuged at 4°C for 20 min at 30000 rpm using a TLS 55 rotor (TL100 ultracentrifuge, Beckman, USA). The first 0.5 ml of each gradient were collected, mixed with 1.5 ml isotonic 50% Percoll® suspension, and submitted to a second ultra-centrifugation for 30 min at the same speed. Twenty fractions (100-µl each) were collected and stored at -80°C for further analyses. In experiments using quinacrine-loaded cells, fraction aliquots were examined under the fluorescence microscope to visualise granule-associated fluorescence. The fractions of the second gradient were analysed for nucleotide concentration and by immuno-slot blot (71), using antibodies against cellular markers MUC5AC and VAMP-8 (mucin granules), MUC1 (plasma membrane), GM 130 and p230 (Golgi), protein disulfide isomerase (PDI, endoplasmic reticulum), LAMP-1 (lysosome), and mitochondrial cytochrome oxidase subunits III / IV and ATP-synthase α-subunit.

Quantification of adenyl purines via etheno-derivatization and HPLC analysis – Cell cultures were rinsed and incubated as above, except that ATP hydrolysis inhibitors were

omitted due to interference with the detection of etheno-derivatives. To quantify adenyl species within isolated mucin granules, purified granules were disrupted with ice-cold 5% trichloroacetic acid followed by ethyl ether extraction, as previously described (173). Samples were derivatised with chloroacetaldehyde and the resulting fluorescent etheno-species analyzed by HLPC, as previously described (25).

ATP hydrolysis - Isolated mucin granules (2 µg protein) were re-suspended in ice-cold 100 µl HEPES-buffered HBSS (pH 7.4) containing 0.1 µCi [^{3}H]ATP (100 µM). Reactions were initiated by transferring the tubes to a 37°C water bath followed by the immediate addition of either vehicle or 0.1% triton X-100. At the end of the incubation, samples were heated (2 min at 95°C) to inactivate ATPase activities. The resulting [^{3}H]-species were separated by HPLC, as previously described (173).

Statistics – Student's paired t-test was performed using Excel 2003; $p < 0.01$ was accepted to indicate statistical significance.

3. Results

PAR agonists elicit release of ATP associated with mucins in WD-HBE cells. In **Chapter III**, we indicated that basolateral, but not mucosal, addition of the serine protease thrombin resulted in enhanced mucosal ATP release from WD-HBE cultures. Since cellular responses to thrombin and other serine proteases are mediated by members of the family of PARs, we investigated whether PAR stimulation in WD-HBE cells elicited mucin secretion coordinate with ATP release. Expression of PARs was verified in WD-HBE cells by RT-PCR analysis. PAR1, PAR2, and PAR3, but not PAR4 transcripts were amplified in WD-HBE cultures (**Fig. 4.1A**). Thrombin (50 nM, 5 min), a physiological agonist for PAR1 and PAR3 (208) promoted both mucin secretion (**Fig. 4.1B**) and ATP release (**Fig. 4.1C**) into the

apical bath of WD-HBE cultures. Activation of PARs by their cognate proteases involves proteolytic cleavage of the amino-terminal exodomain of the receptor, generating a new amino terminus that functions as a tethered ligand (208). Synthetic peptides, mimicking the tethered ligand, can selectively activate PAR1 and PAR2 independently of receptor cleavage. Human PAR3 is not activated by PAR3 mimicking peptides (208). Basolateral incubation of WD-HBE cells for 5 min with PAR1 and PAR2 activating peptides (PAR1-AP and PAR2-AP, respectively) resulted in enhanced mucosal mucin secretion and ATP release (**Fig. 4.1B, C**). PAR activation did not elicit mucin or ATP release into the basolateral bath (not shown).

PARs promote Ca^{2+}-dependent mucin secretion from Calu-3 cells. Goblet cells are sparsely expressed in WD-HBE cell cultures, making purification of goblet cell granules difficult. Therefore, airway goblet-like Calu-3 cells (71) were utilized as a cell model to investigate the contribution of mucin granule exocytosis to ATP release. Based on a previous study suggesting the presence of Ca^{2+}-mobilizing PARs in Calu-3 cells (198), the expression of PAR transcripts in these cells was examined by RT-PCR. As illustrated in **Figure 4.2A**, transcripts for PAR1, PAR2, and PAR3, but not for PAR4, could be amplified in these cells.

Consistent with the concept that all PARs couple to Gq and phospholipase C activation (208), Calu-3 cells loaded with Fura-2 AM displayed increased intracellular Ca^{2+} mobilization in response to thrombin (50 nM), PAR1-AP (100 µM), or PAR2-AP (100 µM) (**Fig. 4.2B**). As shown in **Figure 4.2C**, thrombin-evoked Ca^{2+} mobilization was negligible in PAR1-AP-pretreated cells, suggesting that desensitization of PAR1 prevented Calu-3 cells from responding to thrombin. Control experiments indicated that PAR2-AP-evoked responses were not affected by PAR1-AP pre-treatment (**Fig. 4.2C**). Although the data cannot rule out a contribution of PAR3 to thrombin-evoked responses, the nearly identical

efficacies of thrombin and PAR1-AP and the PAR1-AP desensitization effect on thrombin in eliciting Ca^{2+} mobilization suggest that PAR1 is the major thrombin receptor expressed in Calu-3 cells. Our results suggest that PAR2 is also robustly expressed in these cells.

The secreted mucin MUC5AC is highly expressed in Calu-3 cells as revealed by fluorescence microscopy analyses that identified ~ 1-µm diameter MUC5AC-immunoreactive granules in 30-40% of Calu-3 cell cultures (71). Having verified that Calu-3 cells express Ca^{2+}-mobilizing PARs, we asked whether activation of these receptors resulted in enhanced mucin secretion. Incubation of the cells with thrombin, PAR1-AP, or PAR2-AP (5 min) resulted in marked (~70%) loss of MUC5AC intracellular immunoreactive granules (**Fig. 4.3A and B**), suggesting that PAR agonists elicited mucin granule secretion from these cells. To further verify the effect of PARs on mucin secretion, polarized monolayers of Calu-3 cells were stimulated basolaterally with PAR agonists and the MUC5AC content in the extracellular solution assessed by immuno-slot blot analysis. Incubation of cells with thrombin, PAR1-AP, or PAR2-AP resulted in enhanced secretion of MUC5AC into the apical extracellular solution (**Fig. 4.3C**). Similarly to previous observations with ionomycin-stimulated Calu-3 cells (71), negligible mucin secretion to the basolateral solution was observed in PAR-stimulated Calu-3 cells (not shown). Thus, PAR-elicited mucin secretion reflects an exocytotic process associated with the apical plasma membrane of Calu-3 cells.

It has been well-established that receptor-mediated mucin secretion reflects a Ca^{2+}-dependent process (32). Incubation of Calu-3 cells with BAPTA AM to chelate intracellular Ca^{2+} impaired thrombin-induced mucin secretion, as assessed by the fluorescence microscopy observation of MUC5AC-immunostained cells (**Fig. 4.4A**) and immuno-slot blot analysis of Calu-3 cell apical secretions (**Fig. 4.4B**). Consistent with the notion that actin

cytoskeleton remodelling is required for mucin granule exocytosis (32, 71), thrombin-promoted mucin secretion was inhibited by cytochalasin D (which disrupts the actin cytoskeleton), ML7 (a myosin light chain kinase inhibitor), and H1152, an inhibitor of Rho kinase, a known upstream effector of myosin light change kinase and actin cytoskeleton remodeling during exocytosis (32) (**Fig. 4.4A and B).** PAR1-AP- and PAR2-AP-stimulated cells also displayed reduced MUC5AC secretion when pre-incubated with the Rho kinase inhibitor H1152 (**Fig. 4.4A and B**). Moreover, changes in the organization of actin cytoskeleton were observed in PAR-stimulated Calu-3 cells labeled with fluorescent phalloidin as previously described in thrombin-stimulated non-epithelial cells (95) (not shown).

PAR-promoted mucin secretion is associated with enhanced release of ATP. Incubation of Calu-3 cells with PAR agonists resulted in enhanced release of ATP into the mucosal (but not basolateral) compartment (**Fig. 4.5**). Maneuvers that affected mucin granule exocytosis in Calu-3 cells, such as chelating intracellular Ca^{2+} (BAPTA-AM), inhibiting Rho kinase (HH152) and myosin light chain kinase (ML7), or disruption of the actin cytoskeleton (cytochalasin D), reduced, although did not abolish, ATP release in thrombin-stimulated Calu-3 cells (**Fig. 4.5**). Bafilomycin A_1, an inhibitor of the vesicular H^+ / ATPase that loads ATP into specialized granules in secretory cells (213), also partially inhibited (~ 30% inhibition) ATP release from thrombin-stimulated Calu-3 cells (**Fig. 4.5**). Altogether, our results are consistent with the hypothesis that a vesicular / granular component, e.g., mucin granules, contributed at least in part to ATP release from PAR-stimulated Calu-3 cells.

Isolated mucin granules contain adenine nucleotides. These results, together with our previous observation that Ca^{2+}-regulated mucin granule secretion is accompanied by

enhanced ATP release (71), suggest that mucin granules are a source of exocytotic ATP release. To more definitively assess this possibility, we utilized a strategy that takes advantage of the fluorescent dye quinacrine that labels Calu-3 cell granules (71) to isolate mucin granules from these cells. A representative image of quinacrine-labelled Calu-3 cells displaying strong granular fluorescence is shown in **Figure 4.6A**. Stimulation of the cells with thrombin, PAR1-AP, or PAR2-AP resulted in loss of granules containing quinacrine fluorescence (**Fig. 4.6B**).

Next, we subjected quinacrine-labelled Calu-3 cells to sub-cellular fractionation and fluorescently labelled granules were isolated using two consecutive continuous Percoll® gradients. Quinacrine-labelled granules (1-2 μm diameter) were concentrated within a fraction (**Fig. 4.7A**) that was also enriched in MUC5AC (**Fig. 4.7B and C**).

VAMP-8 has been proposed as the R-SNARE in goblet cell granule exocytosis (32) based on its broad participation in exocrine secretion (214). Therefore, we investigated whether VAMP-8 is associated with airway epithelial mucin granule secretion and, hence, could serve as an additional marker for granule purification. RT-PCR analysis indicated that VAMP-8 transcripts were present in native airway epithelial tissues and in Calu-3 and WD-HBE cell cultures (not shown). Importantly, VAMP-8 immunoreactivity co-localised with MUC5AC in the mucin granule fraction (i.e., fraction 4, **Fig. 4.7C**), and in granules of intact Calu-3 cells (**Fig. 4.7D**, left panel). Addition of thrombin to Calu-3 cell cultures resulted in decreased VAMP-8 immunoreactivity, which re-distributed to a diffused intracellular pattern, concomitantly with the loss of MUC5AC granule staining (**Fig. 4.7D**, right panel). Collectively, these data suggest VAMP-8 should be a valid marker for mucin granule isolation.

92

The MUC5AC / VAMP-8-containing fraction exhibited negligible amounts of MUC1 (plasma membrane marker), GM 130 and p230 (Golgi markers), protein disulfide isomerase (endoplasmic reticulum marker), LAMP-1 (lysosomal marker), or mitochondrial markers cytochrome oxidase subunit III / IV and ATP-synthase α-subunit (**Fig. 4.7C**). Thus, we conclude by these independent markers, MUC5AC and VAMP-8, that we had purified a mucin granule population.

We next measured the adenyl nucleotide content of the various fractions. ATP was concentrated in the same fraction as MUC5AC and VAMP-8 (i.e., fraction 4, **Fig. 4.8A**). ATP levels within isolated mucin granules were 0.003 - 0.01 fmoles / cell or 500-900 pmoles / mg protein, and represented < 2 % of the total cellular ATP content.

In addition, ATP metabolites were abundant in the MUC5AC / VAMP-8- enriched fraction (**Fig. 4.8A**). Indeed, in isolated mucin granules, ADP and AMP were the prevalent species (approximately 60% and 30%, respectively), while ATP and adenosine comprised ~ 10 % and ~ 2 % of total purines, respectively (**Fig. 4.8B**). This pattern of nucleotide distribution within mucin granules clearly contrasted with that observed in the whole cell lysate, where ATP represented the dominant (~ 70 %) adenyl species (**Fig. 4.8B**). These data suggest that an ATP hydrolyzing activity was present in the lumen of the mucin granule. Using [^{3}H]ATP as radiotracer, an ATPase activity was revealed in mucin granules permeabilized with Triton X-100 (150 ± 16 nmol ATP / min / mg protein, n = 2).

ADP and AMP accompanied ATP release from PAR-stimulated cells. The relatively high levels of ADP and AMP, relative to ATP, in mucin granules (**Fig. 4.8B**) suggest that these nucleotide species are co-released with ATP and mucins. To examine this possibility directly, the adenyl purine content of Calu-3 cell surface liquid was assessed by etheno-

93

derivatization. A marked increase in ADP, AMP, and ATP accumulation was observed in mucosal samples from cells stimulated with thrombin (50 nM, 5 min), relative to control cells (**Fig. 4.9**). The net increase in ATP concentration (28 ± 3 nM) measured with this assay was ~50% lower than that observed using the luciferase assay (57 ± 5 nM, **Fig. 4.5**). This difference is consistent with the fact that β,γ-met-ATP and ebselen, which efficiently block extracellular ATP hydrolysis on airway epithelia [as illustrated in **Chapters II and III**], were included in the luciferase assay but not in the derivatization protocol, due to interference of the blockers in the detection of etheno-species. Importantly, the net increase in mass of ATP, ADP, and AMP combined following thrombin addition (95 ± 11 nM, **Fig. 4.9**) substantially exceeded the mass of ATP release detected in the presence of ATPase inhibitors (57 ± 5 nM, **Fig. 4.5**). The most likely interpretation of these data is that mucin granule release of ADP / AMP contributed, at least in part, to the accumulation of these species in Calu-3 cell surface liquid.

4. Discussion

Gel-forming mucins, the principal polymeric species of the airway mucus, are condensed inside specialized granules and released from cells via Ca^{2+}-regulated exocytotic mechanisms (215-216). Mucin release requires synchronized secretion of ions / water for mucin dispersion into the ASL, but these transport activities are not expressed on goblet cells (215). Thus, the mechanisms by which electrolyte transport and mucin secretion activities are synchronized are poorly understood. Given that mucin secretion is accompanied by enhanced nucleotide release (71) and that ASL nucleotides and nucleosides regulate airway epithelial electrolyte transport activities (71, 206), we hypothesized that mucin granules themselves are the source of coordinately released nucleotides. We tested this hypothesis by (i)

characterizing the contribution of receptor-mediated mucin secretion to nucleotide release, and (ii) quantifying the nucleotide content within isolated mucin granules.

Our results demonstrate that primary cultures of WD-HBE cells and immortalized Calu-3 cells express functional PAR1 and PAR2, which upon activation, promote Ca^{2+}-dependent mucin secretion and ATP release onto the apical surface. The observation that thrombin-promoted ATP release was partially inhibited by maneuvers that deplete ATP from vesicular compartments (e.g., bafilomycin A_1) suggests that thrombin-elicited ATP release was mediated, at least in part, by an exocytotic mechanism (**Fig. 4.5**). Moreover, ATP release was reduced under conditions that inhibited mucin exocytosis (i.e., intracellular calcium chelating with BAPTA AM, actin cytoskeleton disruption with cytochalasin D, and inhibition of Rho and myosin light chain kinases with H1152 and ML7, respectively; **Fig. 4.5**), also consistent with a mucin granule secretion contribution to ATP release.

Previously, the presence of ATP in the mucin granules had been hypothesized based on the premise that mucin molecule packaging and granule integrity are energy dependent processes (217). Direct testing of this hypothesis has been challenging because the scant numbers of goblet cells within normal airway epithelia and granule fragility has hampered the isolation of intact mucin granules. Taking advantage of Calu-3 cell cultures that comprise up to 40% goblet-like mucin granule expressing cells (71), we were able to obtain a sub-cellular fraction highly enriched with mucin granules. Employing a cell cavitation method and applying two successive continuous Percoll® gradients, mucin granules were isolated devoid of measurable amounts of other cellular components. Importantly, a population of isolated mucin granules were intact, since ATP was enriched in the mucin granule-containing fraction (**Fig. 4.8A**). Moreover, AMP and to a greater extent ADP were more abundant than

ATP in this fraction (**Fig. 4.8B**), strongly suggesting that a spectrum of adenyl nucleotides (rather than ATP alone) are released from mucin granules during mucin exocytosis.

It could be argued that the relative high content of ADP / AMP observed in the mucin granule may be due to an artifact consequent to granule isolation, e.g., a phosphatase activity associated with the cytosol-facing side of the granule membrane could have rapidly hydrolyzed ATP upon disruption of the mucin granule. This possibility seems unlikely since, for nucleotide measurements, mucin granules were disrupted in the presence of trichloroacetic acid, which rapidly inactivates enzyme activities. Thus, the relative high content of ADP / AMP relative to ATP in the lumen of granules suggests the presence of metabolic activities, e.g., energy-dependent and / or phosphorylation reactions, inside the granule. Supporting this notion, an activity capable of hydrolyzing exogenous [^{3}H]ATP with a rate of 150 ± 16 nmol ATP / min x mg protein was detected in isolated granules following granule permeabilisation with Triton X-100. Thus, ATP, ADP, and AMP likely co-exist within intact mucin granules. While mucin granule isolation was performed at 4°C, a condition that minimizes ATPase activities, the relative abundance of adenyl species within isolated mucin granules in living cells remains to be determined. Nevertheless, the net increase in mass of ADP / AMP in secretions from PAR-stimulated cells (**Fig. 4.9**) surpassed that predicted from the hydrolysis of ATP released alone (**Fig. 4.5**). Thus, the data strongly suggest that an intracellular pool contributed to ADP and AMP release. This conclusion is consistent with the predictions of a recently described mathematical model of nucleotide regulation in ASL. According to this model, AMP and ADP are predicted to be released from airway epithelia via an exocytotic mechanism (100).

Our results suggest that mucin granules release ADP / AMP in preference to ATP. Such a pattern of nucleotide release from goblet cells offers a potential physiological advantage to the airway of selectively activating ion / water transport activities on neighboring ciliated cells, while minimizing autocrine feedback on mucin secretion from goblet cells (see a proposed model of ASL nucleotide regulation in **Figure 4.10**). Specifically, released ADP and AMP can be rapidly hydrolyzed to produce adenosine, which selectively promotes liquid secretion via an A_{2b} receptor / CFTR-mediated mechanism on ciliated cells (7, 25). In contrast, adenosine receptors are not expressed in goblet cells, and this feature, plus the relatively low levels of ATP release, prevent autocrine stimulation of further mucin release from goblet cells. Such a mechanism maximises the capacity to hydrate mucins in normal airways, but allows fine control of mucin secretion.

It is worth noting that non-exocytotic mechanisms likely also contribute to ATP release in airway epithelia. In **Chapter III** we demonstrate that thrombin promotes robust release of ATP from WD-HBE cells, which are largely dominated by non-mucous cells, as well as from lung epithelial A549 cells, which are devoid of mucin granules. ATP release from these cells was partially inhibited by inhibitors of connexin/pannexin hemichannels, suggesting the involvement of conductive mechanisms. A prediction in this scenario is that conductive nucleotide release e.g., from non-mucous cells, would reflect cytosolic nucleotide concentrations, i.e., ATP would be the predominant released species. Our observation that significant amounts of AMP and ADP are stored within and released from mucin granules in thrombin-stimulated Calu-3 cells is predicted to reduce the contribution of the cytosolic pool to nucleotide release in goblet cell metaplasic airway epithelia.

An additional contribution of our study was the identification of VAMP-8 as the vesicle SNARE protein associated with MUC5AC granules in airway epithelial goblet cells (**Fig. 4.7**). Although investigation on the contribution of VAMP-8 to mucin secretion is beyond the scope of the current study, the fact that VAMP-8 immunostaining re-distributed upon agonist-stimulated MUC5AC secretion (**Fig. 4.7D**) provides the first experimental evidence of a functional role for VAMP-8 in goblet cell granule exocytosis, as previously speculated (32).

Thrombin was utilized as a tool to initiate agonist-mediated ATP release in our studies. However, thrombin has been reported to be present in the airways of patients with bronchial asthma and allergic rhinitis (218-219) and to stimulate mucin secretion through PAR1 activation in airway epithelial cells(219). PAR2 is not activated by thrombin but is activated by trypsin, tryptase, catepsin G, and proteinase 3, and its expression is up regulated in respiratory epithelium subsequent to inflammation in asthma and COPD (218). Activation of PAR2 has been linked to mucin secretion in gastrointestinal epithelial cells (220-221) but, according to one study, PAR2 promotes only modest mucin secretory responses in airway epithelial cells (210). Our data, however, suggest that, like PAR1, PAR2 promotes robust mucin secretion (and ATP release) in two airway epithelial cell models. Because chronic airway inflammation is accompanied by goblet cell metaplasia (32), a thrombin and/or trypsin-like PAR-dependent mucin and ATP secretagogue activity may be a significant feature of chronic lung diseases.

In summary, our results demonstrated that mucin granules are an important source of releasable ATP, ADP, and AMP, providing paracrine signaling to ciliated cells for mucin hydration. By releasing predominantly ADP and AMP, mucin granules have the capacity to

minimize autocrine stimulation of mucin release, while favoring adenosine formation, selectively activating ion / water secretion from ciliated cells. Lastly, the observation that both PAR1 and PAR2 agonists elicited robust mucin secretion from polarized monolayers of goblet-like Calu-3 cells suggests that similar processes may be a feature of chronic muco-obstructive lung diseases.

Figure 4.1. PAR agonists stimulate mucin and ATP release from WD-HBE cells. A, RT-PCR analysis indicating that PAR1, PAR2, and PAR3 (but not PAR4) transcripts were amplified in WD-HBE cells; RT, reverse transcriptase. B, C, WD-HBE cultures were incubated basolaterally with vehicle, 50 nM thrombin, 100 μM PAR1-AP, or 100 μM PAR2-AP for 5 min at 37° C. The apical bath was analyzed for mucin content by immuno-slot blot (B) and ATP content by the luciferin-luciferase assay (C). Experiments were performed in quadruplicate with cultures from three different donors. The results are expressed as the mean ± SEM (*, $p < 0.01$).
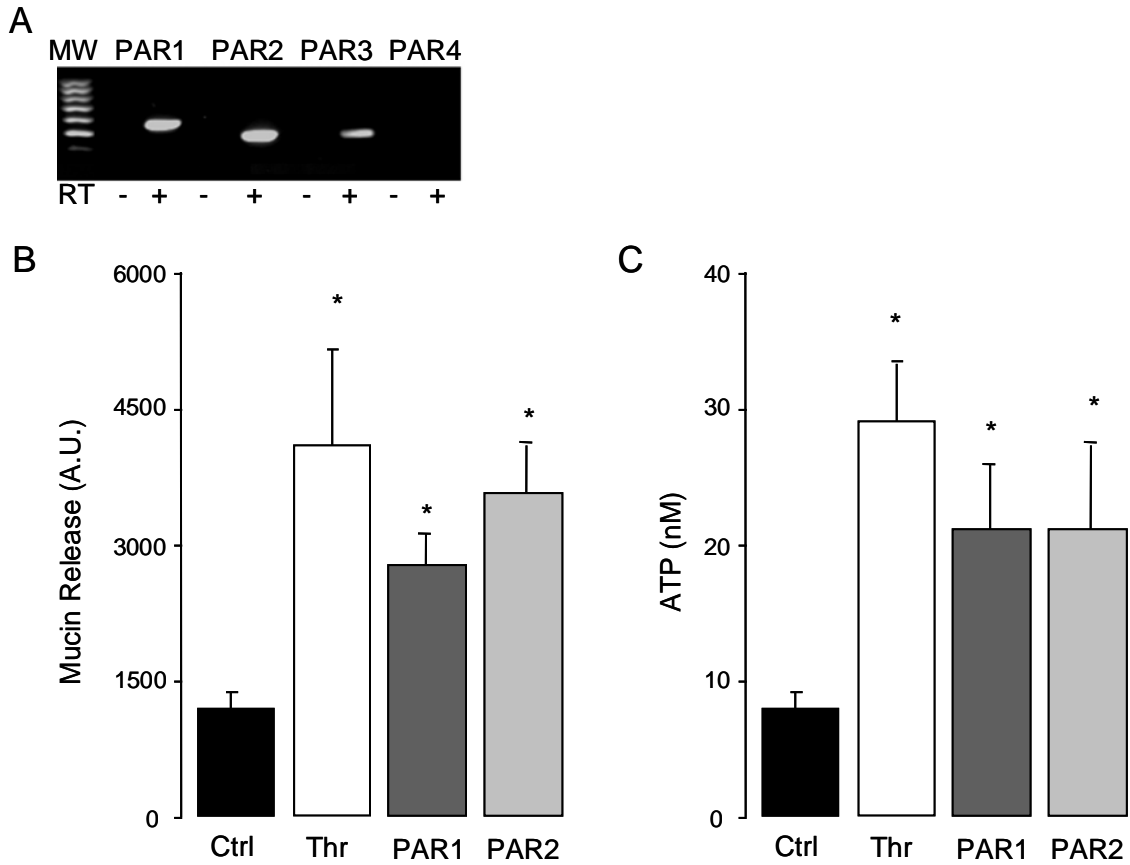
Figure 4.2. Calu-3 cells express PARs. A, RT-PCR analysis indicating that PAR1, PAR2, and PAR3 (but not PAR4) transcripts were expressed in Calu-3 cells. B, C, Intracellular calcium mobilization was assessed in Calu-3 cells loaded with Fura-2. Cells were challenged with 50 nM thrombin, 100 µM PAR1-AP, or 100 µM PAR2-AP added independently (B) or consecutively (C). The tracings are representative of three independent experiments performed in duplicate.
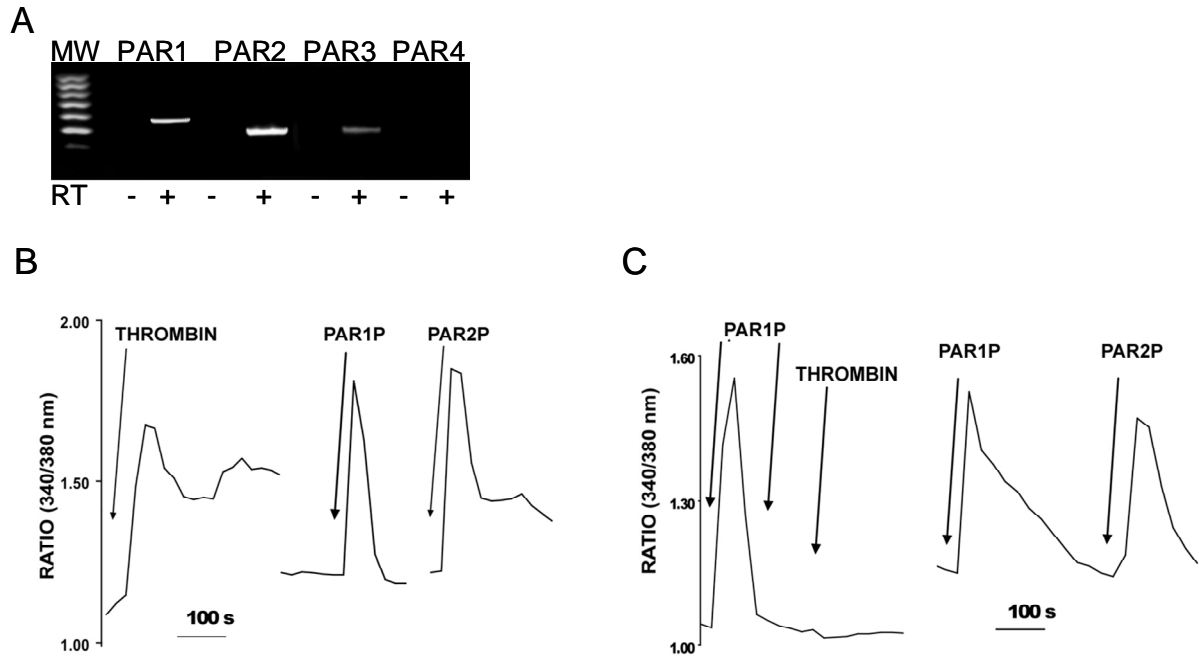
Figure 4.3. PAR agonists stimulate mucin release from Calu-3 cells. Calu-3 cells were challenged with vehicle, 50 nM thrombin, 100 µM PAR1-AP, or 100 µM PAR2-AP for 5 min at 37°C. A, Mucin granule content was determined by immunostaining with a MUC5AC antibody followed by confocal microscopy analysis (bar = 100 µm). B, Quantification of MUC5AC immunostaining in Calu-3 cultures. C, Mucin release in the lumenal bath was assessed by slot blot as in Figure 4.1. The results of a representative experiment are illustrated, and the data are expressed in arbitrary units and are the mean ± SEM (n = 4; *, P< 0.01). Similar results were obtained in three independent experiments.
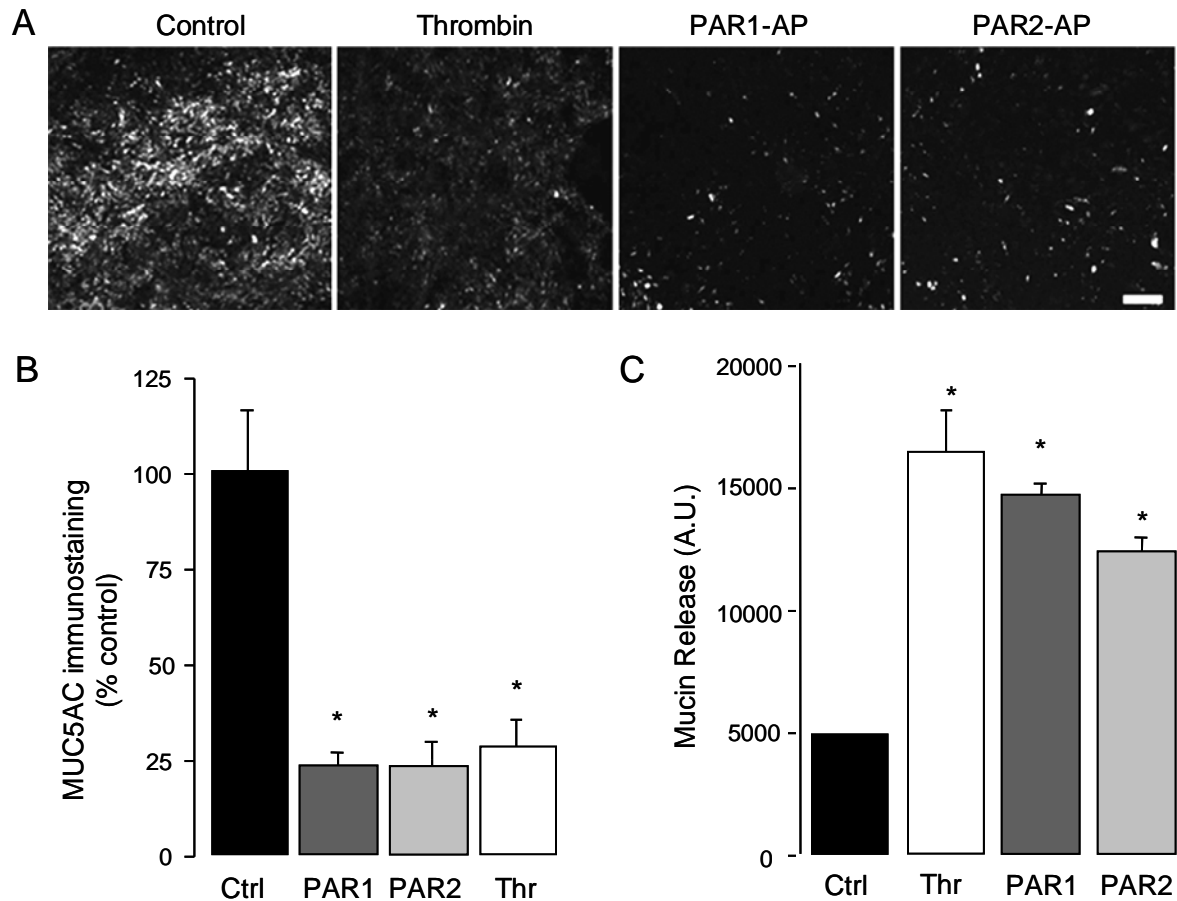
Figure 4.4. PAR-stimulated mucin release is Ca^{2+} and cytoskeleton dependent. Calu-3 cells were pre-incubated for 30 min at 37 °C with either vehicle, 10 μM BAPTA AM, 5 μM cytochalasin D, 100 nM H1152, 10 μM Y27632, or 1 μM ML7. Cells were challenged with vehicle, 50 nM thrombin, 100 μM PAR1-AP, or 100 μM PAR2-AP for 5 min at 37°C. A, Mucin granule content was quantified by immunostaining as in Figure 4.3. B, Mucin release in the apical bath was assessed by slot blot as in Figure 4.1. Experiments were performed three times, each condition in quadruplicate. The results of a representative experiment are illustrated and data are expressed as percentage of control (mean ± SEM; *, p< 0.01 vs. control).
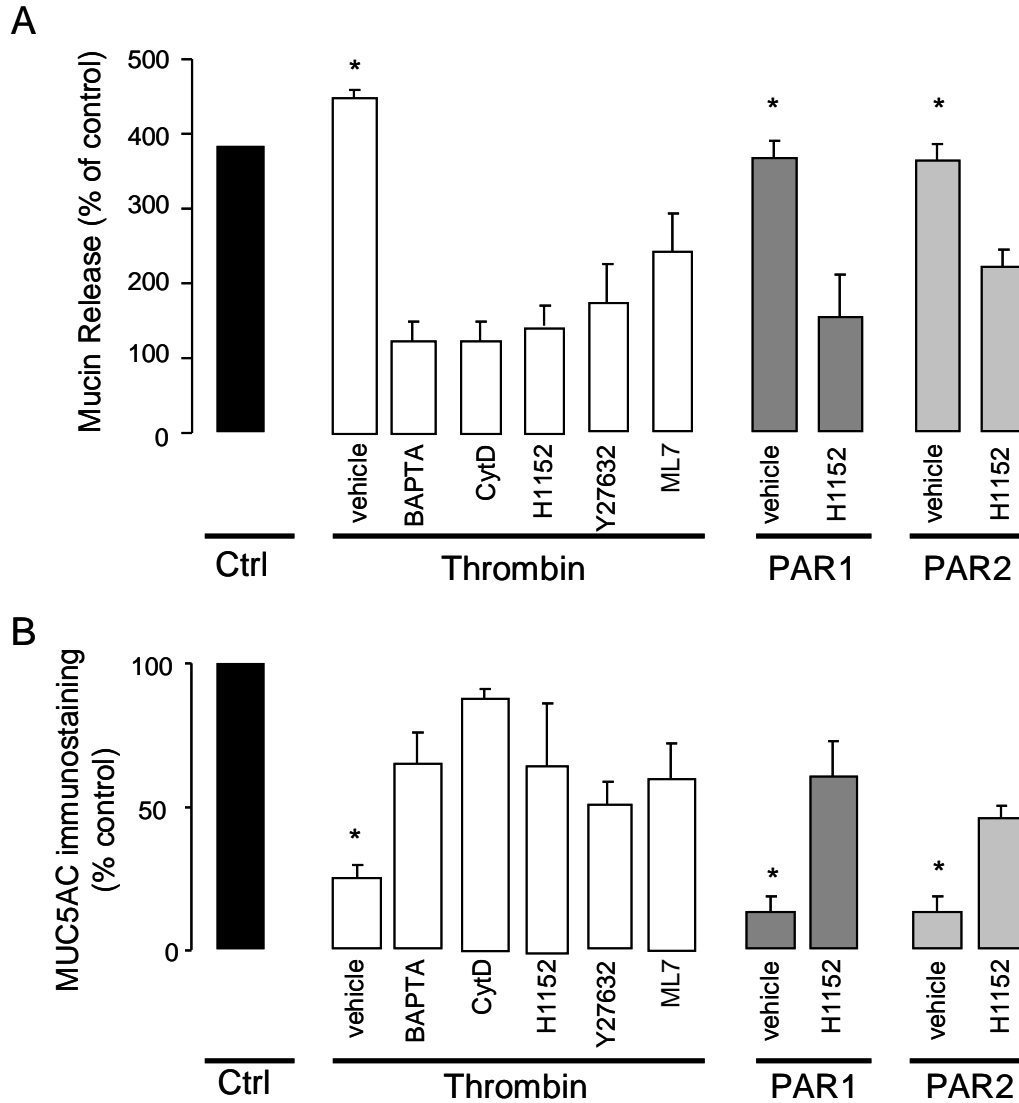
Figure 4.5. PAR-stimulated ATP release involves a vesicular, Ca^{2+}-, and cytoskeleton-dependent mechanism. Calu-3 cells were pre-incubated with inhibitors as in Figure 4.4, or with 4 μM Bafilomycin A_1 for 30 min at 37 °C. Mucosal ATP release following the addition of the indicated PAR agonists (5 min at 37°C) was assessed using the luciferin-luciferase assay in the presence of blockers of ecto-nucleotidases. Experiments were performed in quadruplicate with three independent cultures. The results of a representative experiment are illustrated, and the data are expressed as the difference between PAR agonist and basal values (basal ATP values, 15 ± 5 nM), (mean $\pm$ SEM; *, $p < 0.01$ compared to thrombin stimulation; #, $p < 0.01$ compared to PAR1-AP and PAR2-AP stimulation).
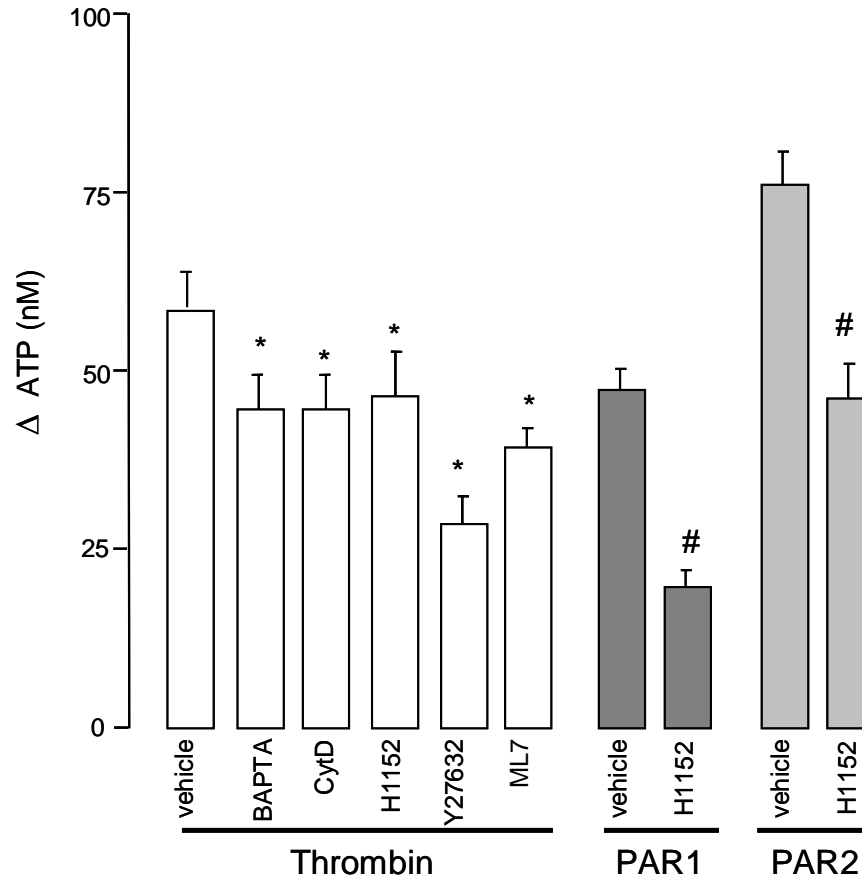
Figure 4.6. PAR agonists stimulate secretion of quinacrine-labelled granules. Calu-3 cell mucin granules were loaded with quinacrine (10 µM, 20 min at 37°C). Cells were mounted in a confocal microscope and real-time images of the DIC / Nomarski illumination (grey) and fluorescence (green) channels acquired every 30 s (see Methods). Cells were challenged with vehicle (control), 50 nM thrombin, 100 µM PAR1-AP, or 100 µM PAR2-AP. A, Overlay of the DIC and fluorescence confocal images of quinacrine-labelled Calu-3 cells in control conditions; bar = 10 um. B, Representation of the change in fluorescence intensity associated with 1 µm-granules after 5 min incubation with vehicle or PAR agonists (n = 3; mean ± SEM; *, $p < 0.01$).

A

B
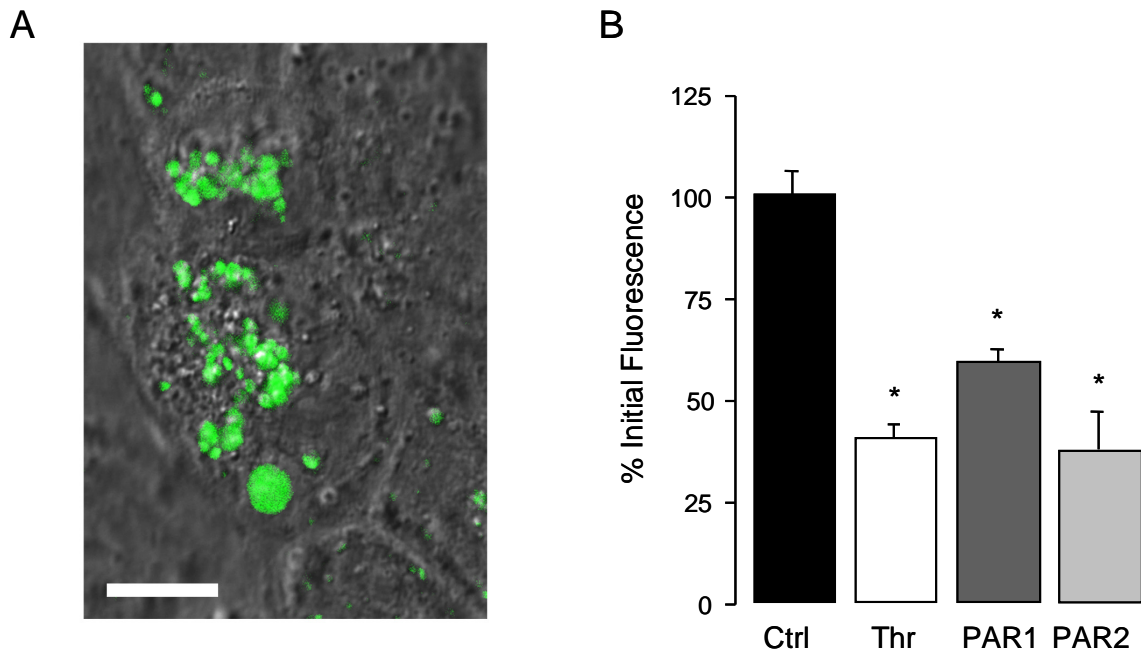
Figure 4.7. Isolation of mucin granules from Calu-3 cells. Mucin granules were isolated from Calu-3 cells using two consecutive Percoll® gradients as described in Methods; the results of a representative isolation experiment are illustrated. A, Confocal microscopy image (DIC / fluorescence channel overlay) of an isolated mucin granule from Calu-3 cultures labelled with quinacrine. B, Image of the immuno-slot blot for MUC5AC representing the first eight fractions of the second gradient. C, The profile of organelle distribution in the second gradient fractions was assessed by immuno-slot blot using specific antibodies that recognize the indicated cellular markers. The quantification of the densitometry data for each organelle marker is expressed as % of the total lysate content. D, Localization of VAMP-8 and MUC5AC was assessed by immunostaining under resting (control; left panels) or thrombin-stimulated (50 nM, 5 min at 37° C; right panels) conditions in Calu-3 cells; bar = 10 µm.

106
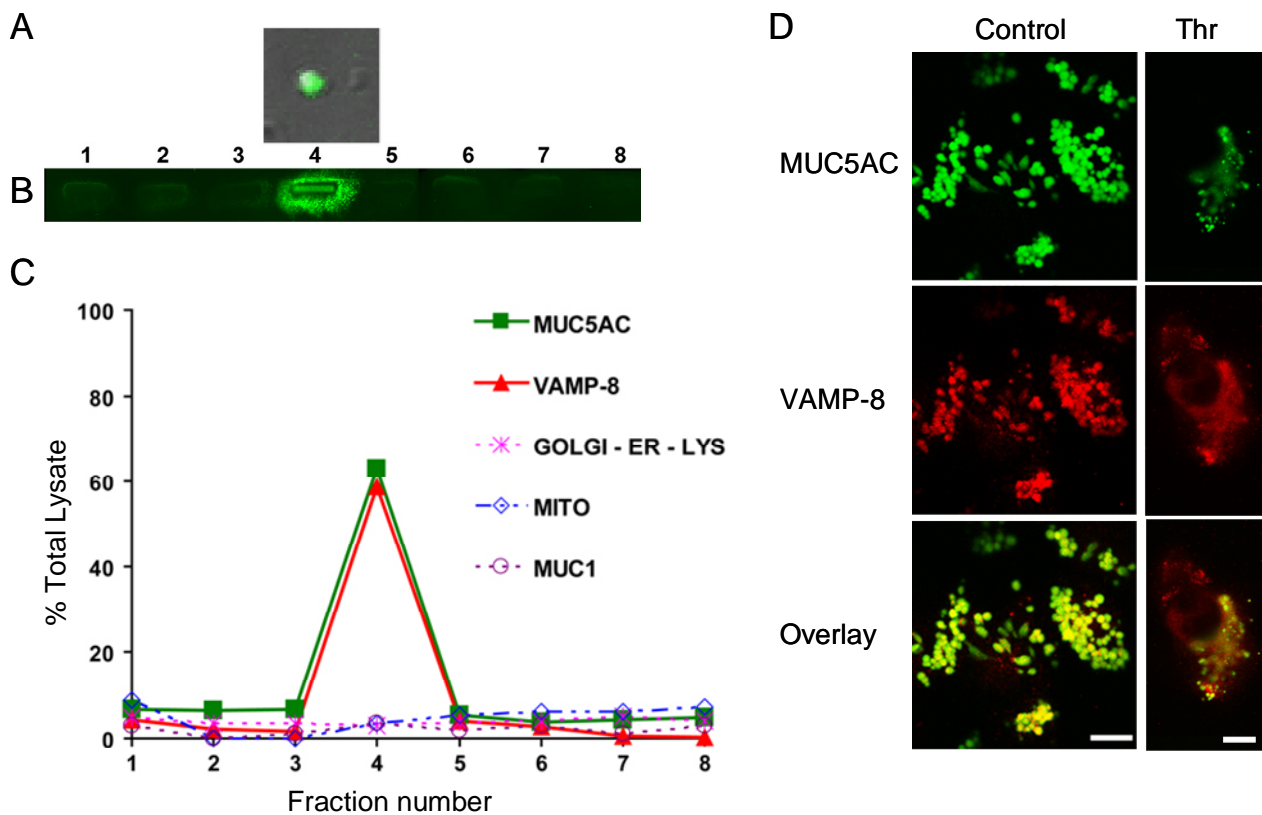
Figure 4.8. Isolated mucin granules contain ATP and other nucleotides. A, Quantification of the amounts of ATP and total adenyl purine in each of the fractions collected in the second gradient was performed by etheno-derivatization and HPLC analysis. Data are expressed as the concentration of ATP (left axis) and total adenine-containing species (right axis); note that left and right axes represent different concentration ranges. B, Quantification of the content of adenyl purine species (ATP, ADP, AMP, and adenosine) in the total cell lysate and isolated mucin granule fraction (i.e. fraction 4) was performed by etheno-derivatization and HPLC analysis. Data are the average of four independent granule isolations and represent the percentage distribution of each species with respect to the total adenyl purine content in the fraction (mean ± SEM). Note: the total adenyl purine mass in the mucin granule fraction represented < 5 % of the cell lysate content.
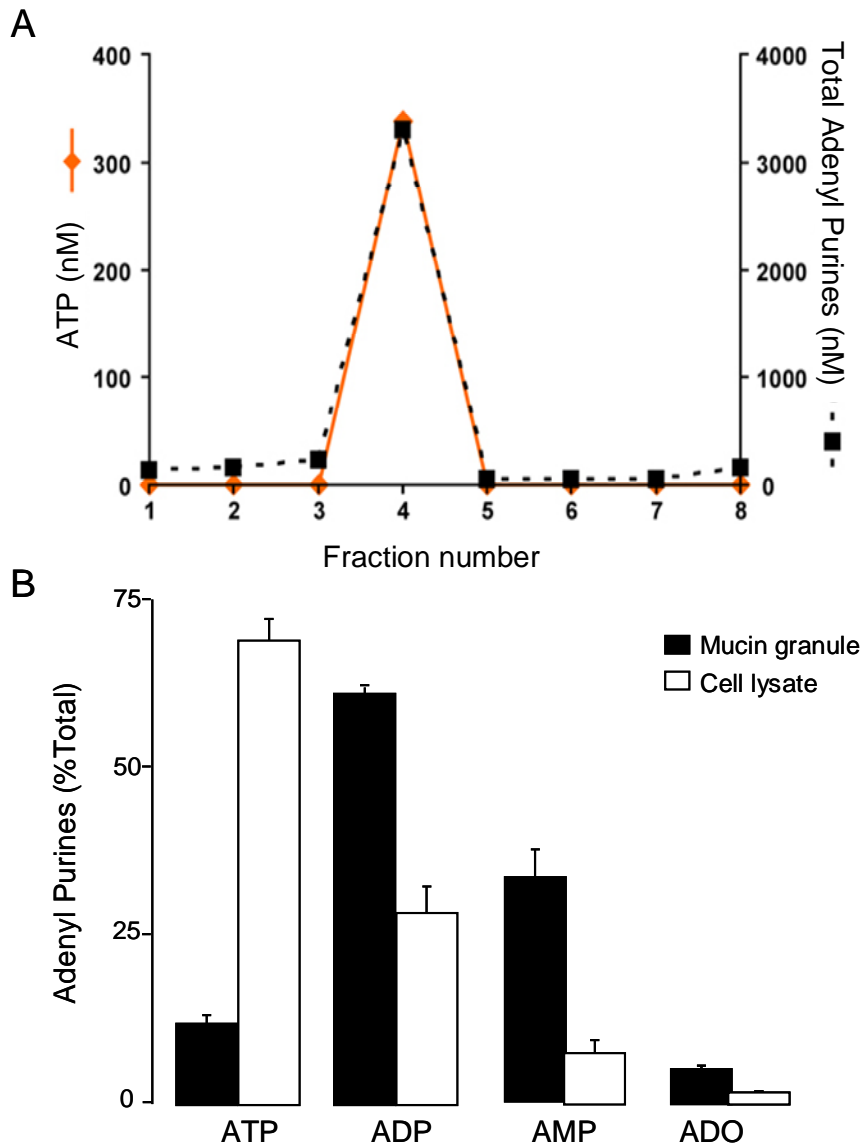
Figure 4.9. Nucleotide composition of Calu-3 cell secretions. Calu-3 cells were stimulated with thrombin (50 nM, 5 min at 37°C) and the apical bath was collected and analyzed for adenyl purines as above. The results of a representative experiment are illustrated, and data are expressed as the mean ± SEM; * , $p < 0.01$ compared to non-stimulated (basal) levels. Similar results were obtained in two independent experiments performed in quadruplicate.
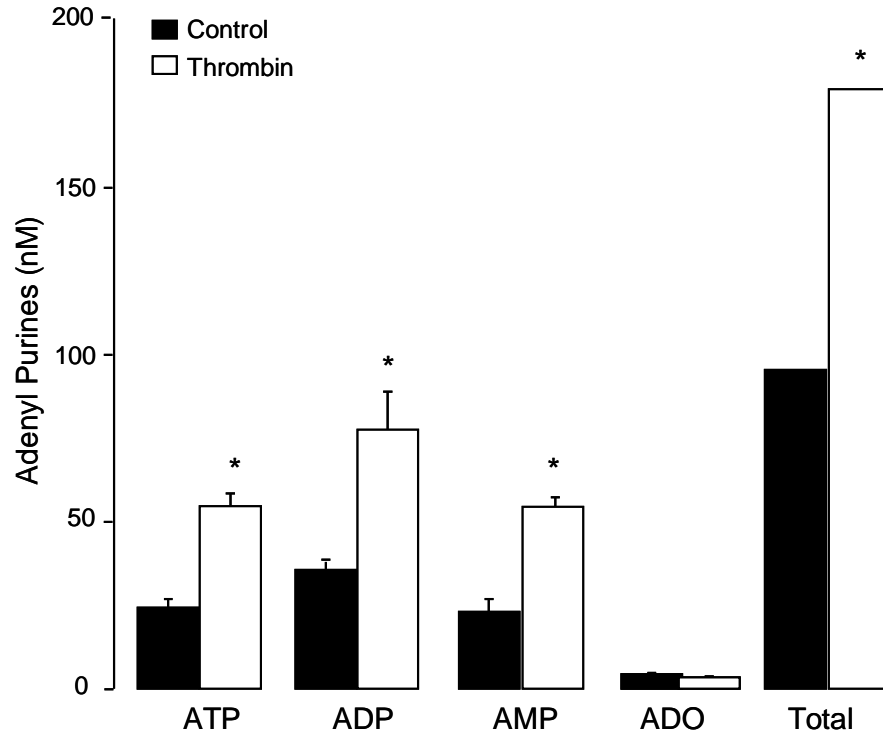
Figure 4.10. Model of adenyl nucleotide regulation in ASL. The schematics represent a ciliated and goblet cell of the airway surface epithelium. Mucin exocytosis from goblet cells is accompanied by release of adenyl nucleotides present in mucin granules as co-cargo molecules. ADP is the prevalent species followed by AMP and ATP. In ASL, ADP and AMP (and ATP) are rapidly metabolised by ecto-nucleotidases into adenosine. Adenyl purines have autocrine and paracrine regulatory activities on epithelial cells. For example, adenosine stimulates the A_{2b} receptor on ciliated cells. CFTR, which is expressed in ciliated cells, is activated by A_{2b} receptor-promoted cAMP formation. Thus, chloride secretion is increased and sodium absorption is reduced (by CFTR-mediated inhibition of ENaC), which generates the driving gradient for water secretion necessary to disperse newly secreted mucins into the ASL. ATP released from mucin granules stimulates $P2Y_2$ receptors on goblet cells for further mucin secretion, and on ciliated cells resulting in activation of TMEM16A or CaCC, activation of CFTR, and inhibition of ENaC.
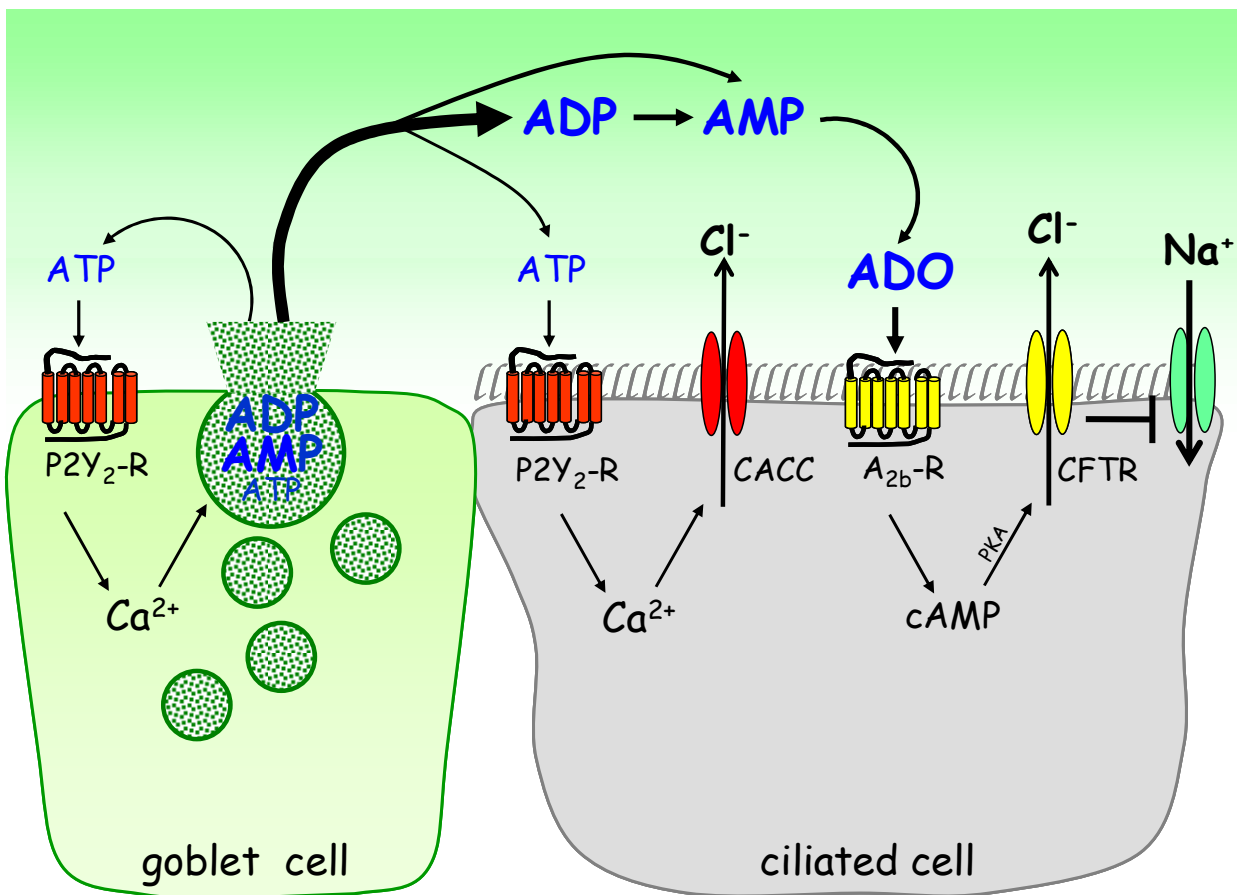
CHAPTER V

Rho-dependent pannexin 1-mediated ATP release from airway epithelia

1. Introduction

The MCC process that removes foreign particles and pathogens from the airways is the primary innate defense mechanism in the lung (222). Nucleotides and nucleosides within the ASL regulate key components of MCC via activation of epithelial cell surface purinergic receptors (206, 223). ATP activates the G_q-coupled $P2Y_2$-R that promotes mucin secretion and ciliary beat frequency, and regulates electrolyte transport and ASL volume production by inhibiting sodium absorption (21, 32, 45, 56-57, 61, 162) and promoting CaCC activity (18, 29, 35, 48-49, 163). Adenosine, generated from the hydrolysis of ATP, activates the G_s-coupled A_{2b}-R that promotes cyclic AMP-regulated CFTR Cl^- channel activity (164) and increases CBF (21). While ATP and adenosine are naturally occurring signaling molecules in ASL (7, 11, 25-27), the mechanisms of airway epithelial ATP release are poorly understood.

The lung epithelia exhibit a complex cellular composition, and thus, several mechanisms and pathways likely are involved in the release of nucleotides into the airways. Studies with goblet-like cell models indicate that ATP and other nucleotides are released concomitantly with MUC5AC, a secretory mucin, during Ca^{2+}-regulated exocytosis of mucin granules (71). Thus, mucin secreting granules may constitute an important source of ASL ATP, providing a pathway for paracrine signaling to ciliated cells, i.e., for mucus hydration and clearance. A vesicular mechanism of nucleotide release may also operate in non-mucous cells. For example, by selectively manipulating the levels of expression of Golgi-resident nucleotide-sugar transporters in 16HBE14o$^-$ cells, a cell line that mimics aspects of ciliated epithelia, Sesma *et al.* demonstrated that the Golgi lumen is an important source of extracellular UDP-sugar constitutively released from cells (94). Although not formally demonstrated, a similar mechanism may apply for the constitutive release of ATP.

Mechanical forces during tidal breathing and coughing and cell swelling during hypotonic gland secretions are ubiquitous stimuli imparting robust ATP release from the airways, but the mechanism involved in mechanically-promoted airway epithelial ATP release are not well-defined (7, 26, 87, 105, 224). Recently, Ransford *et al.* reported that ATP release from hypotonically-swollen WD-HBE cell cultures was nearly 60% inhibited by non-selective hemichannel blockers or by knocking down pannexin 1, via shRNA (207). Thus, pannexin 1 is a candidate ATP release pathway in hypotonically swollen WD-HBE cells. However, regulatory signaling elements transducing hypotonic/mechanical stress into ATP release have not been identified.

In **Chapter III**, we described that activation of G protein-coupled PAR resulted in enhanced release of ATP from WD-HBE cells, which was attenuated by non-selective inhibitors of connexins/pannexin hemichannels. PAR-elicited ATP release reflected a Rho-dependent mechanism, suggesting a link between Rho activation and hemichannel opening. In the present study we tested the hypothesis that ATP release from mechanically stimulated airway epithelial cells involves a Rho-regulated opening of pannexin 1-hemichannels.

2. Methods

Reagents- 2-Phenyl-1,2-benzisoselenazol-3(2H)-one (ebselen), β,γ-methylene ATP (β,γ-metATP), carbenoxolone, flufenamic acid, and luciferase from *Photinus pyralis* were obtained from Sigma (St. Louis, MO. Luciferin was obtained from BD PharMingen (Franklin Lakes, NJ). The Rho Activation Assay Biochem Kit was purchased from Cytoskeleton (Denver, CO). ML-7 and H1152 were purchased from Calbiochem. HC67047 was a kind gift from Dr. David Clapham (Hydra Biosciences). The pannexin 1 blocking peptide WRQAAFVDSY ([10]Panx1) (196), and its scrambled version, ([Scr]Panx1) SADYRVAFWQ,

112

generated using the online software at Genscript (http://www.genscript.com/scrambled_library.html) were synthesized at the UNC Microprotein Sequencing and Peptide Synthesis Facility. Other chemicals were from sources previously reported (25, 71).

Cell culture and incubations- Primary cultures of WD-HBE cells were provided by the Cystic Fibrosis/Pulmonary Research and Treatment Center Tissue Procurement and Cell Culture Core at UNC. WD-HBE cells were grown on 12-mm Transwell supports (Costar) and maintained at air–liquid interface, as previously described (25, 225). A549 lung epithelial cells were grown to confluence on plastic dishes as described in **Chapter III**. Cells were rinsed twice with HBSS supplemented with 1.6 mM $CaCl_2$, 1.8 mM $MgCl_2$, and 25 mM HEPES pH 7.4 (HBSS+) and pre-incubated as indicated below in the corresponding assay sections. Hypotonic challenge was applied by gently replacing one third of the volume of the extracellular solution with a HEPES-buffered (pH 7.4) solution containing 1.8 mM $MgCl_2$ and 1.6 mM $CaCl_2$, thus reducing the solution tonicity to 200 mOsm, as previously described (26). A saline-based (isotonic) solution containing the above additions was used for volume replacement in control cultures.

For experiments involving phasic motion-promoted shear stress, WD-HBE cultures were placed on the platform of an in-house designed device, which was subjected to rotational go/stop cycles (28 cycles/min) inside a humidified incubator (7). The change in velocity caused by this phasic motion was similar to changes seen during in vivo inspiration during normal tidal breathing, as previously described (7).

Measurement of ATP release- ATP concentrations in WD-HBE and A549 cells were quantified off-line via a LB953 AutoLumat luminometer (Berthold), as described in **Chapter**

III. Calibration curves using known concentrations of ATP were generated at the end of each experiment. None of the reagents used during ATP release measurements interfered with the luciferase reaction.

RT-PCR analysis- Total RNA was prepared using the RNeasy Mini Kit (Qiagen, Inc., Valencia, CA) and reverse-transcribed using SuperScript III reverse transcriptase (RT; Invitrogen Corporation, Carlsbad, CA). RT-PCR was performed using the following cycling conditions: 4 min/94°C, 1 min/72°C, 45 s/94°C, 1 min/55°C, and 1 min/72°C; 36 cycles. Amplified products were sequenced at the UNC Genome Analysis Facility. Primer compositions are indicated in **Table 5.1.**

Semi-quantitative RT-PCR was performed in a Lightcycler PCR machine® thermal cycler (10 min/95ºC; 5 s/55ºC, 8 s/72ºC; 45 cycles), as described **in Chapter III**. GAPDH served as a housekeeping gene for normalization between samples, and was included in each cycling run. The melting temperature of the PCR product for each reaction was monitored to ensure that only a single product of the correct size was amplified. Primers for GAPDH were: forward, 5'-GAAGTTGAAGGTCGGAGTCA-3', and reverse, 5'-GATCTCGCTCCTGGAAGATG-3'. Other primer pairs are indicated in **Table 5.1.**

Uptake of propidium iodide- WD-HBE cells were rinsed and challenged for 5 min in the presence of 20 µM propidium iodide (added apically). At the end of the incubation, the bathing solution was replaced with HBSS+ containing 4% paraformaldehyde. Acquisition of confocal images and quantification of nuclei staining were performed as described in Chapter III.

siRNA- Oligonucleotides targeting human pannexin 1 (5'-GCATCAAATCAGGGATCCT-3') and its scrambled control (5'-

GCTTGACCCACGGTATAA-3'), were purchased from Dharmacon Inc. A549 cells were transfected with 1 µg oligonucleotide using the Amaxa Nucleofector Device™ and Cell Line Nucleofector® Kit T (Amaxa Biosystems, Gaithersburg, MD), following the manufacturer instructions. Assays were performed 48 h after transfections.

Overexpression of dominant negative mutants of RhoGEF and RhoA- pcDNA3.1 vectors encoding p115RGS and RhoA(T19N) were kindly provided by Dr. T. K. Harden (176-177). A549 cells were transfected with empty vector or vector containing the desired insert using the Amaxa Nucleofector Device™.

RhoA pulldown assay- Measurements of GTP-bound RhoA were performed using the Rho Activation Assay Biochem Kit, following to the manufacturer instructions, as described in **Chapter III**.

MLC phosphorylation- Proteins were resolved by SDS-PAGE and duplicated membranes were separately blotted with anti-phospho-MLC(Ser19) antibody (1:500) or anti-MLC (1:1000) antibodies (Cell Signaling Technology Inc. Danvers, MA) followed by goat anti-rabbit Alexa Fluor®680 secondary antibody (Invitrogen, Eugene, Oregon). Immunoblots were revealed and quantified as described in **Chapter III**.

Cell volume regulation- Changes in cell height were measured to estimate cell volume changes, as described previously (26). In brief, WD-HBE cells were loaded with 5 µM calcein-AM (Molecular Probes, Eugene, Oregon) for 30 min at 37 °C. The apical surface of cultures was equilibrated for 10 min with 33 µl HBSS+ and the osmolarity of the solution was reduced to 200 mOsm, as indicate above. Xz-scanning images were obtained every second for initial 15 s, then every 5 s for next 75 s.

Data Analysis- Differences between means were determined by unpaired Student's t-test and were considered significant when $p < 0.05$.

3. Results

Hypotonic stress promotes pannexin 1-mediated dye uptake and ATP release. Connexins and pannexins form non-junctional hemichannels and they have been proposed to release ATP in receptor- and hypotonic shock-stimulated airway epithelial cells [(207) and **Chapter III**]. However, whether connexin/pannexin hemichannels form functional pores at the WD-HBE cell surface and, if so, how are they regulated, is not well-understood.

As an initial test for the expression of functional hemichannels on WD-HBE cells, the uptake of the hemichannel-permeable reporter dye propidium iodide was investigated. Propidium iodide displays low intrinsic fluorescence, but its fluorescence increases 20- to 30-fold upon binding to nucleic acids. Under resting conditions, a small number of HBE cells displayed nuclear labeling with propidium iodide, but nuclear fluorescence increased sharply upon exposure of the cells to hypotonic challenge (**Fig. 5.1A and B**). The time-course of propidium iodide uptake following the hypotonic challenge was nearly identical to that of ATP release (**Fig. 5.1B**). Both propidium iodide uptake (**Fig. 5.1C**) and ATP release (**Fig. 5.1D**) were markedly impaired in the presence of 10 µM carbenoxolone, a licorice root derivative that preferentially albeit not selectively inhibits pannexin hemichannels over connexin hemichannels and volume regulated anion channels (226-228). Control experiments indicated that carbenoxolone did not affect hypotonicity-induced cell swelling (**Fig. 5.4A**). Consistent with the notion that released ATP promotes regulatory volume decrease (RVD) in hyponically-swollen WD-HBE cells (26), carbenoxolone delayed RVD (**Fig. 5.4B**). Flufenamic acid, a potent inhibitor of connexin hemichannels (229) that displays low affinity

towards pannexin 1 (226) had no significant effect on ATP release and propidium iodide uptake in WD-HBE cells (**Fig 5.1C and D**). The potential involvement of pannexin 1 in ATP release and dye uptake was further tested by assessing the effect of the pannexin 1-selective blocking peptide [10]Panx1. [10]Panx1 (30 µM), but not its scrambled control, completely blocked the uptake of propidium iodide in hypotonically-challenged WD-HBE cells (**Fig. 5.1C**). ATP release was in parallel inhibited by [10]Panx1 (**Fig. 5.1D**). These results strongly suggest that pannexin 1 is an important mediator of ATP release from WD-HBE cells. It is worth noting, however, that inhibition of ATP release by [10]Panx1 (50-60%) was less robust than the nearly 100% inhibition observed on dye uptake (compare **Figs. 5.1C and 5.1D**), suggesting that mechanisms additional to hemichannel opening contribute to ATP release in these cells.

RT-PCR analysis confirmed the expression of pannexin 1 in WD-HBE cells (**Fig. 5.2A**). Sequencing analysis of the product of the PCR reaction indicated the insertion of GGT ATG AAC ATA 66 bp upstream of the termination codon of pannexin 1, suggesting that the 426 amino acid-long pannexin 1b [Gene Bank NP_056183.2 (230)] is the major pannexin 1 sub-variant expressed in WD-HBE cells. Brain-specific pannexin 2 (230) and pannexin 3 could not be amplified in these cultures (**Fig. 5.2A**).

Experiments illustrated also in **Figure 5.2** indicated the presence of pannexin 1 transcripts in lung carcinoma A549 cells (**Fig. 5.2B**). Like WD-HBE cells, A549 cells displayed enhanced propidium iodide uptake (**Fig. 5.2C**) and ATP release (**Fig. 5.2D**) in response to hypotonic challenge, which were inhibited by carbenoxolone and [10]Panx1. Also similar to WD-HBE cells, [10]Panx1 nearly completely blocked dye uptake while robustly, but not completely, impaired ATP release.

Unlike WD-HBE cells, A549 cells can be efficiently transfected with cDNA expression vectors and siRNA oligonucleotides [as described in **Chapter III**]. Thus, we took advantage of these cells to further assess, via siRNA, the involvement of pannexin 1 in ATP release and dye uptake. A549 cells transfected with pannexin 1 siRNA olygonucleotides (but not its scrambled version) exhibited a ~50% reduction of pannexin 1 transcript levels (**Fig. 5.3A).** The siRNA approach was selective for pannexin 1 since it did not affect the expression of connexin 43 transcripts (**Fig. 5.3A**). Pannexin 1 siRNA-transfected cells exhibited ~50% reduced hypotonic challenge-promoted ATP release (**Fig. 5.3B**) and propidium iodide uptake (**Fig. 5.3C**).

Collectively, the data in **Figures 5.1-5.3** strongly suggest that pannexin 1 mediates the uptake of propidium iodide and contributes to the release of ATP in hypotonic stress-stimulated airway epithelial cells.

Rho GTPases regulate ATP release from hypotonically stimulated airway epithelial cells. Based on our studies in **Chapter III** suggesting that Rho GTPases are important regulators of ATP release in cells stimulated with the serine protease thrombin, we examined the possibility that Rho signaling is involved in ATP release from hypotonic-stress stimulated WD-HBE cells. Therefore, the effects of inhibitors of ROCK and ROCK downstream effectors were investigated in WD-HBE cell cultures subjected to hypotonicity-induced cell swelling (26). Hypotonic challenge-promoted ATP release was reduced in the presence the ROCK inhibitor H1152 (**Fig. 5.5**). The regulatory domain of MLC is a major downstream effector of ROCK. By phosphorylating and inactivating MLC phosphatase, ROCK facilitates MLC phosphorylation by MLCK (187). Consistent with the possibility that MLC phosphorylation was involved in ATP release from hypotonicity-stimulated WD-HBE cells,

the MLCK inhibitor ML-7 markedly reduced ATP release from these cells (**Fig. 5.5A**). ML-7 and H1152 had no effect on hypotonic stress-elicited cell swelling (**Fig. 5.3C**). These results suggest that hypotonic stress promoted Rho/ROCK activation and enhanced MLC phosphorylation upstream of ATP release.

To directly verify that hypotonic stress induces Rho activation and MLC phosphorylation in WD-HBE cells, RhoA-GTP and MLC phosphorylation were measured by the pulldown assay and phospho-MLC (Ser19) immunoblot, respectively. As illustrated in **Figure 5.5B and C**, hypotonic stress enhanced RhoA activation and MLC phosphorylation, respectively, relative to control cells. Consistent with the notion that ROCK and MLCK act on MLC (187), H1152 and ML-7 reduced MLC phosphorylation in hypotonicity challenged WD-HBE cells (**Fig. 5.5C**).

While the above-described experiments indicated that RhoA was activated in response to hypotonic challenge, evidence that Rho activation is involved in ATP release relies on pharmacological inhibitors with less than ideal selectivity. To more conclusively assess the involvement of Rho in ATP release, the effect of a dominant negative mutant of RhoA, RhoA(T19N), which tightly binds to Rho-GEF but does not promote downstream effector activation, was examined. A549 lung epithelial cells transiently transfected with RhoA(T19N) cDNA. Transfected cells displayed reduced hypotonic shock-evoked ATP release, relative to empty vector-trasnfected cells (**Fig. 5.6A**). Unlike RhoA(T19N), cell transfection with p115-RGS, which inhibits the coupling between $G\alpha_{12/13}$ and p115-RhoGEF in response to GPCR activation [see **Chapter III**] had no effect on hypotonic shock-promoted ATP release (**Fig. 5.6A**). As expected, RhoA activation and MLC phosphorylation were impaired in cells transfected with RhoA(T19N) (**Figs. 5.6B**).

Rho signaling regulates dye uptake in airway epithelial cells. Having determined that ATP release from hypotonic stress-stimulated cells (i) reflects a Rho-dependent process (**Figs. 5.5 and 5.6**) and (ii) is associated with pannexin 1 activation (**Figs. 5.1 - 5.3**), the potential link between Rho signaling and hemichannel opening was examined. Both the Rho kinase inhibitor H1152 and the MLCK inhibitor ML-7 caused a nearly complete inhibition of hypotonic challenge-promoted propidium iodide uptake in WD-HBE cells (**Fig. 5.7A and B**). Moreover, transfection of A549 cells with RhoA(T19N) markedly reduced the uptake of propidium iodide in these cells (**Fig. 5.7C**).

Shear stress promotes airway epithelial ATP release in a Rho kinase-, MLCK-, and pannexin 1-dependent manner. Hypotonic shock was utilized above as a tool to initiate cell swelling-mediated ATP release. In addition to cell swelling triggered *in vivo* by hypotonic gland secretions (103), the airways are continuously exposed to shear stress during tidal breathing and coughing, which impart ATP release-dependent MCC activities (7). However, how shear stress elicits ATP release is not known. A hypothesis derived from our studies in **Chapter III** and current observations (**Figs. 5.1-5.7**) is that Rho GTPases and pannexin hemichannels are upstream regulators and effectors, respectively, of ATP release. Therefore, we examined the effects of pannexin 1 blockers and Rho kinase/MLCK inhibitors in the release of ATP from shear stress-stimulated WD-HBE cell cultures. Using a specially-designed device, WD-HBE cell cultures were subjected to acceleration/deceleration cycles to deliver phasic shear stress over the apical cell membrane with profiles similar to airflow-induced shear stress (7). Consistent with an involvement of Rho signaling, shear stress-induced ATP release was partially inhibited by H1152 and ML-7 (**Fig. 5.8**). Moreover, shear

stress-elicited ATP release was also reduced in the presence of carbenoxolone or the pannexin 1 blocking peptide [10]Panx1 (but not its scrambled control peptide) (**Fig. 5.8**).

TRPV4 as a potential effector upstream of ATP release. The transient receptor potential vanilloid (TRPV) 4 channel is a broadly expressed cation channel that acts as a sensor of various physical stimuli such as heat, osmotic stress, shear stress, and stretch (231-233). Particularly relevant to our study, it has been recently reported that TRPV4 mediated ATP release in response to osmotic stress in the thick ascending limb of the renal medulla (234) and in stretch-stimulated urothelia (235). Since TRPV4 is abundantly expressed in the airways, we hypothesized that TRPV4 transduces mechanical stimuli into Rho/pannexin 1-mediated ATP release in airway epithelia. An initial assessment of this hypothesis indicated that ruthenium red (10 µM), a non-selective inhibitor of TRP channels, markedly inhibited hypotonic stress-promoted ATP release in WD-HBE cells (data not shown). Consequently, the effect of the highly selective TRPV4 inhibitor HC67047 was examined. As depicted in **Figure 5.9**, pre-incubation of the cells for 30 min in the presence of 10 µM HC67047 markedly impaired ATP release (**Fig. 5.9A**) and dye uptake (**Fig. 5.9B and C**) in hypotonicity-challenged WD-HBE cells. Control experiments indicated that HC67047 did not affect hypotonic-stress-elicited cell swelling (**Fig. 5.4C**), indicating that the target of the TRPV4 inhibitor was located downstream to the cell volume change and plasma membrane stretching triggered by the osmotic challenge. Lastly, HC67047 completely impaired hypotonic stress-promoted RhoA-GTP formation, but had no effect on the Rho response to thrombin activation of PARs (**Fig. 5.9D**).

4. Discussion

A key physiological component of lung function involves the complex and not well-defined mechanism that controls MCC activities. Nucleotides (e.g., ATP) and nucleosides (i.e., adenosine) are present in physiologically relevant concentrations in ASL both *in vivo* and *in vitro*. Compelling evidence suggests that these molecules acting on epithelial cell surface purinergic receptors are major regulators of electrolyte transport, cilia beating, and mucin secretion (206). However, the mechanisms that control the release of nucleotides into ASL are incompletely understood.

We now demonstrate that WD-HBE cells display hypotonic stress-promoted uptake of the hemichannel probe propidium iodide with kinetics overlapping that of ATP release. We further show that the non-selective hemichannel inhibitor carbenoxolone, the pannexin 1-selective blocking peptide [10]Panx1, and pannexin 1 siRNA markedly decreased dye uptake, in addition to reducing ATP release. Thus, pannexin 1 is functionally expressed at the airway epithelial plasma membrane, i.e. as an ATP (and dye) permeable channel. However, the major finding of the current study is that the pannexin 1-associated activities are controlled by Rho GTPases and their downstream effectors. Specifically, we demonstrated that hypotonic stress elicited MLC phosphorylation in a Rho kinase-dependent manner and that inhibition of MCL phosphorylation (with the Rho kinase inhibitor H1152 or the MLC kinase inhibitor ML-7) decreased ATP release and impaired dye uptake (**Fig.5.5A and 5.7A**). Furthermore, our results show that hypotonic stress promotes RhoA activation in airway epithelial cells (**Fig 5.5**) and that selective inhibition of RhoA activation (using a RhoA dominant negative mutant) resulted in impaired MLC phosphorylation, dye uptake, and ATP release (**Fig. 5.6 and 5.7**). Taken together, these results strongly suggest that RhoA/Rho

kinase activation (and subsequent MLC phosphorylation) is an early step upstream of pannexin 1-mediated ATP release in hypotonic stress-stimulated epithelia. We have not addressed the mechanism by which Rho contributed to pannexin 1-mediated ATP release. However, given the actions exerted by Rho/Rho kinase on cytoskeleton components [e.g., regulating MLC phosphorylation and actin polymerization (189)], one speculation is that Rho-promoted membrane-cytoskeletal rearrangements facilitates pannexin 1 interaction with regulators.

Our study provides new clues as to the potential mechanism by which hypotonic challenge resulted in Rho activation. We demonstrated that TRP channel inhibitors markedly reduce ATP release from WD-HBE cells. We also demonstrated that the highly selective TRPV4 inhibitor HC67047 not only reduced hypotonic stress-triggered ATP release but impaired dye uptake and Rho activation (**Fig. 5.9**). The most compelling interpretation of these results is that TRPV4, which is a mechano- and osmo-sensor Ca^{2+} (and Mg^{2+}) channel abundantly expressed in the airways, transduces hypotonic cell swelling (and likely shear stress) into Rho activation. Although we have not investigated the signaling that links TRPV4 with Rho, Ca^{2+}-elicited RhoGEF activation likely is involved. This hypothesis is in part based on a recent study illustrating that TRPC6 (a distant relative of TRPV4) contributes to RhoA activation in endothelial cells via Ca^{2+}-dependent protein kinase C activation and subsequent phosphorylation and inhibition of GDP dissociation inhibitor-1 (GDI-1) and phosphorylation and activation of p115RhoGEF (236). In this regard, however, our data suggest that the $G\alpha_{12/13}$/p115-RhoGEF pathway, a major mechanism for Rho activation in PAR-stimulated cells [discussed in **Chapter III**], is not involved in hypotonic stress-elicited Rho activation. Specifically, thrombin-promoted RhoA activation was not affected by the TRPV4 inhibitor

(**Fig. 5.9B**), and transfection of cells with p115-RGS, a dominant negative mutant of p115RhoGEF, resulted in inhibition of thrombin-promoted ATP release without affecting hypotonic stress-evoked ATP release (**Fig. 5.6A**). Whether hypotonic stress/TRPV4/Ca^{2+} activates p115-RhoGEF (or other RhoGEF) independently of $G_{\alpha12/13}$, remains to be elucidated.

The airways are continuously exposed to mechanical forces, e.g. shear stress imparted by airflow during tidal breathing and coughing, which promote MCC functions via ATP release (7, 105). Our data demonstrate mechanical shear stress-promoted ATP release that was diminished by inhibitors of Rho kinase, MLC kinase, and pannexin 1. Although the mechanism of shear stress-promoted ATP release remains less extensively investigated than hypotonic stress- or receptor-promoted nucleotide release, our results suggest that common signaling pathways and effectors operate in response to these physiologically relevant stimuli.

It is worth nothing, however, that pathways in addition to pannexin 1 likely contribute to ATP release in WD-HBE cells. Indeed, our results in **Figures 5.1, 5.5, and 5.7** indicate that residual ATP release activity is evident under conditions in which dye uptake has been completely or nearly completely abrogated by [10]Panx1 or H1152. While these results suggest that connexins do not contribute to the residual ATP release, volume-regulated channels, maxi-anion channels (121), and vesicle exocytosis (94, 170) are potential mechanisms for pannexin1-independent nucleotide release.

In sum, we have shown that pannexin1 is an important contributor to ATP release in hypotonic stress- and shear stress-stimulated airway epithelia. Our data also indicate that hypotonic stress induces Rho activation upstream of pannexin hemichannel opening, and that

TRPV4 channels likely transduce hypo-osmotic stress into RhoA-promoted pannexin 1-mediated ATP release.

Table 5.1. Primers used for standard PCR amplification of pannexins (Panx) and connexin 43 (Conx 43). Sequences are indicated in the 5'→3' order.

Panx 1 forward	GAGGTATCTGAAAGCCACTTCAAGTACCC
Panx 1 reverse	TATGGTACCGCGCAAGAAGAATCCAGAAGTC
Panx 2, forward	ACCAAGAACTTCGCAGAGGA
Panx 2 reverse	CCACGTTGTCGTACATGAGG
Panx 3 forward	AGCTCCGATCTGCTGTTCAT
Panx 3 reverse	AGGGTTCTAAGCCAGCCAAT
Conx 43 forward	GGGTTAAGGGAAAGAGCGACC
Conx 43 reverse	CCCCATTCGATTTTGTTCTGC

Figure 5.1. **Hypotonicity-induced dye uptake and ATP release in WD-HBE cells.** A, uptake of propidium iodide was assessed on real-time in response to a 33% hypotonic stress, as described in Methods. The images represent propidium iodide-associated nuclear fluorescence; bar, 100 μm. B, time-course of hypotonic stress-promoted ATP release and propidium iodide uptake. Results are expressed as the percent of nuclei displaying fluorescence. Similar results were obtained in at least three separate experiments performed in quadruplicate. C and D, WD-HBE cells were pre-incubated for 15 min with vehicle or with 10 μM carbenoxolone (CBX), 100 μM flufenamic acid (FFA), 100 μM ^{10}Panx1 or its scrambled control (^{src}Panx1), and challenged for 5 min with isotonic solution (Iso), or hypotonic solution (Hypo) containing the indicated drugs. The results are the mean ± SEM, n = 4. Dye uptake (C) and ATP release (D) were assessed as above. (*) indicates significant inhibition of hypotonic responses, p < 0.01.

127
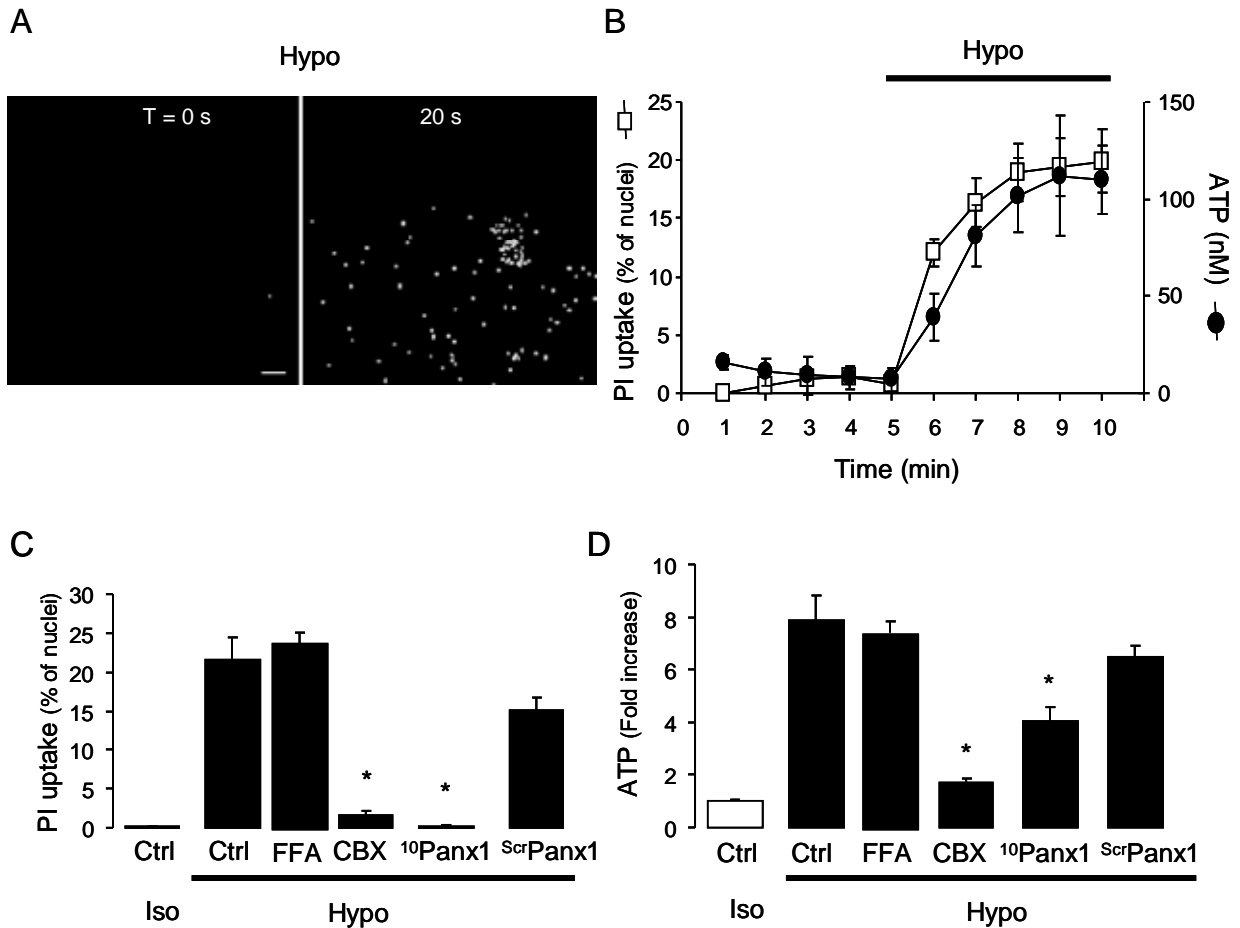
Figure 5.2. **Hypotonicity-induced dye uptake and ATP release in A549 cells.** A, pannexin 1, 2 and 3 mRNA expression in WD-HBE cells was determined by RT-PCR analysis, using primers listed in **Table 5.1**. Results are representative of six independent WD-HBE cell RNA preparations. As positive controls (Panx-Ctrls) we used pcDNA3.1 expressing human pannexin 1 (Panx 1), brain (Panx 2), and skin (Panx 3). B, expression of pannexin transcripts in A549 cells was assessed by RT-PCR as above in panel A. C, uptake of propidium iodide was assessed after 5 min incubation in isotonic (Iso) or hypotonic (Hypo) solution, as described in Figure 5.1C. Values are the mean ± SEM. Similar results were obtained in at least three separate experiments performed in quadruplicate. (*), p < 0.01. D, cells were pre-incubated with vehicle or with the indicated concentrations of carbenoxolone (CBX, 15 min), 25 min with either [10]Panx1 or [Scr]Panx1, and challenged for 5 min with isotonic or hypotonic solution containing the indicated drugs. ATP concentrations were measured and analyzed as described in Figure 5.1D. Values are the mean ± SEM of six independent experiments performed sextuplicate.
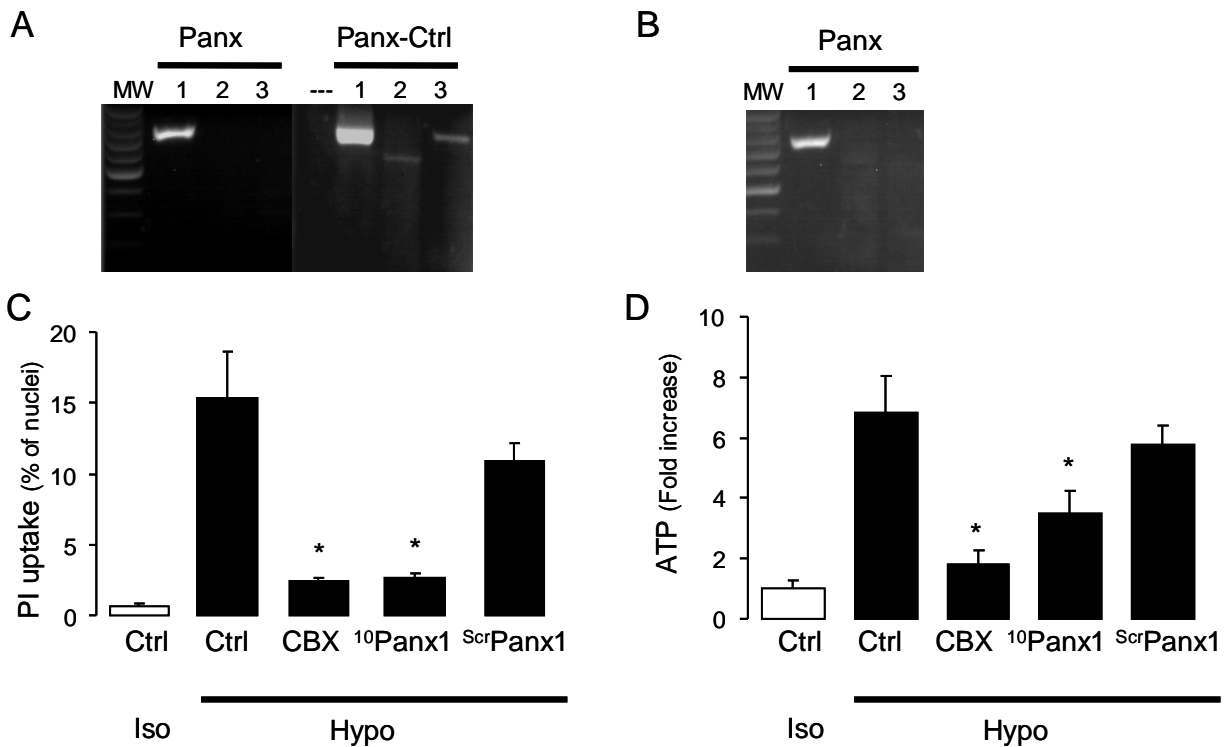
Figure 5.3. **Pannexin 1 mediates hypotonicity-induced ATP release.** A, pannexin 1 siRNA reduces pannexin 1 (Panx1), but not connexin 43 (Cx43), mRNA expression (mean ± SEM, n = 4). B, ATP release was measured in A549 cells transfected with either pannexin 1 siRNA (Panx1-siRNA), its scramble oligonucleotide (scr-siRNA), or vehicle (control), and incubated for 5 min in isotonic (Iso) or hypotonic (Hypo) solutions. The data represent the mean ± SEM of three separate experiments performed in triplicate. C, cells transfected as above were challenged for 5 min with isotonic (Iso) or hypotonic (Hypo) solutions containing propidium iodide. Cells were fixed, and dye uptake was measured as described in Figure 5.1C. The data represent the mean ± SEM of at least three independent experiments performed in quadruplicate. (*), $p < 0.01$.
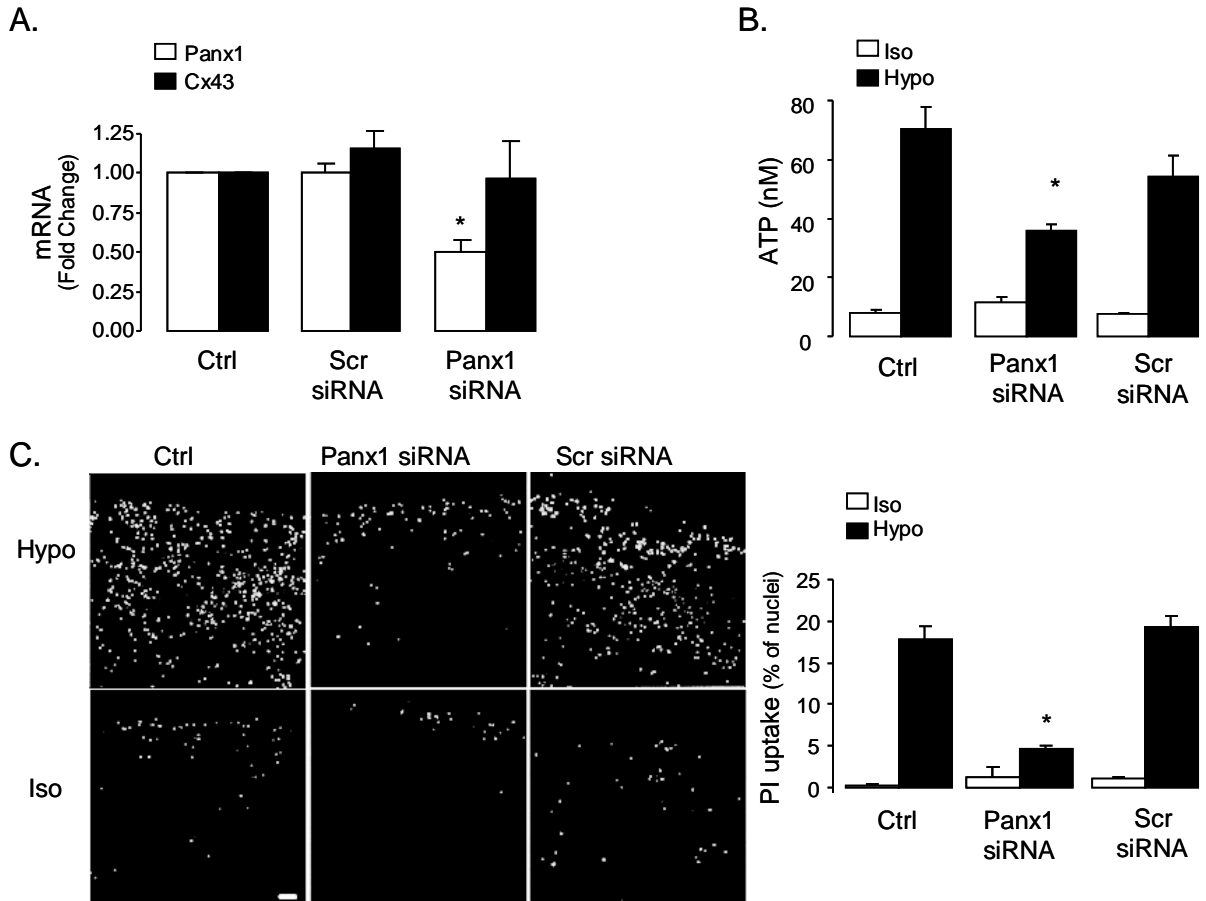
Figure 5.4. Effect of reagents on hypotonicity-induced cell swelling. A, calcein-labeled WD-HBE cells were preincubated for 15 min with 10 µM carbenoxolone (CBX). Representative xz images of cells upon isotonic/hypotonic challenge. B, time-course of the effect of carbenoxolone on hypotonicity-elicited cell swelling and RVD. The data represent the mean ± SEM of three independent experiments performed in triplicate. (*), $p < 0.05$. C, Quantification of cell height in swelling and RVD phases in cells incubated in the presence of vehicle (Ctrl), 1 µM H1552 (45 min pre-incubation), 1 µM ML-7 (45 min pre-incubation), 10 µM carbenoxolone (CBX), 10 µM HC67047 (30 min pre-incubation), and challenged with hypotonic solution containing the indicated drugs. (*) indicates significant inhibition of RVD, $p < 0.05$, (mean ± SEM, n = 4).
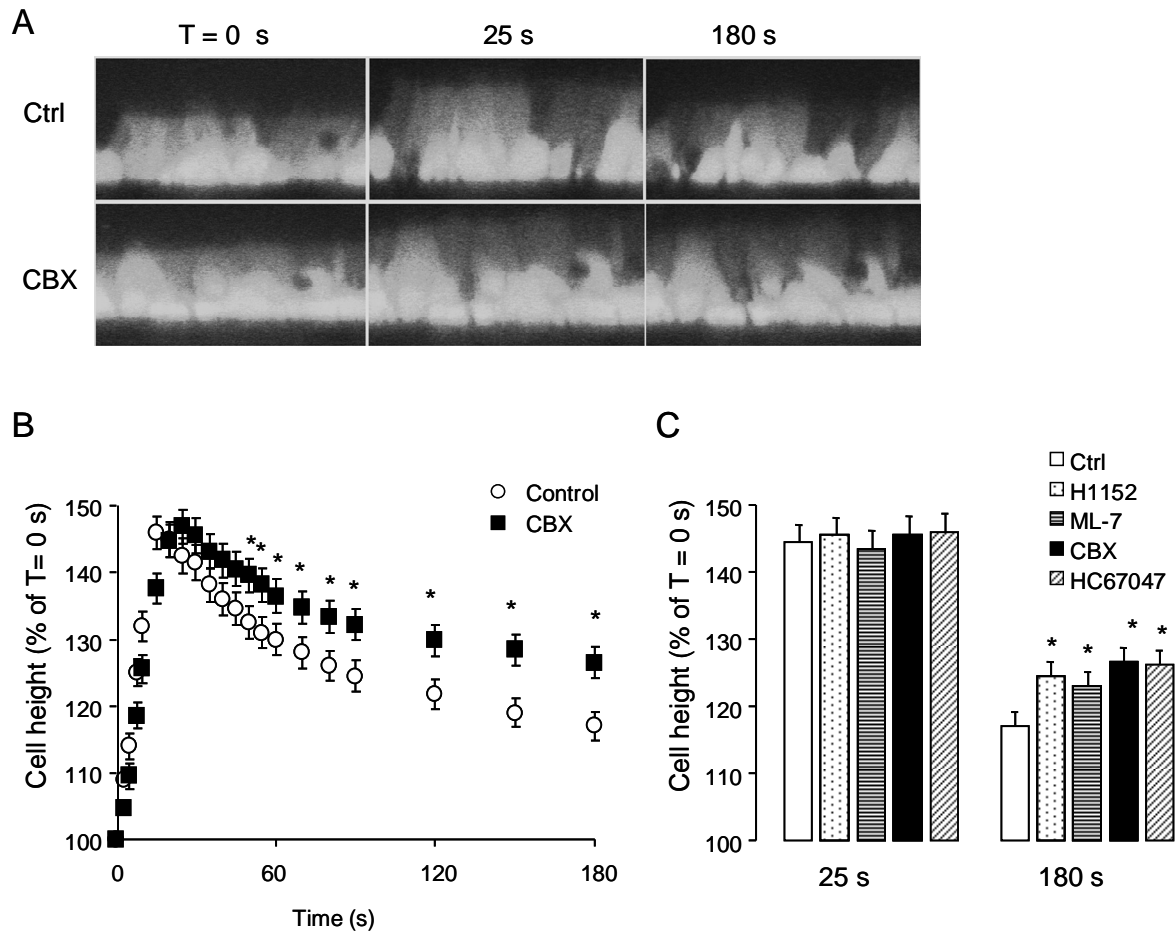
Figure 5.5. Hypotonicity-induced ATP release is associated with Rho activation and MLC phosphorylation. A, WD-HBE cells were pre-incubated for 45 min with 1 µM H1152 or 1 µM ML-7, and ATP release was measured after a 5 min incubation in hypotonic solution (Hypo) or isotonic control (Iso). B, total RhoA and RhoA-GTP were measured in cells incubated for 5 min in the presence of 5 U/ml apyrase with isotonic (Iso) or hypotonic solution (Hypo). RhoA activation is expressed as fold increase over control (right panel); values are the mean ± SEM of seven independent experiments. C, effect of 1 µM H1152 or 1 µM ML-7 on hypotonicity-promoted MLC phosphorylation. Quantification of p-MLC is indicated on the right panel; mean ± SD, n = 4.
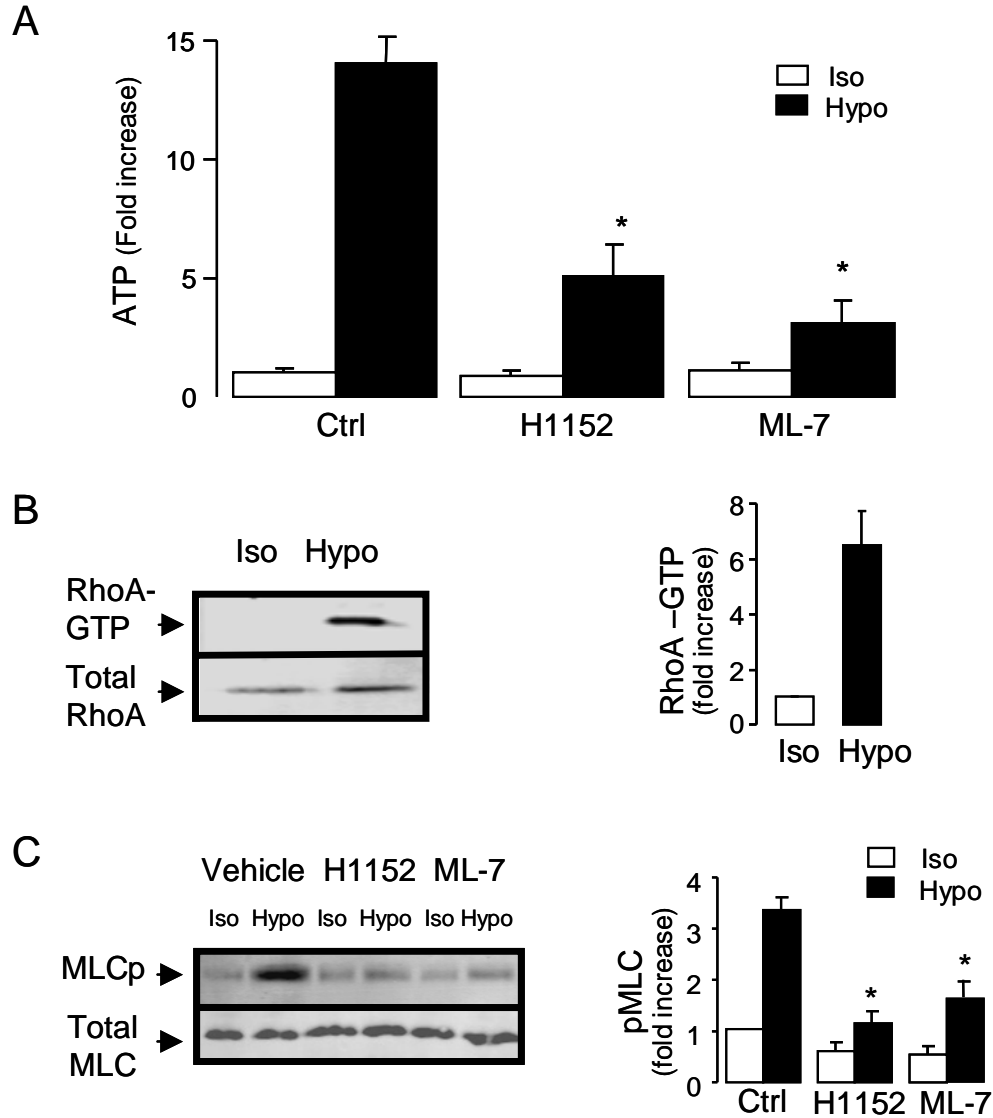
Figure 5.6. RhoA activation mediates ATP release in response to hypotonic stress. A549 cells were transfected with empty vector, p115-RGS, or RhoA(T19N). A, hypotoncity-elicited ATP release was assessed 48 h post transfection. Values are the mean ± SEM of three independent experiments performed in quadruplicate. B and C, RhoA activation and MLCp in response to hypotonic stress were measured in cells transfected as above. Values are expressed as fold increase over isotonic in empty vector-transfected cells (mean ± SEM, n = 4).
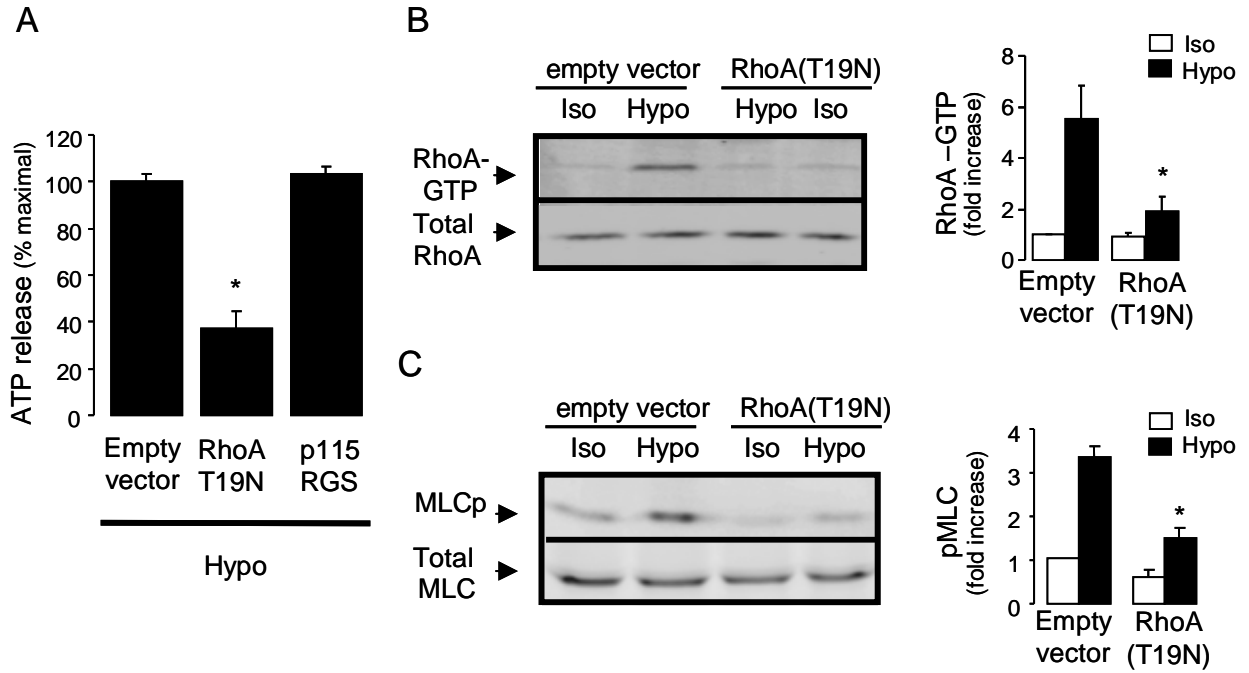
Figure 5.7. **RhoA activation is required for propidium iodide uptake.** A and B, WD-HBE cells were pre-incubated for 45 min with vehicle, 1 µM H1152, or 1 µM ML-7, and incubated for 5 min with isotonic (Iso) or hypotonic (Hypo) solution in the presence of propidium iodide. The data are the mean ± SEM, n = 4. Bar, 100 µm. (*), $p < 0.01$. C, A549 cells transfected with an empty vector or RhoA(T19N) were incubated for 5 min in isotonic (Iso) or hypotonic (Hypo) solution, and propidium iodide uptake measured, as described above. The results represent the mean ± SEM of four separate experiments performed in triplicate, (*), $p < 0.05$.
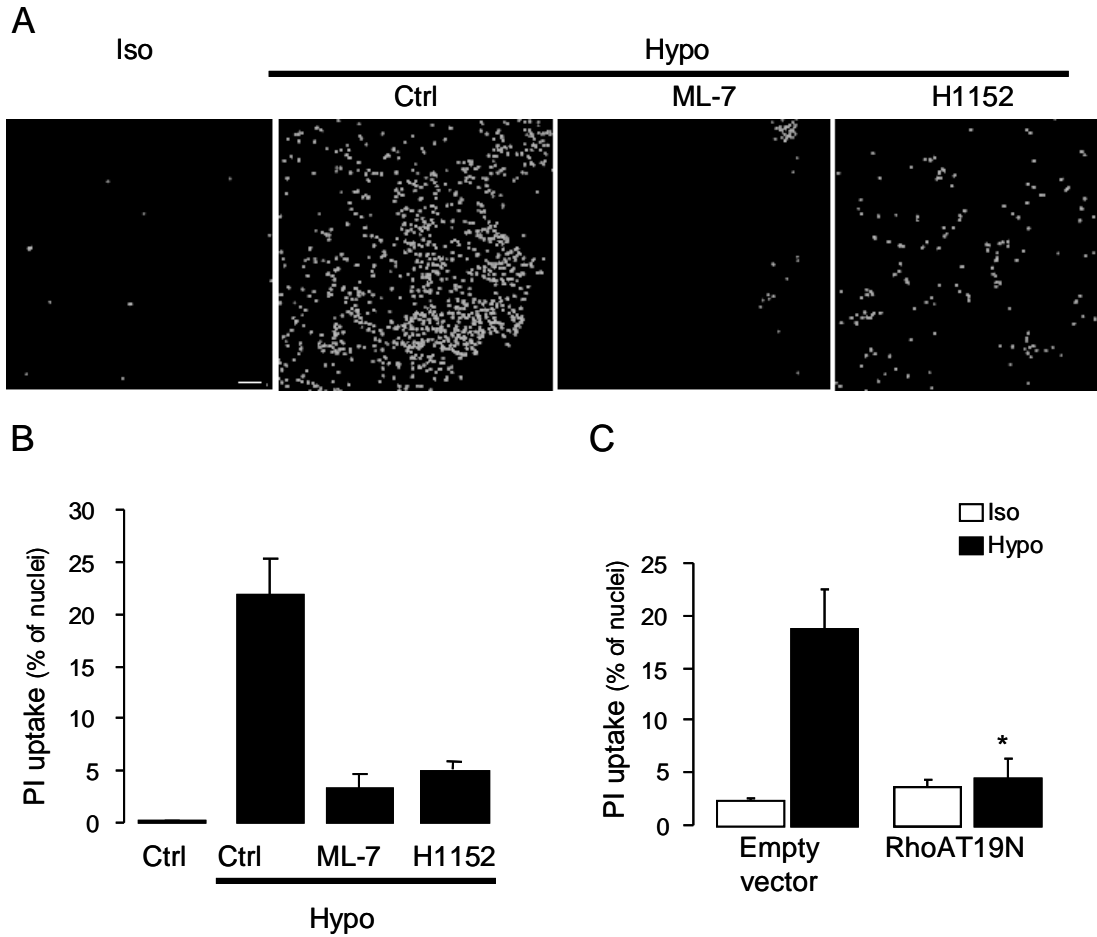
Figure 5.8. Pannexin 1, Rho kinase and MLC kinase contribute to shear stress-induced ATP release. A, ATP concentrations were measured in cells under static conditions or subjected to shear stress for 25 min in the presence of vehicle (Ctrl), 1 μM H1552 (20 min pre-incubation), 1 μM ML-7 (20 min pre-incubation), 10 μM carbenoxolone (CBX), 30 μM [10]Panx1, or 30 μM [Scr]Panx1. Values represent the mean ± SEM of at least six separate experiments performed in quadruplicate. (*) indicates significant inhibition of shear-stress responses, $p < 0.05$.
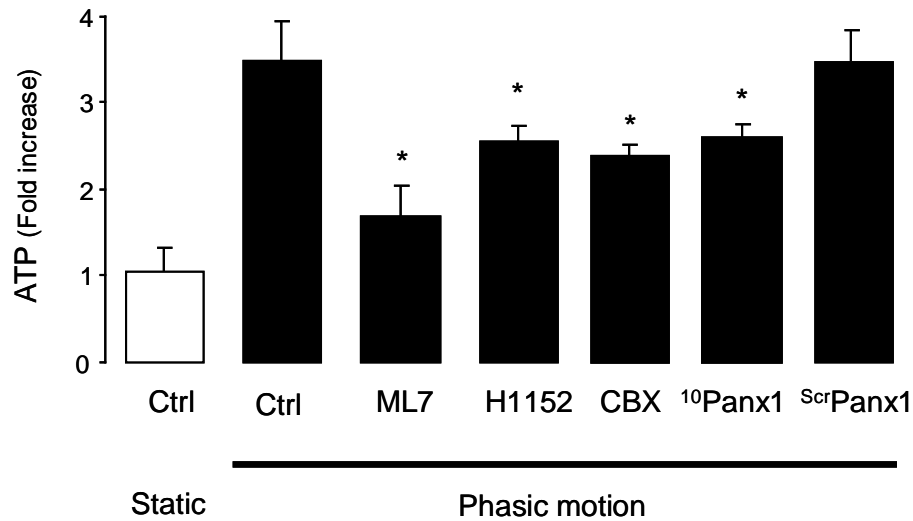
Figure 5.9. Hypotonic challenge-induced Rho activation and pannexin 1 mediated ATP release is sensitive to TRPV4 inhibition. A, WD-HBE cells were pre-incubated for 30 min with vehicle or 10 μM HC67047 followed by a 5 min hypotonic challenge, and ATP release was measured as indicated in Methods. B, RhoA activation was measured in cells pre-incubated as above and challenged for 5 min (in the presence of apyrase) with isotonic (Iso) or hypotonic (Hypo) solution, or 30 nM basolateral thrombin (Thr). C, were preincubated with HC67047 as above and propidium iodide uptake was assessed as described in Figure 5.1C. The data are the mean ± SEM, n = 4. (*), $p < 0.05$.
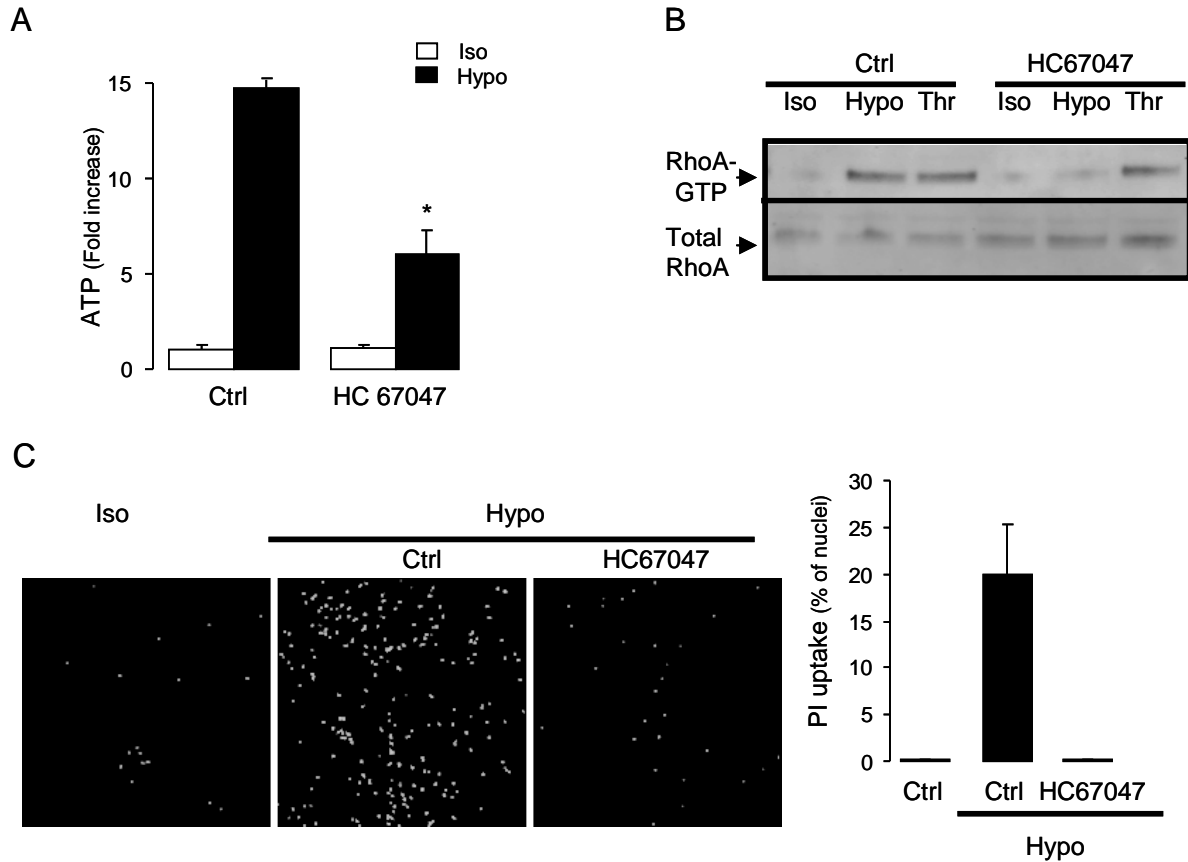
CHAPTER VI

General Discussion

1. Overview of results

ATP and adenosine within the ASL bathing the airway epithelia regulate key components of the MCC mechanisms that protect the lung against foreign particles and pathogens. However, it is not completely understood how these molecules are generated in the ASL. The work within this dissertation has unveiled a major mechanism responsible for ATP release in ciliated cell-dominated human airway epithelia. It demonstrates that pannexin 1 acts as an ATP release pathway, and that Rho GTPases are key regulators of ATP release upstream of pannexin 1. An additional important contribution of the present work is the identification and characterization of signaling initiated by activation of PARs localized at the basolateral surface of WD-HBE cells. PAR studies not only were crucial on our findings on Rho-dependent pannexin-1 mediated ATP release from ciliated epithelia, but greatly contribute to identify a major pathway for ATP release from goblet cells, i.e., mucin granule secretion.

Collectively, these findings greatly improved the current understanding of nucleotide-mediated regulation of airway epithelial cell functions, and provide new avenues for therapeutic strategies that will aid individuals with chronic lung diseases characterized by deficient MCC, such as CF.

2. Signaling elements involved in ATP release

The airway epithelia are continuously exposed to physical forces that impart ATP release-regulated MCC activities. In WD-HBE cell cultures, stimuli that mimic these forces, i.e., shear stress, cyclic compressive stress, and hypotonic challenge-promoted cell swelling, induce robust ATP release (7, 26, 105). However, it is not known how mechanical stresses are transduced into biochemical signaling, and hence, delineating a systematic strategy for identifying signaling elements regulating ATP release in airway epithelial cells has proven

problematic. Furthermore, a major limitation in studies of the mechanisms that regulate ATP release from airway epithelial cells is the paucity of pharmacological tools to promote nucleotide release in these cells. Previously, few studies from our and other labs reported that Ca^{2+}-mobilizing GPCRs (e.g., P2Y-R and PAR) promote ATP release from astrocytoma and endothelial (95, 154-156). Based on these studies, we reasoned that investigating the effect of GPCR activation on ATP release from airway epithelial cells would provide a strategy to identify mechanistic elements upstream of ATP release.

Our observations described in **Chapter III** are the first that demonstrate the occurrence of robust ATP release in GPCR-stimulated lung epithelial cells, including physiologically relevant cultures of WD-HBE cells. Using a highly sensitive luciferin-luciferase assay for ATP quantification in real-time (described in detail **in Chapter II**), we observed that the PAR agonist thrombin elicited rapid and robust release of ATP from lung epithelial A549 cells in a Ca^{2+}-dependent manner. In contrast, the $P2Y_2$-R agonist UTP caused negligible ATP release, despite promoting robust Ca^{2+}-responses. Therefore, signals in addition to Ca^{2+} participate in receptor-promoted ATP release. PAR-induced ATP release was associated with activation of Rho GTPases, and was diminished in cells transfected with dominant negative mutants of Rho A and p115-Rho GEF. The involvement of Rho in ATP release was further supported by the observation that ATP release from thrombin-stimulated A549 and WD-HBE cells decreased in the presence of ROCK inhibitors. Thus, thrombin-induced ATP release involves activation of the $G_{12/13}$/RhoA/ROCK signaling pathway. ROCK activation is known to promote phosphorylation of the myosin regulatory light chain. Consistent with this concept, we found that MLC is an effector of ROCK upstream of ATP release.

Based on the observations with PAR-stimulated cells, the involvement of Rho/ROCK and MLC in hypotonic stress-induced ATP release was investigated. We demonstrated that hypotonicity-promoted ATP release from WD-HBE cells was accompanied by activation of RhoA and enhanced phosphorylation of MLC. Inhibition of ROCK and MLCK diminished hypotonic challenge-induced ATP release. Furthermore, hypotonicity-induced ATP release was impaired in airway epithelial cells transfected with the RhoA dominant negative mutant (RhoAT19N).

Altogether, these results strongly suggest that activation of RhoA/ROCK and MLCK are necessary for ATP release in both receptor- and mechanically-stimulated WD-HBE cells. Although we have not investigated signaling downstream of MLC phosphorylation, it is possible that Rho/ROCK activation and MLC phosphorylation promote cytoskeletal rearrangement leading to insertion or activation of an ATP channel, e.g., pannexin 1 (see further below).

3.   Pathways for regulated ATP release from airway epithelial cells

ATP release has been proposed to occur either via (i) cytosolic ATP release through channels or transporters, or (ii) exocytotic release of ATP-enriched vesicles. However, unambiguous assessment of the contribution of conductive or exocytotic ATP release in airway epithelial cells has remained elusive.

The work presented in this dissertation provides a quantitative and molecular understanding of the contribution of conductive and exocytotic pathways in the release of nucleotides from ciliated and goblet epithelial cells, respectively.

Connexin hemichannels, and more recently pannexin hemichannels, have been proposed as pathways for ATP release in several cell types (141, 150, 152, 195, 237). In airway epithelial cells, circumstantial evidence suggests that connexin hemichannels have contribute to ATP release under low extracellular Ca^{2+} (141, 238), a situation unlikely to be found under physiological conditions. While connexins have been shown to be functionally expressed as plasma membrane hemichannels and may allow the exit of ATP, it remains to be demonstrated whether they may open and release ATP under physiological $[Ca^{2+}]_{ex}$ concentrations, i.e., ~ 2 mM. In contrast to connexins, pannexins are exported to the cell surface as glycosylated proteins, and therefore, it is unlikely for pannexons to form gap junctions (147, 239). Thus, pannexons in the non-junctional plasma membrane are predicted to comprise the predominant structural state (240). Pannexons open under physiological extracellular calcium concentrations and at resting membrane potentials in response to mechanical stress, thus, pannexons are appealing candidates for ATP-releasing channels.

In our studies of PAR-induced ATP release from WD-HBE cell cultures, we found that non-selective blockers of connexin/pannexin hemichannels diminished both ATP release and the uptake of the hemichannel-permeable dye propidium iodide, suggesting that ATP release from thrombin-stimulated cells occurs via hemichannels. We expanded these observations to illustrate that ATP release from hypotonically- and shear stress-stimulated WD-HBE cells was reduced in the presence of hemichannel inhibitors. Confocal microscopy studies verified that hypotonicity-induced ATP release was associated with the rapid uptake of the hemichannel-permeable reporter dye propidium iodide, which was inhibited by carbenoxolone, a potent and selective pannexin 1 inhibitor. RT-PCR analysis of WD-HBE cells revealed the expression of pannexin 1, but not pannexin 2 or 3. A pannexin 1-selective

blocking peptide (but not its scrambled control) nearly completely abolished hypotonicity-induced propidium iodide uptake, and diminished ATP release from WD-HBE cells. Moreover, siRNA against pannexin 1 diminished hypotonicity-evoked responses. Highly relevant to these observations, propidium iodide uptake was inhibited by ROCK and MLCK inhibitors, and by transfecting cells with RhoAT19N. Collectively, our data suggest that pannexin 1 acts as an ATP release pathway in hypotonically-stimulated WD-HBE cells, which consist mostly of non-mucus cells, and that hemichannel opening is regulated by RhoA/ROCK/MLCK.

It is noteworthy to mention that the pannexin 1-selective blocking peptide abolished the uptake of propidium iodide induced by hypotonic challenge, but only partially diminished ATP release, suggesting that additional mechanisms are involved in the release of ATP from WD-HBE cells. Based on published studies, it is possible that this residual ATP release occurs via maxi-anion channels (121), VSOAC channels (228), or vesicles (94).

While investigating PAR-promoted ATP release we found that goblet-like airway epithelial Calu-3 cells, express PAR1, PAR2, and PAR3. Since Calu-3 cells do not express Ca^{2+}-mobilizing P2Y or muscarinic receptors, we hypothesized that PAR activation would provide a physiological approach to promote Ca^{2+}-regulated mucin secretion. Confocal studies illustrated that incubation of cells with thrombin, PAR1-AP, and PAR2-AP resulted in loss of MUC5AC immunoreactive granules. In addition, extracellular solutions were analyzed by slot blot and showed enhanced secretion of MUC5AC. Noteworthy, PAR-induced mucin secretion was accompanied by ATP release. HPLC analysis detected a marked increase relative to control in ADP, AMP, and adenosine, in addition to ATP, in samples stimulated with thrombin. MUC5AC-containing granules were isolated and showed

to contain ATP, ADP, and AMP. In sum, isolated mucin granules contain a significant pool of adenine nucleotides susceptible to release upon agonist-promoted mucin secretion. These findings are in good agreement with a mathematical model predicting that ADP and AMP within vesicles are an important source of ASL adenosine (100).

4. Protease activated receptors in the airway epithelia

The protease thrombin not only cleaves fibrinogen and other soluble protein substrates, but also triggers a host of responses in platelets, endothelial, epithelial, and other cells trough the cleavage of cell surface receptors, PARs. PARs are GPCRs that convert an extracellular proteolytic cleavage event into a signaling cascade: PARs carry a thethered ligand, which remains occult until an NH_2-terminal fragment of the receptor is proteolytically removed. Four PARs have been cloned and characterized (241). PAR 1, 3, and 4 are targets for thrombin. In contrast, PAR2 is resistant to thrombin but is activated by trypsin and other proteases (241-242).

Several studies have reported that PARs are expressed, at least at the mRNA level, in various cell types of the respiratory tract, including epithelial cells, endothelial cells, alveolar cells, smooth muscle cells, mast cells, and alveolar macrophages (218). In addition to thrombin and trypsin, proteases that may be present in the respiratory tract and activate PARs include mast cell tryptase (which activates PAR2), mast cell chymase (that activates PAR1) and neutrophil cathepsin G (activating PAR2 and PAR4), and exogenous enzymes such as the house dust mite Der p1 (which activates PAR2)(218).

Our studies have defined for the first time a physiological role for PAR3. We showed that thrombin activation of PAR3 promotes Ca^{2+}-mobilization, RhoA activation, and ATP release from A549 cells. RT-PCR analysis identified transcripts for the previously poorly

142

characterized PAR3, but not for other PARs in A549 cells. Transfection of cells with human PAR3 cDNA increased thrombin-induced RhoA activation, inositol phosphate formation, and ATP release. Conversely, siRNA against PAR3 diminished thrombin-evoked responses. Collectively, these data indicate that (i) PAR3 is capable of triggering signaling, and (i) PAR3 mediates thrombin actions in A549 cells. Furthermore, our studies indicated that activation of PAR1, PAR2, and possibly PAR3 promote ATP release and mucin secretion from Calu-3 cells. In sum, our studies demonstrate that serine proteases acting via basolateral PAR1, PAR2, and/or PAR3 in airway epithelial cells act as potent and robust stimuli for ATP release.

It has been reported that PAR expression is up-regulated during chronic inflammatory diseases, such as asthma and COPD (218), which are characterized by goblet cell metaplasia and mucus plug formation (32). Thus, a corollary of our findings is that PAR-dependent mucin (and ATP) secretagogue activity may contribute to the pathogenesis of these diseases.

5. Future Directions

This dissertation research has shed new light on mechanisms that participate in regulated ATP release from airway epithelial cells, i.e., Rho/ROCK/MLCK, and provides compelling evidence for a role of pannexin 1 as an ATP release pathway. While this research provides essential basic knowledge regarding these pathways in health, it remains to be investigated whether increased or diminished activity of these pathways participates in the maintenance of chronic lung diseases, e.g., COPD, asthma, and CF.

Our studies suggest that an osmotically/mechanically activated sensor transduces cell swelling into Rho activation. Based on recent literature suggesting that TRPV4 mediates osmotic stress-induced ATP release in urethelial and renal epithelial cells (234-235), and our

143

observations that pharmacological inhibitors of TRPV4 diminished hypotonic stress-induced RhoA activation (and ATP release), we propose that TRPV4 fulfills such a role. Future studies should define, unambiguously, the involvement of TRPV4 in hypotonic challenge- and shear stress-promoted ATP release from airway epithelial cells.

How activation of TRP channels results in Rho activation is not known. Rho GTPases are regulated by: (1) GEFs, which replace GDP with GTP thereby activating Rho proteins; (2) GTPase-activating proteins, which inactive Rho by by converting Rho-GTP to inactive Rho-GDP; and (3) guanine nucleotide dissociation inhibitors, which sequester Rho-GDP from GEF. It has been recently proposed that Rho GTPases act downstream of GEFs as second messengers of osmotic stress (243-244). Our findings indicated that PAR-stimulated ATP release requires $G\alpha_{12/13}$/p115RhoGEF activation upstream of RhoA, however, transfection of cells with a p115RGS did not affect hypotonic stress-induced ATP release, suggesting that $G\alpha_{12/13}$ is not activated by hypotonic challenge. It remains to be investigated whether p115RhoGEF or other GEFs transduce TRPV4 activation into Rho-dependent ATP release.

It has been also reported that hypertonic stress induces the phosphorylation of the actin-binding ezrin-moesin-radixin (EMR) proteins (244), which act as upstream activators of Rho by sequestering Rho GDI (245). On speculative grounds and based on the fact that TRPC4 and TRP5 are associated with EMR proteins (246-247), hypotonic challenge may promote TRPV4-mediated ERM-phosphorylation resulting in Rho activation.

The discovery of pannexin 1 as a major contributor to ATP release from airway epithelial cells opens several potential lines of investigation. For example, proteomic analysis of pannexin 1 immunoprecipitates should identify partners of pannexin 1. Eventually, these

studies would lead to elucidate the role of cytoskeleteal components and other effectors in Rho/ROCK/MLCK-regulated pannexin 1-mediated ATP release.

Since ASL ATP and adenosine are important molecules in health and disease, the role of pannexin 1 under these conditions grants further investigation. For example, ATP and adenosine are key players in the asthma inflammatory cascade (248-249). A recent study showed that intranasal administration of carbenoxolone attenuated several asthma features in a mouse asthma model (250), and suggested that pannexin 1-mediated ATP release is an important contributor to these features. Generating a pannexin 1 (-/-) mice would be a major step in assessing this hypothesis.

The therapeutic potential of enhanced ATP release into the ASL has been studied in diseases characterized by ASL volume dehydration, such as CF. Phase II clinical trials of aerosolized non-hydrolysable nucleotides delivered to the airways of patients with mild CF lung disease indicate a significant improvement in lung function (251-252). However, in most patients with CF lung disease, aerosolized nucleotides have to permeate trough the dehydrated and compact mucus layer, and reach the airway cell surface to activate $P2Y_2$-Rs. In this scenario, enhancing endogenous ATP release seems an advantageous alternative. Based on our findings with pannexin 1, future studies should test in CF/COPD mouse models whether overexpression of pannexin 1 in the airway epithelium reverses the obstructive lung phenotype.

REFERENCES

1.   Knowles MR, Boucher RC. Mucus clearance as a primary innate defense mechanism for mammalian airways. Journal of Clinical Investigation. 2002;109(5):571-7.

2.   Matsui H, Davis CW, Tarran R, Boucher RC. Osmotic water permeabilities of cultured, well-differentiated normal and cystic fibrosis airway epithelia. Journal of Clinical Investigation. 2000;105(10):1419-27.

3.   Matsui H, Grubb BR, Tarran R, Randell SH, Gatzy JT, Davis CW, et al. Evidence for periciliary liquid layer depletion, not abnormal ion composition, in the pathogenesis of cystic fibrosis airways disease. Cell. 1998;95(7):1005-15.

4.   Button B, Boucher RC. Role of mechanical stress in regulating airway surface hydration and mucus clearance rates. Respiratory Physiology and Neurobiology. 2008;163(1-3):189-201.

5.   Sims DE, Horne MM. Heterogeneity of the composition and thickness of tracheal mucus in rats. American Journal of Physiology. 1997;273(5 Pt 1):L1036-41.

6.   Rubin BK. Physiology of airway mucus clearance. Respiratory Care. 2002;47(7):761-8.

7.   Tarran R, Button B, Picher M, Paradiso AM, Ribeiro CM, Lazarowski ER, et al. Normal and cystic fbrosis airway surface liquid homeostasis: The effects of phasic shear stress and viral infections. Journal of Biological Chemistry. 2005;280:35751-9.

8.   Tarran R, Grubb BR, Gatzy JT, Davis CW, Boucher RC. The relative roles of passive surface forces and active ion transport in the modulation of airway surface liquid volume and composition. Journal of General Physiology. 2001;118(2):223-36.

9.   Mall M, Grubb BR, Harkema JR, O'Neal WK, Boucher RC. Increased airway epithelial Na+ absorption produces cystic fibrosis-like lung disease in mice. Nature Medicine. 2004;10(5):487-93.

10.   Lazarowski ER, Paradiso AM, Watt WC, Harden TK, Boucher RC. UDP activates a mucosal-restricted receptor on human nasal epithelial cells that is distinct from the P2Y(2) receptor. Proceedings of the National Academy of Sciences of the USA. 1997;94(6):2599-603.

11.   Donaldson SH, Lazarowski ER, Picher M, Knowles MR, Stutts MJ, Boucher RC. Basal nucleotide levels, release, and metabolism in normal and cystic fibrosis airways. Molecular Medicine. 2000;6(11):969-82.

12.   Donaldson SH, Picher M, Boucher RC. Secreted and cell-associated adenylate kinase and nucleoside diphosphokinase contribute to extracellular nucleotide metabolism on human

airway surfaces. American Journal of Respiratory Cell and Molecular Biology. 2002;26(2):209-15.

13.   Picher M, Boucher RC. Human Airway Ecto-adenylate Kinase. A mechanism to propagate ATP signaling on airway surfaces. Journal of Biological Chemistry. 2003;278(13):11256-64.

14.   Picher M, Burch LH, Hirsh AJ, Spychala J, Boucher RC. Ecto 5'-nucleotidase and non-specific alkaline phosphatase: two AMP-hydrolyzing ectoenzymes with distinct roles in human airways. Journal of Biological Chemistry. 2003;278(15):13468-79.

15.   Picher M, Burch LH, Boucher RC. Metabolism of P2 receptor agonists in human airways: Implications for mucociliary clearance and cystic fibrosis. Journal of Biological Chemistry. 2004;279(19):20234-41.

16.   Picher M, Boucher RC. Biochemical evidence for an ecto alkaline phosphodiesterase I in human airways. American Journal of Respiratory Cell and Molecular Biology. 2000;23(2):255-61.

17.   Hirsh AJ, Stonebraker JR, van Heusden CA, Lazarowski ER, Boucher RC, Picher M. Adenosine deaminase 1 and concentrative nucleoside transporters 2 and 3 regulate adenosine on the apical surface of human airway epithelia: implications for inflammatory lung diseases. Biochemistry. 2007;46(36):10373-83.

18.   Mason SJ, Paradiso AM, Boucher RC. Regulation of transepithelial ion transport and intracellular calcium by extracellular ATP in human normal and cystic fibrosis airway epithelium. British Journal of Pharmacology. 1991;103(3):1649-56.

19.   Lazarowski ER, Mason SJ, Clarke L, Harden TK, Boucher RC. Adenosine receptors on human airway epithelia and their relationship to chloride secretion. British Journal of Pharmacology. 1992;106(4):774-82.

20.   Parr CE, Sullivan DM, Paradiso AM, Lazarowski ER, Burch LH, Olsen JC, et al. Cloning and Expression of A Human-P(2U) Nucleotide Receptor, A Target for Cystic-Fibrosis Pharmacotherapy. Proceedings of the National Academy of Sciences of the USA. 1994;91(8):3275-9.

21.   Morse DM, Smullen JL, Davis CW. Differential effects of UTP, ATP, and adenosine on ciliary activity of human nasal epithelial cells. American Journal of Physiology Cell Physiology. 2001;280(6):C1485-C97.

22.   Cobb BR, Ruiz F, King CM, Fortenberry J, Greer H, Kovacs T, et al. A(2) adenosine receptors regulate CFTR through PKA and PLA(2). American Journal of Physiology. 2002;282(1):L12-L25.

23.   Douillet CD, Robinson WP, III, Zarzaur BL, Lazarowski ER, Boucher RC, Rich PB. Mechanical Ventilation Alters Airway Nucleotides and Purinoceptors in Lung and

Extrapulmonary Organs. American Journal of Respiratory Cell and Molecular Biology. 2005;32(1):52-8.

24.   Esther CR, Alexis NE, Clas ML, Lazarowski ER, Donaldson SH, Pedrosa Ribeiro CM, et al. Extracellular Purines are Biomarkers of Neutrophilic Airway Inflammation. European Respiratory Journal. 2008;31(5):949-56.

25.   Lazarowski ER, Tarran R, Grubb BR, van Heusden CA, Okada S, Boucher RC. Nucleotide release provides a mechanism for airway surface liquid homeostasis. Journal of Biological Chemistry. 2004;279(35):36855-64.

26.   Okada SF, Nicholas RA, Kreda SM, Lazarowski ER, Boucher RC. Physiological regulation of ATP release at the apical surface of human airway epithelia. Journal of Biological Chemistry. 2006;281 (32):22992-3002.

27.   Huang PB, Lazarowski ER, Tarran R, Milgram SL, Boucher RC, Stutts MJ. Compartmentalized autocrine signaling to cystic fibrosis transmembrane conductance regulator at the apical membrane of airway epithelial cells. Proceedings of the National Academy of Sciences of the USA. 2001;98(24):14120-5.

28.   Rollins BM, Burn M, Coakley RD, Chambers LA, Hirsh AJ, Clunes MT, et al. A2B adenosine receptors regulate the mucus clearance component of the lung's innate defense system. American Journal of Respiratory Cell and Molecular Biology. 2008;39(2):190-7. PMCID: 2542455.

29.   Cressman VL, Lazarowski E, Homolya L, Boucher RC, Koller BH, Grubb BR. Effect of loss of P2Y(2) receptor gene expression on nucleotide regulation of murine epithelial Cl-transport. Journal of Biological Chemistry. 1999;274(37):26461-8.

30.   Lethem MI, Dowell ML, Van Scott M, Yankaskas JR, Egan T, Boucher RC, et al. Nucleotide regulation of goblet cells in human airway epithelial explants: normal exocytosis in cystic fibrosis. American Journal of Respiratory Cell and Molecular Biology. 1993;9(3):315-22.

31.   Conway JD, Bartolotta T, Abdullah LH, Davis CW. Regulation of mucin secretion from human bronchial epithelial cells grown in murine hosted xenografts. American Journal of Physiology. Lung Cell and Molecular Physiology. 2003;284(6):L945-L54.

32.   Davis CW, Dickey BF. Regulated airway goblet cell mucin secretion. Annual Review in Physiology. 2008;70:487-512.

33.   Kunzelmann K, Schreiber R, Konig J, Mall M. Ion transport induced by proteinase-activated receptors (PAR2) in colon and airways. Cell Biochemistry and Biophysics. 2002;36(2-3):209-14.

34.   Ma HP, Chou CF, Wei SP, Eaton DC. Regulation of the epithelial sodium channel by phosphatidylinositides: experiments, implications, and speculations. Pflugers Archives. 2007;455(1):169-80.

35.   Rock JR, O'Neal WK, Gabriel SE, Randell SH, Harfe BD, Boucher RC, et al. Transmembrane protein 16A (TMEM16A) is a Ca2+-regulated Cl- secretory channel in mouse airways. Journal of Biological Chemistry. 2009;284(22):14875-80. PMCID: 2685669.

36.   Taylor AL, Schwiebert LM, Smith JJ, King C, Jones JR, Sorscher EJ, et al. Epithelial P2X purinergic receptor channel expression and function. Journal of Clinical Investigation. 1999;104(7):875-84.

37.   Homolya L, Watt WC, Lazarowski ER, Koller BH, Boucher RC. Nucleotide-regulated calcium signaling in lung fibroblasts and epithelial cells from normal and P2Y(2) receptor (-/-) mice. Journal of Biological Chemistry. 1999;274(37):26454-60.

38.   Mall M, Wissner A, Gonska T, Calenborn D, Kuehr J, Brandis M, et al. Inhibition of amiloride-sensitive epithelial Na(+) absorption by extracellular nucleotides in human normal and cystic fibrosis airways. American Journal of Respiratory Cell and Molecular Biology. 2000;23(6):755-61.

39.   Clarke LL, Boucher RC. Chloride secretory response to extracellular ATP in human normal and cystic fibrosis nasal epithelia. American Journal of Physiology. 1992;263(2 Pt 1):C348-56.

40.   Knowles MR, Clarke LL, Boucher RC. Activation by extracellular nucleotides of chloride secretion in the airway epithelia of patients with cystic fibrosis. New England Journal of Medicine. 1991;325(8):533-8.

41.   Hentchel-Franks K, Lozano D, Eubanks-Tarn V, Cobb B, Fan L, Oster R, et al. Activation of airway cl- secretion in human subjects by adenosine. American Journal of Respiratory Cell and Molecular Biology. 2004;31(2):140-6.

42.   Cobb BR, Fan LJ, Kovacs TE, Sorscher EJ, Clancy JP. Adenosine Receptors and Phosphodiesterase Inhibitors Stimulate Cl- Secretion in Calu-3 Cells. American Journal of Respiratory Cell and Molecular Biology. 2003;29:410-8.

43.   Cheng SH, Rich DP, Marshall J, Gregory RJ, Welsh MJ, Smith AE. Phosphorylation of the R domain by cAMP-dependent protein kinase regulates the CFTR chloride channel. Cell. 1991;66(5):1027-36.

44.   Rowe SM, Miller S, Sorscher EJ. Cystic fibrosis. New England Journal of Medicine. 2005;352(19):1992-2001.

45.   Jia Y, Mathews CJ, Hanrahan JW. Phosphorylation by protein kinase C is required for acute activation of cystic fibrosis transmembrane conductance regulator by protein kinase A. Journal of Biological Chemistry. 1997;272(8):4978-84.

46.   Seavilleklein G, Amer N, Evagelidis A, Chappe F, Irvine T, Hanrahan JW, et al. PKC phosphorylation modulates PKA-dependent binding of the R domain to other domains of CFTR. American Journal of Physiology. Cell Physiology. 2008;295(5):C1366-75.

47.   Chappe F, Loewen ME, Hanrahan JW, Chappe V. Vasoactive intestinal peptide increases cystic fibrosis transmembrane conductance regulator levels in the apical membrane of Calu-3 cells through a protein kinase C-dependent mechanism. Journal of Pharmacology and Experimental Therapy. 2008;327(1):226-38.

48.   Yang YD, Cho H, Koo JY, Tak MH, Cho Y, Shim WS, et al. TMEM16A confers receptor-activated calcium-dependent chloride conductance. Nature. 2008;455(7217):1210-5.

49.   Caputo A, Caci E, Ferrera L, Pedemonte N, Barsanti C, Sondo E, et al. TMEM16A, a membrane protein associated with calcium-dependent chloride channel activity. Science. 2008;322(5901):590-4.

50.   Schroeder BC, Cheng T, Jan YN, Jan LY. Expression cloning of TMEM16A as a calcium-activated chloride channel subunit. Cell. 2008;134(6):1019-29.

51.   Donaldson SH, Hirsh A, Li DC, Holloway G, Chao J, Boucher RC, et al. Regulation of the epithelial sodium channel by serine proteases in human airways. Journal of Biological Chemistry. 2002;277(10):8338-45.

52.   Carattino MD, Hughey RP, Kleyman TR. Proteolytic processing of the epithelial sodium channel gamma subunit has a dominant role in channel activation. Journal of Biological Chemistry. 2008;283(37):25290-5.

53.   Bruns JB, Carattino MD, Sheng S, Maarouf AB, Weisz OA, Pilewski JM, et al. Epithelial Na+ channels are fully activated by furin- and prostasin-dependent release of an inhibitory peptide from the gamma-subunit. Journal of Biological Chemistry. 2007;282(9):6153-60.

54.   Boucher RC, Stutts MJ, Knowles MR, Cantley L, Gatzy JT. Na+ transport in cystic fibrosis respiratory epithelia. Abnormal basal rate and response to adenylate cyclase activation. Journal of Clinical Investigation. 1986;78(5):1245-52.

55.   Huang P, Gilmore E, Kultgen P, Barnes P, Milgram S, Stutts MJ. Local regulation of cystic fibrosis transmembrane regulator and epithelial sodium channel in airway epithelium. Proceedings of the American Thoracic Society. 2004;1(1):33-7.

56.   Devor DC, Pilewski JM. UTP inhibits Na+ absorption in wild-type and DeltaF508 CFTR-expressing human bronchial epithelia. American Journal of Physiology. 1999;276(4 Pt 1):C827-C37.

57.   Kunzelmann K, Bachhuber T, Regeer R, Markovich D, Sun J, Schreiber R. Purinergic inhibition of the epithelial Na+ transport via hydrolysis of PIP2. The Federation of American Societies for Experimental Biology Journal. 2005;19(1):142-3.

58.   Pochynyuk O, Tong Q, Medina J, Vandewalle A, Staruschenko A, Bugaj V, et al. Molecular determinants of PI(4,5)P2 and PI(3,4,5)P3 regulation of the epithelial Na+ channel. Journal of General Physiology. 2007;130(4):399-413.

59.   Pochynyuk O, Tong Q, Staruschenko A, Stockand JD. Binding and direct activation of the epithelial Na+ channel (ENaC) by phosphatidylinositides. Journal of Physiology. 2007;580(Pt. 2):365-72.

60.   Pochynyuk O, Bugaj V, Vandewalle A, Stockand JD. Purinergic control of apical plasma membrane PI(4,5)P2 levels sets ENaC activity in principal cells. American Journal of Physiology. Renal Physiology. 2008;294(1):F38-F46.

61.   Yue G, Malik B, Eaton DC. Phosphatidylinositol 4,5-bisphosphate (PIP2) stimulates epithelial sodium channel activity in A6 cells. Journal of Biological Chemistry. 2002;277(14):11965-9.

62.   Adler KB, Schwarz JE, Anderson WH, Welton AF. Platelet activating factor stimulates secretion of mucin by explants of rodent airways in organ culture. Experimental Lung Research. 1987;13(1):25-43.

63.   Adler KB, Li Y. Airway epithelium and mucus: intracellular signaling pathways for gene expression and secretion. American Journal of Respiratory Cell and Molecular Biology. 2001;25(4):397-400.

64.   Martin LD, Rochelle LG, Fischer BM, Krunkosky TM, Adler KB. Airway epithelium as an effector of inflammation: molecular regulation of secondary mediators. European Respiratory Journal. 1997;10(9):2139-46.

65.   Abdullah LH, Davis SW, Burch L, Yamauchi M, Randell SH, Nettesheim P, et al. P2u purinoceptor regulation of mucin secretion in SPOC1 cells, a goblet cell line from the airways. Biochemistry Journal. 1996;316 (Pt 3):943-51.

66.   Davis CW. Goblet Cells: Physiology and Pharmacology. In: Rogers DF, Lethem MI, editors. Airway Mucus: Basic Mechanisms and Clinical Prspectives. Basel/Switzerland: Birkhauser Verlag; 1997. p. 149-77.

67.   Evans CM, Williams OW, Tuvim MJ, Nigam R, Mixides GP, Blackburn MR, et al. Mucin is produced by clara cells in the proximal airways of antigen-challenged mice. American Journal of Respiratory Cell and Molecular Biology. 2004;31(4):382-94.

68.   Zhu Y, Ehre C, Abdullah LH, Sheehan JK, Roy M, Evans CM, et al. Munc13-2-/- baseline secretion defect reveals source of oligomeric mucins in mouse airways. Journal of Physiology. 2008;586(7):1977-92. PMCID: 2375724.

69.   Abdullah LH, Conway JD, Cohn JA, Davis CW. Protein kinase C and Ca2+ activation of mucin secretion in airway goblet cells. AmJPhysiol. 1997;273(1 Pt 1):L201-L10.

70.   Kemp PA, Sugar RA, Jackson AD. Nucleotide-mediated mucin secretion from differentiated human bronchial epithelial cells. American Journal of Respiratory Cell and Molecular Biology. 2004.

71.   Kreda SM, Okada SF, van Heusden CA, O'Neal W, Gabriel S, Abdullah L, et al. Coordinated release of nucleotides and mucin from human airway epithelial Calu-3 cells. Journal of Physiology. 2007;584(Pt 1):245-59.

72.   Ehre C, Zhu Y, Abdullah LH, Olsen J, Nakayama KI, Nakayama K, et al. nPKCepsilon, a P2Y2-R downstream effector in regulated mucin secretion from airway goblet cells. American Journal of Physiology. Cell Physiology. 2007;293(5):C1445-54.

73.   Park J, Fang S, Crews AL, Lin KW, Adler KB. MARCKS regulation of mucin secretion by airway epithelium in vitro: interaction with chaperones. American Journal of Respiratory Cell and Molecular Biology. 2008;39(1):68-76.

74.   Li Y, Martin LD, Spizz G, Adler KB. MARCKS protein is a key molecule regulating mucin secretion by human airway epithelial cells in vitro. Journal of Biological Chemistry. 2001;276(44):40982-90.

75.   Singer M, Martin LD, Vargaftig BB, Park J, Gruber AD, Li Y, et al. A MARCKS-related peptide blocks mucus hypersecretion in a mouse model of asthma. Nature Medicine. 2004;10(2):193-6.

76.   Shah AS, Ben-Shahar Y, Moninger TO, Kline JN, Welsh MJ. Motile cilia of human airway epithelia are chemosensory. Science. 2009;325(5944):1131-4.

77.   Lieb T, Forteza R, Salathe M. Hyaluronic acid in cultured ovine tracheal cells and its effect on ciliary beat frequency in vitro. Journal of Aerosol Medicine and Pulmonary Drug Delivery. 2000;13(3):231-7.

78.   Parekh AB, Putney JW, Jr. Store-operated calcium channels. Physiology Reviews. 2005;85(2):757-810.

79.   Vig M, Kinet JP. The long and arduous road to CRAC. Cell Calcium. 2007;42(2):157-62.

80.   Lorenzo IM, Liedtke W, Sanderson MJ, Valverde MA. TRPV4 channel participates in receptor-operated calcium entry and ciliary beat frequency regulation in mouse airway epithelial cells. Proceedings of the National Academy of Sciences of the USA. 2008;105(34):12611-6.

81.   Zhang L, Sanderson MJ. Oscillations in ciliary beat frequency and intracellular calcium concentration in rabbit tracheal epithelial cells induced by ATP. Journal of Physiology. 2003;546(Pt 3):733-49.

82.   Salathe M, Pratt MM, Wanner A. Cyclic AMP-dependent phosphorylation of a 26 kD axonemal protein in ovine cilia isolated from small tissue pieces. American Journal of Respiratory Cell and Molecular Biology. 1993;9(3):306-14.

83.   Wyatt TA, Forget MA, Adams JM, Sisson JH. Both cAMP and cGMP are required for maximal ciliary beat stimulation in a cell-free model of bovine ciliary axonemes. American Journal of Physiology. Lung Cell and Molecular Physiology. 2005;288(3):L546-51.

84.   Gertsberg I, Hellman V, Fainshtein M, Weil S, Silberberg SD, Danilenko M, et al. Intracellular Ca2+ regulates the phosphorylation and the dephosphorylation of ciliary proteins via the NO pathway. Journal of Genaral Physiology. 2004;124(5):527-40.

85.   Ma W, Silberberg SD, Priel Z. Distinct axonemal processes underlie spontaneous and stimulated airway ciliary activity. Journal of General Physiology. 2002;120(6):875-85.

86.   Lazarowski ER, Mason SJ, Clarke L, Harden TK, Boucher RC. Adenosine receptors on human airway epithelia and their relationship to chloride secretion. British Journal of Pharmacology. 1992;106(4):774-82.

87.   Watt WC, Lazarowski ER, Boucher RC. Cystic fibrosis transmembrane regulator-independent release of ATP - Its implications for the regulation of P2Y(2) receptors in airway epithelia. Journal of Biological Chemistry. 1998;273(22):14053-8.

88.   Grygorczyk R, Hanrahan JW. CFTR-independent ATP release from epithelial cells triggered by mechanical stimuli. American Journal of Physiology. 1997;272(3 Pt 1):C1058-C66.

89.   Seminario-Vidal L, Kreda S, Jones L, O'Neal W, Trejo J, Boucher RC, et al. Thrombin promotes release of ATP from lung epithelial cells through coordinated activation of Rho- and Ca2+-dependent signaling pathways. Journal of Biological Chemistry. 2009;284(31):20638-48.

90.   Lazarowski ER, Harden TK. Quantitation of extracellular UTP using a sensitive enzymatic assay. British Journal of Pharmacology. 1999;127(5):1272-8.

91.   Bodin P, Burnstock G. Evidence that release of adenosine triphosphate from endothelial cells during increased shear stress is vesicular. Journal of Cardiovascular Pharmacology. 2001;38(6):900-8.

92.   Fabbro A, Skorinkin A, Grandolfo M, Nistri A, Giniatullin R. Quantal release of ATP from clusters of PC12 cells. Journal of Physiology. 2004;560(Pt 2):505-17.

93.   Obermuller S, Lindqvist A, Karanauskaite J, Galvanovskis J, Rorsman P, Barg S. Selective nucleotide-release from dense-core granules in insulin-secreting cells. Journal of Cell Science. 2005;118(Pt 18):4271-82.

94.   Sesma JI, Esther CR, Jr., Kreda SM, Jones L, O'Neal W, Nishihara S, et al. ER/golgi nucelotide sugar transporters contribute to the cellular release of UDP-sugar signaling molecules. Journal of Biological Chemistry. 2009;284(18):12572-83.

95.   Kreda SM, Seminario-Vidal L, Heusden C, Lazarowski ER. Thrombin-promoted release of UDP-glucose from human astrocytoma cells. British Journal of Pharmacology. 2008;153(7):1528-37.

96.   Gatof D, Kilic G, Fitz JG. Vesicular exocytosis contributes to volume-sensitive ATP release in biliary cells. American Journal of Physiology. Gastrointestinal and Liver Physiology. 2004;286(4):G538-G46.

97.   Liu GJ, Kalous A, Werry EL, Bennett MR. Purine release from spinal cord microglia after elevation of calcium by glutamate. Molecular Pharmacology. 2006;70(3):851-9.

98.   Coco S, Calegari F, Pravettoni E, Pozzi D, Taverna E, Rosa P, et al. Storage and release of ATP from astrocytes in culture. Journal of Biological Chemistry. 2003;278(2):1354-62.

99.   Kreda S, Seminario-Vidal L, Okada S, van Heusden C, Boucher RC, Lazarowski E. Differential regulation of ATP release by airway epithelial cells. Pediatric Pulmonology. 2008;43 (S31)(S31):246.

100. Zuo P, Picher M, Okada SF, Lazarowski ER, Button B, Boucher RC, et al. Mathematical model of nucleotide regulation on airway epithelia. Implications for airway homeostasis. Journal of Biological Chemistry. 2008;283(39):26805-19.

101. Basser PJ, McMahon TA, Griffith P. The mechanism of mucus clearance in cough. Journal of Biomechanical Engineering. 1989;111(4):288-97.

102. Levitzky MG. Pulmonary Physiology. 3rd ed. New York: McGraw-Hill; 1991.

103. Wine JJ, Joo NS. Submucosal glands and airway defense. Proceedings of the National Academy of Sciences of the USA. 2004;1(1):47-53.

104. Homolya L, Steinberg AD, Boucher RC. Cell to cell communication in response to mechanical stress via bilateral release of ATP and UTP in polarized epithelia. Journal of Cell Biology. 2000;150(6):1349-60.

105. Button B, Picher M, Boucher RC. Differential effects of cyclic and constant stress on ATP release and mucociliary transport by human airway epithelia. Journal of Physiology. 2007;580(Pt. 2):577-92.

106. Tatur S, Kreda S, Lazarowski E, Grygorczyk R. Calcium-dependent release of adenosine and uridine nucleotides from A549 cells. Purinergic Signalling. 2008;4(2):139-46.

107. Golledge J, Turner RJ, Harley SL, Springall DR, Powell JT. Circumferential deformation and shear stress induce differential responses in saphenous vein endothelium exposed to arterial flow. Journal of Clinical Investigation. 1997;99(11):2719-26.

108. Miyazaki H, Shiozaki A, Niisato N, Marunaka Y. Physiological significance of hypotonicity-induced regulatory volume decrease: reduction in intracellular Cl- concentration

acting as an intracellular signaling. American Journal of Physiology. Renal Physiology. 2007;292(5):F1411-7.

109. Strange K, Emma F, Jackson PS. Cellular and molecular physiology of volume-sensitive anion channels. American Journal of Physiology. 1996;270(3 Pt 1):C711-30.

110. Wang Y, Roman R, Lidofsky SD, Fitz JG. Autocrine signaling through ATP release represents a novel mechanism for cell volume regulation. Proceedings of the National Academy of Sciences of the USA. 1996;93:12020-5.

111. Sabirov RZ, Dutta AK, Okada Y. Volume-dependent ATP-conductive large-conductance anion channel as a pathway for swelling-induced ATP release. Journal of General Physiology. 2001;118(3):251-66.

112. Boudreault F, Grygorczyk R. Cell swelling-induced ATP release and gadolinium-sensitive channels. American Journal of Physiology. 2002;282(1):C219-C26.

113. Hisadome K, Koyama T, Kimura C, Droogmans G, Ito Y, Oike M. Volume-regulated anion channels serve as an auto/paracrine nucleotide release pathway in aortic endothelial cells. Journal of General Physiology. 2002;119(6):511-20.

114. Okada SF, O'Neal WK, Huang P, Nicholas RA, Ostrowski LE, Craigen WJ, et al. Voltage-dependent Anion Channel-1 (VDAC-1) Contributes to ATP Release and Cell Volume Regulation in Murine Cells. Journal of General Physiology. 2004;124(5):513-26.

115. Dutzler R, Campbell EB, MacKinnon R. Gating the selectivity filter in ClC chloride channels. Science. 2003;300(5616):108-12.

116. Colombini M. Structure and mode of action of a voltage dependent anion-selective channel (VDAC) located in the outer mitochondrial membrane. Annals of the **New York** Academy of Sciences. 1980;341:552-63.

117. Zalman LS, Nikaido H, Kagawa Y. Mitochondrial outer membrane contains a protein producing nonspecific diffusion channels. Journal of Biological Chemistry. 1980;255(5):1771-4.

118. Bahamonde MI, Fernandez-Fernandez JM, Guix FX, Vazquez E, Valverde MA. Plasma membrane voltage-dependent anion channel mediates antiestrogen-activated maxi Cl-currents in C1300 neuroblastoma cells. Journal of Biological Chemistry. 2003;278(35):33284-9.

119. Bell PD, Lapointe JY, Sabirov R, Hayashi S, Peti-Peterdi J, Manabe K, et al. Macula densa cell signaling involves ATP release through a maxi anion channel. Proceedings of the National Academy of Sciences of the USA. 2003;100(7):4322-7.

120. Sabirov RZ, Sheiko T, Liu H, Deng D, Okada Y, Craigen WJ. Genetic demonstration that the plasma membrane maxianion channel and voltage-dependent anion channels are unrelated proteins. Journal of Biological Chemistry. 2006;281(4):1897-904.

121. Sabirov RZ, Okada Y. The maxi-anion channel: a classical channel playing novel roles through an unidentified molecular entity. Journal of Physiological Science. 2009;59(1):3-21.

122. Reisin IL, Prat AG, Abraham EH, Amara JF, Gregory RJ, Ausiello DA, et al. The cystic fibrosis transmembrane conductance regulator is a dual ATP and chloride channel. Journal of Biological Chemistry. 1994;269(32):20584-91.

123. Schwiebert EM, Egan ME, Hwang TH, Fulmer SB, Allen SS, Cutting GR, et al. CFTR regulates outwardly rectifying chloride channels through an autocrine mechanism involving ATP. Cell. 1995;81(7):1063-73.

124. Jiang Q, Mak D, Devidas S, Schwiebert EM, Bragin A, Zhang Y, et al. Cystic fibrosis transmembrane conductance regulator-associated ATP release is controlled by a chloride sensor. Journal of Cell Biology. 1998;143(3):645-57.

125. Cantiello HF. Electrodiffusional ATP movement through CFTR and other ABC transporters. Pflugers Archives. 2001;443 Suppl 1:S22-7.

126. Reigada D, Mitchell CH. Release of ATP from retinal pigment epithelial cells involves both CFTR and vesicular transport. American Journal of Physiology. Cell Physiology. 2005;288(1):C132-C40.

127. Abraham EH, Prat AG, Gerweck L, Seneveratne T, Arceci RJ, Kramer R, et al. The multidrug resistance (mdr1) gene product functions as an ATP channel. Proceedings of the National Academy of Sciences of the USA. 1993;90(1):312-6.

128. Reddy MM, Quinton PM, Haws C, Wine JJ, Grygorczyk R, Tabcharani JA, et al. Failure of the cystic fibrosis transmembrane conductance regulator to conduct ATP. Science. 1996;271(5257):1876-9.

129. Shestopalov VI, Panchin Y. Pannexins and gap junction protein diversity. Cellular and Molecular Life Sciences. 2008;65(3):376-94.

130. Bruzzone R, Barbe MT, Jakob NJ, Monyer H. Pharmacological properties of homomeric and heteromeric pannexin hemichannels expressed in Xenopus oocytes. Journal of Neurochemistry. 2005;92(5):1033-43.

131. Penuela S, Celetti SJ, Bhalla R, Shao Q, Laird DW. Diverse subcellular distribution profiles of pannexin 1 and pannexin 3. Cell Communication and Adhesion. 2008;15(1):133-42.

132. Muller DJ, Hand GM, Engel A, Sosinsky GE. Conformational changes in surface structures of isolated connexin 26 gap junctions. EMBO Journal. 2002;21(14):3598-607.

133. Gomez-Hernandez JM, de Miguel M, Larrosa B, Gonzalez D, Barrio LC. Molecular basis of calcium regulation in connexin-32 hemichannels. Proceedings of the National Academy of Sciences of the USA. 2003;100(26):16030-5.

134. Ebihara L, Berthoud VM, Beyer EC. Distinct behavior of connexin56 and connexin46 gap junctional channels can be predicted from the behavior of their hemi-gap-junctional channels. Biophysics Journal. 1995;68(5):1796-803.

135. Ebihara L, Liu X, Pal JD. Effect of external magnesium and calcium on human connexin46 hemichannels. Biophysics Journal. 2003;84(1):277-86.

136. Li H, Liu TF, Lazrak A, Peracchia C, Goldberg GS, Lampe PD, et al. Properties and regulation of gap junctional hemichannels in the plasma membranes of cultured cells. The Journal of Cell Biology. 1996;134(4):1019-30.

137. Pfahnl A, Dahl G. Gating of cx46 gap junction hemichannels by calcium and voltage. Pflugers Arch. 1999;437(3):345-53.

138. Quist AP, Rhee SK, Lin H, Lal R. Physiological role of gap-junctional hemichannels. Extracellular calcium-dependent isosmotic volume regulation. The Journal of Cell Biology. 2000;148(5):1063-74.

139. Valiunas V. Biophysical properties of connexin-45 gap junction hemichannels studied in vertebrate cells. Journal of General Physiology. 2002;119(2):147-64.

140. Cotrina ML, Lin JH, Alves-Rodrigues A, Liu S, Li J, Azmi-Ghadimi H, et al. Connexins regulate calcium signaling by controlling ATP release. Proceedings of the National Academy of Sciences of the USA. 1998;95(26):15735-40.

141. Arcuino G, Lin JH, Takano T, Liu C, Jiang L, Gao Q, et al. Intercellular calcium signaling mediated by point-source burst release of ATP. Proceedings of the National Academy of Sciences of the USA. 2002;99(15):9840-5.

142. Hofer A, Dermietzel R. Visualization and functional blocking of gap junction hemichannels (connexons) with antibodies against external loop domains in astrocytes. Glia. 1998;24(1):141-54.

143. White TW, Bruzzone R. Intercellular communication in the eye: clarifying the need for connexin diversity. Brain Research Reviews. 2000;32(1):130-7.

144. Contreras JE, Saez JC, Bukauskas FF, Bennett MV. Gating and regulation of connexin 43 (Cx43) hemichannels. roceedings of the National Academy of Sciences of the USA. 2003;100(20):11388-93.

145. Retamal MA, Yin S, Altenberg GA, Reuss L. Voltage-dependent facilitation of Cx46 hemichannels. American Journall of Physiology - Cell Physiology. 2010;298(1):C132-9.

146. Gonzalez D, Gomez-Hernandez JM, Barrio LC. Species specificity of mammalian connexin-26 to form open voltage-gated hemichannels. The Federation of American Societies for Experimental Biology Journal. 2006;20(13):2329-38.

147. Penuela S, Bhalla R, Gong XQ, Cowan KN, Celetti SJ, Cowan BJ, et al. Pannexin 1 and pannexin 3 are glycoproteins that exhibit many distinct characteristics from the connexin family of gap junction proteins. Journal of Cell Science. 2007;120(Pt 21):3772-83.

148. Zoidl G, Petrasch-Parwez E, Ray A, Meier C, Bunse S, Habbes HW, et al. Localization of the pannexin1 protein at postsynaptic sites in the cerebral cortex and hippocampus. Neuroscience. 2007;146(1):9-16.

149. Boassa D, Qiu F, Dahl G, Sosinsky G. Trafficking dynamics of glycosylated pannexin 1 proteins. Cell Communication and Adhesion. 2008;15(1):119-32. PMCID: 2528835.

150. Locovei S, Bao L, Dahl G. Pannexin 1 in erythrocytes: function without a gap. Proceedings of the National Academy of Sciences of the USA. 2006;103(20):7655-9.

151. Bruzzone R, Hormuzdi SG, Barbe MT, Herb A, Monyer H. Pannexins, a family of gap junction proteins expressed in brain. Proceedings of the National Academy of Sciences of the USA. 2003;100(23):13644-9.

152. Bao L, Locovei S, Dahl G. Pannexin membrane channels are mechanosensitive conduits for ATP. FEBS Letter. 2004;572(1-3):65-8.

153. Boudreault F, Grygorczyk R. Cell swelling-induced ATP release is tightly dependent on intracellular calcium elevations. Journal of Physiology. 2004;561(Pt 2):499-513.

154. Pearson JD, Gordon JL. Vascular endothelial and smooth muscle cells in culture selectively release adenine nucleotides. Nature. 1979;281(5730):384-6.

155. Yang S, Cheek DJ, Westfall DP, Buxton IL. Purinergic axis in cardiac blood vessels. Agonist-mediated release of ATP from cardiac endothelial cells. Circulation Research. 1994;74(3):401-7.

156. Joseph SM, Buchakjian MR, Dubyak GR. Colocalization of ATP release sites and ecto-ATPase activity at the extracellular surface of human astrocytes. Journal of Biological Chemistry. 2003;278:23342.-.

157. Lazarowski ER, Shea DA, Boucher RC, Harden TK. Release of Cellular UDP-Glucose as a Potential Extracellular Signaling Molecule. Molecular Pharmacology. 2003;63(5):1190-7.

158. Lundin A. Use of firefly luciferase in ATP-related assays of biomass, enzymes, and metabolites. Methods in Enzymology. 2000;305:346-70.

159. Taylor AL, Kudlow BA, Marrs KL, Gruenert DC, Guggino WB, Schwiebert EM. Bioluminescence detection of ATP release mechanisms in epithelia. American Journal of Physiology. 1998;275:C1391-C406.

160. Beigi R, Kobatake E, Aizawa M, Dubyak GR. Detection of local ATP release from activated platelets using cell surface-attached firefly luciferase. American Journal of Physiology. 1999;276(1 Pt 1):C267-C78.

161. DeLuca M, McElroy W.D. Purification and Properties of Firefly Luciferase. Methods in Enzymology. 1978;2:3 - 15.

162. Ma HP, Saxena S, Warnock DG. Anionic phospholipids regulate native and expressed epithelial sodium channel (ENaC). Journal of Biological Chemistry. 2002;277(10):7641-4.

163. Zsembery A, Fortenberry JA, Liang L, Bebok Z, Tucker TA, Boyce AT, et al. Extracellular zinc and ATP restore chloride secretion across cystic fibrosis airway epithelia by triggering calcium entry. Journal of Biological Chemistry. 2004;279(11):10720-9.

164. Boucher RC. An overview of the pathogenesis of cystic fibrosis lung disease. Advanced Drug Delivery Reviews. 2002;54(11):1359-71.

165. Rooney SA. Regulation of surfactant secretion. Comparative Biochemistry and Physiology Part A: Molecular and Integrative Physiology. 2001;129(1):233-43.

166. Factor P, Mutlu GM, Chen L, Mohameed J, Akhmedov AT, Meng FJ, et al. Adenosine regulation of alveolar fluid clearance. Proceedings of the National Academy of Sciences of the USA. 2007;104(10):4083-8.

167. Sun CX, Zhong H, Mohsenin A, Morschl E, Chunn JL, Molina JG, et al. Role of A2B adenosine receptor signaling in adenosine-dependent pulmonary inflammation and injury. Journal of Clinical Investigation. 2006;116(8):2173-82.

168. Blackburn MR, Lee CG, Young HW, Zhu Z, Chunn JL, Kang MJ, et al. Adenosine mediates IL-13-induced inflammation and remodeling in the lung and interacts in an IL-13-adenosine amplification pathway. Journal of Clinical Investigation. 2003;112(3):332-44.

169. Lazarowski ER, Boucher RC, Harden TK. Mechanisms of release of nucleotides and integration of their action as P2X- and P2Y-receptor activating molecules. Molecular Pharmacology. 2003;64(4):785-95.

170. Tatur S, Groulx N, Orlov SN, Grygorczyk R. Ca2+-dependent ATP release from A549 cells involves synergistic autocrine stimulation by coreleased uridine nucleotides. Journal of Physiology. 2007;584(Pt 2):419-35.

171. Blum AE, Joseph SM, Przybylski RJ, Dubyak GR. Rho-family GTPases modulate Ca(2+) -dependent ATP release from astrocytes. American Journal of Physiology - Cell Physiology. 2008;295(1):C231-C41.

172. Asokananthan N, Graham PT, Fink J, Knight DA, Bakker AJ, McWilliam AS, et al. Activation of protease-activated receptor (PAR)-1, PAR-2, and PAR-4 stimulates IL-6, IL-8, and prostaglandin E2 release from human respiratory epithelial cells. Journal of Immunology. 2002;168(7):3577-85.

173. Lazarowski ER, Boucher RC, Harden TK. Constitutive release of ATP and evidence for major contribution of ecto-nucleotide pyrophosphatase and nucleoside diphosphokinase to extracellular nucleotide concentrations. Journal of Biological Chemistry. 2000;275(40):31061-8.

174. Joseph SM, Pifer MA, Przybylski RJ, Dubyak GR. Methylene ATP analogs as modulators of extracellular ATP metabolism and accumulation. British Journal of Pharmacology. 2004;142:1002-14.

175. Furstenau CR, Spier AP, Rucker B, Luisa BS, Battastini AM, Sarkis JJ. The effect of ebselen on adenine nucleotide hydrolysis by platelets from adult rats. Chemico-Biological Interactions. 2004;148(1-2):93-9.

176. Hains MD, Wing MR, Maddileti S, Siderovski DP, Harden TK. Galpha12/13- and rho-dependent activation of phospholipase C-epsilon by lysophosphatidic acid and thrombin receptors. Molecular Pharmacology. 2006;69(6):2068-75.

177. Hains MD, Siderovski DP, Harden TK. Application of RGS box proteins to evaluate G-protein selectivity in receptor-promoted signaling. Methods in Enzymology. 2004;389:71-88.

178. Ishihara H, Connolly AJ, Zeng D, Kahn ML, Zheng YW, Timmons C, et al. Protease-activated receptor 3 is a second thrombin receptor in humans. Nature. 1997;386(6624):502-6.

179. Trejo J. Protease-activated receptors: new concepts in regulation of G protein-coupled receptor signaling and trafficking. Journal of Pharmacology and Experimental Therapeutics. 2003;307(2):437-42.

180. Steinhoff M, Buddenkotte J, Shpacovitch V, Rattenholl A, Moormann C, Vergnolle N, et al. Proteinase-activated receptors: transducers of proteinase-mediated signaling in inflammation and immune response. Endocrinology Reviews. 2005;26(1):1-43.

181. Hung DT, Wong YH, Vu TK, Coughlin SR. The cloned platelet thrombin receptor couples to at least two distinct effectors to stimulate phosphoinositide hydrolysis and inhibit adenylyl cyclase. Journal of Biological Chemistry. 1992;267(29):20831-4.

182. Xu WF, Andersen H, Whitmore TE, Presnell SR, Yee DP, Ching A, et al. Cloning and characterization of human protease-activated receptor 4. Proceedings of the National Academy of Sciences of the USA. 1998;95(12):6642-6.

183. Coughlin SR. Thrombin signalling and protease-activated receptors. Nature. 2000;407(6801):258-64.

184. Goel R, Phillips-Mason PJ, Gardner A, Raben DM, Baldassare JJ. Alpha-thrombin-mediated phosphatidylinositol 3-kinase activation through release of Gbetagamma dimers from Galphaq and Galphai2. Journal of Biological Chemistry. 2004;279(8):6701-10.

185. Kurose H. Galpha12 and Galpha13 as key regulatory mediator in signal transduction. Life Sciences. 2003;74(2-3):155-61.

186. Feig LA. Tools of the trade: use of dominant-inhibitory mutants of Ras-family GTPases. Nature Cell Biology. 1999;1(2):E25-E7.

187. Schwartz M. Rho signalling at a glance. Journal of Cell Science. 2004;117(Pt 23):5457-8.

188. Davies SP, Reddy H, Caivano M, Cohen P. Specificity and mechanism of action of some commonly used protein kinase inhibitors. Biochemical Journal. 2000;351(Pt 1):95-105.

189. Riento K, Ridley AJ. Rocks: multifunctional kinases in cell behaviour. Nature Reviews Molecular Cell Biology. 2003;4(6):446-56.

190. Saitoh M, Ishikawa T, Matsushima S, Naka M, Hidaka H. Selective inhibition of catalytic activity of smooth muscle myosin light chain kinase. Journal of Biological Chemistry. 1987;262(16):7796-801.

191. Seye CI, Yu N, Gonzalez FA, Erb L, Weisman GA. The P2Y2 nucleotide receptor mediates vascular cell adhesion molecule-1 expression through interaction with VEGF receptor-2 (KDR/Flk-1). Journal of Biological Chemistry. 2004;279(34):35679-86.

192. Dahl G, Locovei S. Pannexin: to gap or not to gap, is that a question? Union of Biochemistry and Molecular Biology Life. 2006;58(7):409-19.

193. Goodenough DA, Paul DL. Beyond the gap: functions of unpaired connexon channels. Nature Reviews Molecular Cell Biology. 2003;4(4):285-94.

194. Stout CE, Costantin JL, Naus CC, Charles AC. Intercellular calcium signaling in astrocytes via ATP release through connexin hemichannels. Journal of Biological Chemistry. 2002;277(12):10482-8.

195. De Vuyst E, Decrock E, Cabooter L, Dubyak GR, Naus CC, Evans WH, et al. Intracellular calcium changes trigger connexin 32 hemichannel opening. EMBO Journal. 2005;25(1):34-44.

196. Pelegrin P, Surprenant A. Pannexin-1 mediates large pore formation and interleukin-1beta release by the ATP-gated P2X7 receptor. EMBO Journal. 2006;25(21):5071-82.

197. Danahay H, Withey L, Poll CT, van de Graaf SF, Bridges RJ. Protease-activated receptor-2-mediated inhibition of ion transport in human bronchial epithelial cells. American Journal of Physiology. Cell Physiology. 2001;280(6):C1455-C64.

198. Palmer ML, Lee SY, Maniak PJ, Carlson D, Fahrenkrug SC, O'Grady SM. Protease-activated receptor regulation of Cl- secretion in Calu-3 cells requires prostaglandin release and CFTR activation. American Journal of Physiology. Cell Physiology. 2006;290(4):C1189-C98.

199. Paradiso AM, Mason SJ, Lazarowski ER, Boucher RC. Membrane-Restricted Regulation of Ca2+ Release and Influx in Polarized Epithelia. Nature. 1995;377(6550):643-6.

200. Koyama T, Oike M, Ito Y. Involvement of Rho-kinase and tyrosine kinase in hypotonic stress-induced ATP release in bovine aortic endothelial cells. Journal of Physiology. 2001;532(Pt 3):759-69.

201. Hirakawa M, Oike M, Karashima Y, Ito Y. Sequential activation of RhoA and FAK/paxillin leads to ATP release and actin reorganization in human endothelium. Journal of Physiology. 2004;558(Pt 2):479-88.

202. Gavard J, Gutkind JS. Protein kinase C-related kinase and ROCK are required for thrombin-induced endothelial cell permeability downstream from Galpha12/13 and Galpha11/q. Journal of Biological Chemistry. 2008;283(44):29888-96.

203. Ostrowska E, Reiser G. The protease-activated receptor-3 (PAR-3) can signal autonomously to induce interleukin-8 release. Cellular and Molecular Life Sciences. 2008;65(6):970-81.

204. McLaughlin JN, Patterson MM, Malik AB. Protease-activated receptor-3 (PAR3) regulates PAR1 signaling by receptor dimerization. Proceedings of the National Academy of Sciences of the USA. 2007;104(13):5662-7.

205. Boucher RC. Cystic fibrosis: a disease of vulnerability to airway surface dehydration. Trends in Molecular Medicine. 2007;13(6):231-40.

206. Lazarowski ER, Boucher RC. Purinergic receptors in airway epithelia. Current Opinion in Pharmacology. 2009.

207. Ransford GA, Fregien N, Qiu F, Dahl G, Conner GE, Salathe M. Pannexin 1 Contributes to ATP Release in Airway Epithelia. American Journal of Respiratory Cell and Molecular Biology. 2009;41(5):525-34.

208. Russo A, Soh UJ, Trejo J. Proteases display biased agonism at protease-activated receptors: location matters! Molecular Interventions. 2009;9(2):87-96.

209. Kawabata A, Kawao N, Kuroda R, Tanaka A, Itoh H, Nishikawa H. Peripheral PAR-2 triggers thermal hyperalgesia and nociceptive responses in rats. Neuroreport. 2001;12(4):715-9.

210. Lin KW, Park J, Crews AL, Li Y, Adler KB. Protease-activated receptor-2 (PAR-2) is a weak enhancer of mucin secretion by human bronchial epithelial cells in vitro. International Journal of Biochemistry - Cell Biology. 2008;40(6-7):1379-88.

211. Shen BQ, Finkbeiner WE, Wine JJ, Mrsny RJ, Widdicombe JH. Calu-3: a human airway epithelial cell line that shows cAMP-dependent Cl- secretion. American Journal of Physiology. 1994;266(5 Pt 1):L493-L501.

212. Kreda SM, Mall M, Mengos A, Rochelle L, Yankaskas J, Riordan JR, et al. Characterization of Wild-Type and {Delta}F508 Cystic Fibrosis Transmembrane Regulator in Human Respiratory Epithelia. Molecular Biology of the Cell. 2005;16(5):2154-67.

213. Bankston LA, Guidotti G. Characterization of ATP transport into chromaffin granule ghosts - Synergy of ATP and serotonin accumulation in chromaffin granule ghosts. Journal of Biological Chemistry. 1996;271(29):17132-8.

214. Wang CC, Shi H, Guo K, Ng CP, Li J, Gan BQ, et al. VAMP8/endobrevin as a general vesicular SNARE for regulated exocytosis of the exocrine system. Molecular Biology of the Cell. 2007;18(3):1056-63.

215. Verdugo P. Goblet cells secretion and mucogenesis. Annual Reviews in Physiology. 1990;52:157-76.

216. Davis CW, Dowell ML, Lethem M, Van Scott M. Goblet cell degranulation in isolated canine tracheal epithelium: response to exogenous ATP, ADP, and adenosine. American Journal of Physiology. 1992;262(5 Pt 1):C1313-C23.

217. Perez-Vilar J. Mucin granule intraluminal organization. American Journal of Respiratory Cell Molecular Biology. 2007;36(2):183-90.

218. Reed CE, Kita H. The role of protease activation of inflammation in allergic respiratory diseases. Journal of Allergy and Clinical Immunology. 2004;114(5):997-1008.

219. Shimizu S, Shimizu T, Morser J, Kobayashi T, Yamaguchi A, Qin L, et al. Role of the coagulation system in allergic inflammation in the upper airways. Clinical Immunology. 2008;129(2):365-71.

220. Kawabata A, Kinoshita M, Nishikawa H, Kuroda R, Nishida M, Araki H, et al. The protease-activated receptor-2 agonist induces gastric mucus secretion and mucosal cytoprotection. Journal of Clinical Investigation. 2001;107(11):1443-50.

221. Kim MH, Choi BH, Jung SR, Sernka TJ, Kim S, Kim KT, et al. Protease-activated receptor-2 increases exocytosis via multiple signal transduction pathways in pancreatic duct epithelial cells. Journal of Biological Chemistry. 2008;283(27):18711-20.

222. Boucher RC. Regulation of airway surface liquid volume by human airway epithelia. Pflugers Archives. 2003;445(4):495-8.

223. Davis CW, Lazarowski E. Coupling of airway ciliary activity and mucin secretion to mechanical stresses by purinergic signaling. Respiratory Physiology and Neurobiology. 2008;163(1-3):208-13.

224. Grygorczyk R, Tabcharani JA, Hanrahan JW. CFTR channels expressed in CHO cells do not have detectable ATP conductance. Journal of Membrane Biology. 1996;151(2):139-48.

225. Fulcher ML, Gabriel S, Burns KA, Yankaskas JR, Randell SH. Well-differentiated human airway epithelial cell cultures. Methods in Molecular Medicine. 2005;107:183-206.

226. Ma W, Hui H, Pelegrin P, Surprenant A. Pharmacological characterization of pannexin-1 currents expressed in mammalian cells. Journal of Pharmacology and Experimental Therapies. 2009;328(2):409-18.

227. Benfenati V, Caprini M, Nicchia GP, Rossi A, Dovizio M, Cervetto C, et al. Carbenoxolone inhibits volume-regulated anion conductance in cultured rat cortical astroglia. Channels (Austin). 2009;3(5):323-36.

228. Blum AE, Walsh BC, Dubyak GR. Extracellular Osmolarity Modulates G protein-Coupled Receptor Dependent ATP Release from 1321N1 Astrocytoma Cells. American Journal of Physiology - Cell Physiology. 2009.

229. Eskandari S, Zampighi GA, Leung DW, Wright EM, Loo DD. Inhibition of gap junction hemichannels by chloride channel blockers. Journal of Membrane Biology. 2002;185(2):93-102.

230. Baranova A, Ivanov D, Petrash N, Pestova A, Skoblov M, Kelmanson I, et al. The mammalian pannexin family is homologous to the invertebrate innexin gap junction proteins. Genomics. 2004;83(4):706-16.

231. Venkatachalam K, Montell C. TRP channels. Annual Review in Biochemistry. 2007;76:387-417.

232. Wu L, Gao X, Brown RC, Heller S, O'Neil RG. Dual role of the TRPV4 channel as a sensor of flow and osmolality in renal epithelial cells. American Journal of Physiology - Renal Physiology. 2007;293(5):F1699-F713.

233. O'Neil RG, Heller S. The mechanosensitive nature of TRPV channels. Pflugers Archives. 2005;451(1):193-203.

234. Silva GB, Garvin JL. TRPV4 mediates hypotonicity-induced ATP release by the thick ascending limb. American Journal of Physiology - Renal Physiology. 2008;295(4):F1090-F5.

235. Mochizuki T, Sokabe T, Araki I, Fujishita K, Shibasaki K, Uchida K, et al. The TRPV4 cation channel mediates stretch-evoked Ca2+ influx and ATP release in primary urothelial cell cultures. Journal of Biological Chemistry. 2009;284(32):21257-64.

236. Singh I, Knezevic N, Ahmmed GU, Kini V, Malik AB, Mehta D. Galphaq-TRPC6-mediated Ca2+ entry induces RhoA activation and resultant endothelial cell shape change in response to thrombin. Journal of Biological Chemistry. 2007;282(11):7833-43.

237. Schenk U, Westendorf AM, Radaelli E, Casati A, Ferro M, Fumagalli M, et al. Purinergic control of T cell activation by ATP released through pannexin-1 hemichannels. Science Signaling. 2008;1(39):ra6.

238. Guyot A, Hanrahan JW. ATP release from human airway epithelial cells studied using a capillary cell culture system. Journal of Physiology. 2002;545(Pt 1):199-206.

239. Boassa D, Qiu F, Dahl G, Sosinsky G. Trafficking dynamics of glycosylated pannexin 1 proteins. Cell Communication and Adhesion. 2008;15(1):119-32.

240. Huang YJ, Maruyama Y, Dvoryanchikov G, Pereira E, Chaudhari N, Roper SD. The role of pannexin 1 hemichannels in ATP release and cell-cell communication in mouse taste buds. Proceedings of the National Academy of Sciences of the USA. 2007;104(15):6436-41.

241. Ossovskaya VS, Bunnett NW. Protease-activated receptors: contribution to physiology and disease. Physiology Reviews. 2004;84(2):579-621.

242. Shpacovitch VM, Seeliger S, Huber-Lang M, Balkow S, Feld M, Hollenberg MD, et al. Agonists of proteinase-activated receptor-2 affect transendothelial migration and apoptosis of human neutrophils. Experimental Dermatology. 2007;16(10):799-806.

243. Kino T, Takatori H, Manoli I, Wang Y, Tiulpakov A, Blackman MR, et al. Brx mediates the response of lymphocytes to osmotic stress through the activation of NFAT5. Science Signaling. 2009;2(57):ra5.

244. Di Ciano-Oliveira C, Thirone AC, Szaszi K, Kapus A. Osmotic stress and the cytoskeleton: the R(h)ole of Rho GTPases. Acta Physiologica (Oxf). 2006;187(1-2):257-72.

245. Takahashi K, Sasaki T, Mammoto A, Takaishi K, Kameyama T, Tsukita S, et al. Direct interaction of the Rho GDP dissociation inhibitor with ezrin/radixin/moesin initiates the activation of the Rho small G protein. Journal of Biological Chemistry. 1997;272(37):23371-5.

246. Tang Y, Tang J, Chen Z, Trost C, Flockerzi V, Li M, et al. Association of mammalian trp4 and phospholipase C isozymes with a PDZ domain-containing protein, NHERF. Journal of Biological Chemistry. 2000;275(48):37559-64.

247. Mery L, Strauss B, Dufour JF, Krause KH, Hoth M. The PDZ-interacting domain of TRPC4 controls its localization and surface expression in HEK293 cells. Journal of Cell Science. 2002;115(Pt 17):3497-508.

248. Idzko M, Hammad H, van Nimwegen M, Kool M, Willart MA, Muskens F, et al. Extracellular ATP triggers and maintains asthmatic airway inflammation by activating dendritic cells. Nature Medicine. 2007;13(8):913-9.

249. Mohsenin A, Blackburn MR. Adenosine signaling in asthma and chronic obstructive pulmonary disease. Current Opinion in Pulmonary Medicine. 2006;12(1):54-9.

250. Ram A, Singh SK, Singh VP, Kumar S, Ghosh B. Inhaled carbenoxolone prevents allergic airway inflammation and airway hyperreactivity in a mouse model of asthma. International Archives of Allergy and Immunology. 2009;149(1):38-46.

251. Deterding RR, Lavange LM, Engels JM, Mathews DW, Coquillette SJ, Brody AS, et al. Phase 2 randomized safety and efficacy trial of nebulized denufosol tetrasodium in cystic fibrosis. American Journal of Respiratory and Critical Care Medicine. 2007;176(4):362-9.

252. Kellerman D, Rossi Mospan A, Engels J, Schaberg A, Gorden J, Smiley L. Denufosol: a review of studies with inhaled P2Y(2) agonists that led to Phase 3. Pulmonary Pharmacology and Therapeutics. 2008;21(4):600-7.